ROBOTIC FABRICATION WORKFLOW FOR GYROID-LIKE MODULAR SYSTEMS

MERYEM NUREFŞAN YABANİGÜL
116803016

INSTITUTE OF GRADUATE PROGRAMS
HISTORY, THEORY ANS CRITICISM IN ARCHITECTURE
MASTER PROGRAM

Istanbul Bilgi University
2020

ROBOTIC FABRICATION WORKFLOW FOR GYROID-LIKE MODULAR SYSTEMS

GYROİD BENZERİ MODÜLER SİSTEMLERİN ROBOTİK FABRİKASYON İŞ AKIŞI

MERYEM NUREFŞAN YABANİGÜL

116803016

Supervisor : **Assoc. Prof.Dr.TUĞRUL YAZAR** .....

Istanbul Bilgi University

Jury Member : **Asst. Prof. FULYA AKİPEK** .....

Istanbul Bilgi University

Jury Member : **Assoc. Prof. Dr. SEMA ALAÇAM** .....

Istanbul Technical University

Date of Approval: 13.01.2020

Total Page Number: 154

Anahtar Kelimeler

1) Hesaplamalı Tasarım
2) Robotik Fabrikasyon
3) Sıcak Tel Kesici
4) Minimal Yüzey
5) Gyroid

Key Words

1) Computational Design
2) Robotic Fabrication
3) Hot-wire Cutting
4) Minimal Surface
5) Gyroid

ACKNOWLEDGEMENTS

I would like to extend my sincere thanks to Assoc. Professor Dr. A. Tuğrul YAZAR, who has made a great contribution to this research by guided and supported me with his knowledge, time, and understanding.

I am also grateful to Istanbul Bilgi University for supporting this research as a part of Scientific Research Project.

Special thanks to Rahman ÇELEBİ, for providing me the most efficient use of the Istanbul Bilgi University Faculty of Architecture Fabrication Laboratory during the research.

I must express my very profound gratitude to my parents Nilgün YABANİGÜL and Mesut YABANİGÜL for providing me with unfailing support, love and continuous encouragement throughout whatever I pursue, and my family for being there whenever I need.

ABSTRACT

ROBOTIC FABRICATION WORKFLOW FOR GYROID-LIKE MODULAR SYSTEMS

With the involvement of the industrial robots, a new field has been opened in architectural design and fabrication research. In this new field, architectural fabrication methods, material, and tool knowledge developed by researches. The thesis aims to generate a design and fabrication workflow by using robotic fabrication technologies and parametric design. Through this aim, this thesis presents a prototype design and production of a volumetric, porous, and modular system.

The hot wire cutter used in robotic architecture researches produces by melting foamed polymer materials with a heated insulating wire. The tool, which enables faster production compared to other devices, has some limitations in the production of free geometries. With the prototype fabrication to be conducted within the scope of the thesis, it also focused on the boundaries of the tool by producing a non-linear hot wire cutter.

Mathematical objects and robot used as catalysts for generating the workflow. In the thesis, the workflow and product variety of these two catalysts shown during the computational design-research process.

Key Words: Computational Design, Robotic Fabrication, Hot-wire Cutting, Minimal Surface, Gyroid

ÖZET

GYROİD BENZERİ MODÜLER SİSTEMLERİN ROBOTİK FABRİKASYON İŞ AKIŞI

Endüstriyel robotların dahil olması ile mimari tasarım ve üretim araştırmalarında yeni bir alan açılmıştır. Oluşan bu yeni alanda, mimarlık üretim yöntemleri, malzeme ve araç araştırmaları yapılarak bu konulardaki bilgi birikimi geliştirilmektedir. Tezin amacı robot teknolojileri ve parametrik tasarım kullanılarak tasarım ve üretim iş akışı oluşturmaktır. Tezde, bu hedef doğrultusunda hacimli, gözenekli ve modüler sistem prototipi tasarımı ve üretimi sunulmaktadır.

Robotik mimarlık araştırmalarında kullanılan sıcak tel kesici, ısıtılan bir yalıtkan tel ile, köpük haline getirilmiş polimer malzemelerin eritilerek üretim yapar. Diğer araçlara kıyasla daha hızlı üretim yapılmasına olanak sağlayan aracın, serbest geometrilerin üretiminde bazı kısıtlamaları mevcuttur.Tezde yapılacak üretimde bu kısıtlamalara da odaklanılmakta, robotik düz olmayan sıcak tel kesici ile üretim yapılmaktadır.

Üretilmesi hedeflenen iş akışı için matematiksel objeler ve robot katolizör olarak kullanılmıştır. Tezde, hesaplamalı tasarım-araştırma sürecinde bu iki katalizörün iş akışını ve ürün çeşitliliğini gösterilmektedir.

Anahtar Kelimeler: Hesaplamalı Tasarım, Robotik Fabrikasyon, Sıcak Tel Kesici, Minimal Yüzey, Gyroid

TABLE OF CONTENT

LIST OF FIGURES

LIST OF TABLES

LIST OF SYMBOLS

%	Percent
3D	3 Dimension
A	Ampere
Assist.	Assistant
Assoc.	Associate
CAD	Computer Aided Design
CAM	Computer Aided Manufacturing
cm	Centimeter
cm^3	Square Centimeter
CNC	Computer Numerical Control
Dr.	Doctor
EPS	Expanded Polystyrene
ft	Feet
kg	Kilogram
kg/m^3	Kilogram / Cubic Meter
KRL	KUKA Robotic Language
m^2	Square Meter
mm	Millimeter
NiCr	Nickel-Chromium
Prof.	Professor

TPMS	Triply Periodic Minimal Surface
V	Volt

1. INTRODUCTION

1.1. Aim of the Study

The study aims to create a prototype of a volumetric, porous, and modular system. This thesis proposes a design and production workflow for the above aim by utilizing robot technology and parametric modeling.

With the involvement of the industrial robots in architecture discipline, a new field has been opened. In this new area, architectural fabrication methods, material and tool knowledge developed by architecture schools and independent design researchers. It aimed to explore the production methods of the future by expanding the boundaries of robotic production with the researches conducted by researchers from various disciplines.

The hot wire cutter used in robotic architecture researches produces by melting foamed polymer materials with a heated insulating wire. The tool, which enables faster production compared to other tools, has some limitations in the production of free geometries. In the prototype production to be made within the scope of the thesis, it also focused on the limitations of the tool by producing with a non-flat hot wire cutter.

1.2. Scope of the Study

The potentials of the robot arm can be revealed through researches carried out by different disciplines. This study incorporates a multi-disciplinary process by the researcher. It involves the computational design, computer programming, and robotic fabrication.

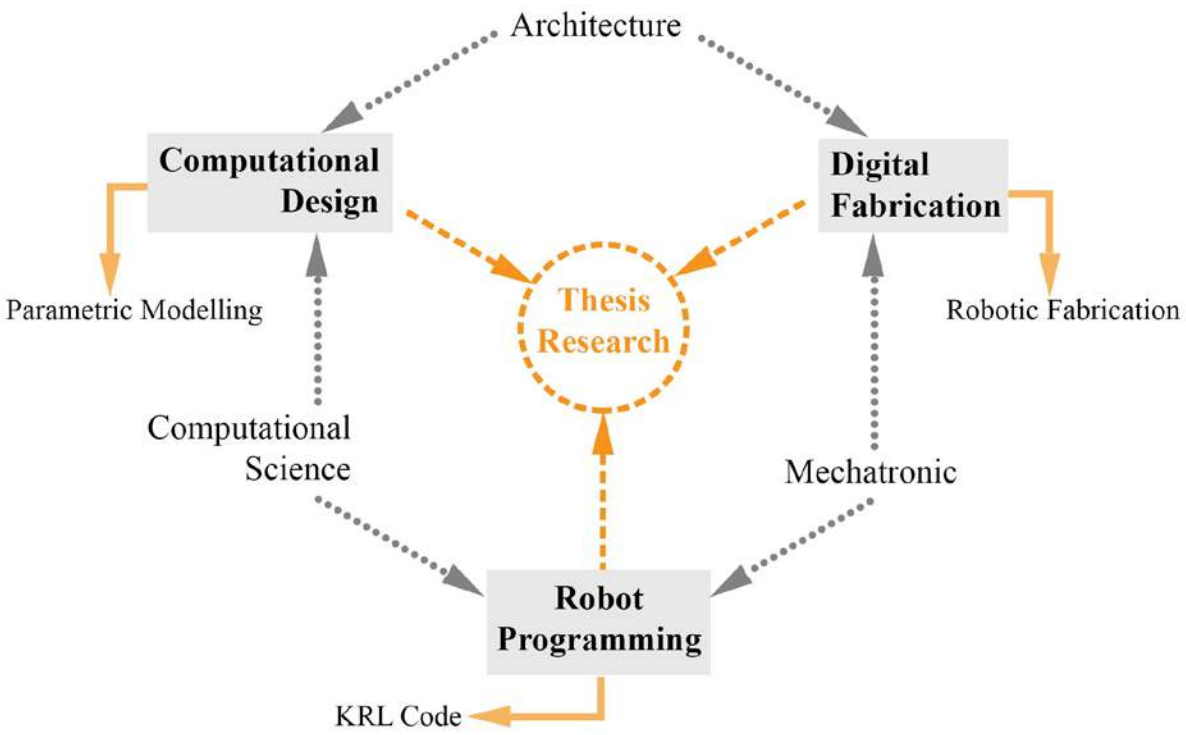

Figure 1.2. The interdisciplinary research system of the thesis

The scope of Computational Design:

Within the scope of the computational design of the research, the focus is on modular masonry structure systems designed in the computer environment.

The scope on Computer Programming:

The robot can programmed in several options. Computer-based robot programming is one of the most common methods among architects. Architects have developed plug-ins like Robots to control the robot.

Another topic to be explored in the computer environment is mathematical objects. New computer software generates and analyses math objects and presents them to designers.

Therefore, on the scope of computer programming, focused topics are dataflow programming in Grasshopper and math objects.

The scope of Robotic Fabrication:

This research contains an industrial robotic arm with an unusual usage. In hotwire robotic production for research purposes, the general use of the wire is straight. In this thesis, robotic hotwire fabrication to be held with a non-linear hotwire cutter system.

1.3. Research Questions

Question 1: Is it possible to design and produce an approximation of a double-curved math object with a robot hotwire cutting technique?

Question 2: What kind of an integrated design and production workflow, along with necessary skills and knowledge sets, are required to answer the first question?

Question 3: What are the performances and potentials of this workflow in terms of the key scope of the research?

1.4. Literature Review

The word “Robot” which comes from “Robota” was first used by a Czech writer named Karel Capek in “Rossum’s Universal Robots” theatrical play in the 1920s. Capek used this word, which means heavy work in the Czech language, for slave machines that Rossum and his son created to serve people (Niku, 2001; Ichbiah, 2005).

In 1927, in the Metropolis film directed by Fritz Lang, Maria appeared as a human-form robot. This term and the concept that it accompanies became widespread by using art in various fields such as literature, cinema, and theater. The word “Robotics” was first used by science fiction writer Isaac Asimov in 1942 in the novel Runaround (Gasparetto & Scalera, 2019).

The Robot term defined as “a robot is a reprogrammable multifunctional manipulator designed to move materials, parts, tools or specialized devices through variable programmed

motions for the performance of a variety of tasks" by the Robot Institute of America (Wallén, 2008).

An example of the articulated human-controlled arm is the teleoperator, designed by Raymond Goertz in the 1940s and 1950s. Articulated arms used for nuclear research in Courtesy Argonne National Labs in the USA. The arms control systems were electrical and controlled behind shields. (Niemeyer, et al. 2008)

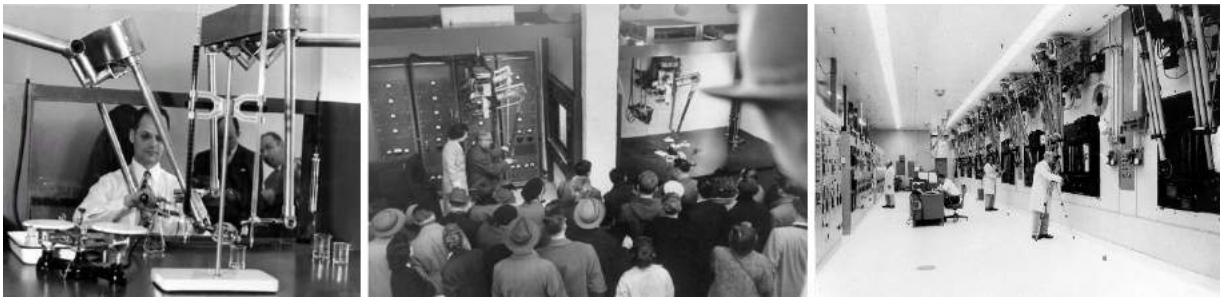

Figure 1.3. Articulated teleoperation arm (URL-20,21)

The programmable industrial articulated robot arms first produced in 1961. In 1956 George Devol and Joseph Engelberger founded a company. As a result of the studies carried out, the first industrial robot arm Unimate developed in 1961. Later on, Unimate was integrated into a conveyor at the General Motors factory and used for a single task. With the development of industrial robot technology, it has significantly affected the speed of mass production (Gasparetto & Scalera, 2019; Ichbiah, 2005).

Figure 1.4. Industrial articulated robot; Unimate, (URL-22)

Although robotic studies thought to be limited to mass production and engineering fields, recent research has spread to many disciplines, including architecture, cinema, and health. With robots, the ability to produce far beyond the existing boundaries in architectural production has

accelerated research on issues such as materials and architectural production (Braumann & Brell-Cokcan, 2012).

Articulated robots, which are used extensively in the automotive industry, are used in a wide variety of tasks, such as welding or spray paint, since they are suitable for replacing or adding parts in the latest joint. In particular, articulated robotic arms have been involved in architectural research, as they can be used in a wide range of tasks and a wide range of domains compared to other production tools. Research is carried out not only in architectural design offices but also in architecture faculties in universities such as ETH Zurich, TU Vienna, Stuttgart, Architecture Association, and Michigan.

Leading examples of robotic fabrication research have been conducted since 2006 at the Gramazio & Kohler research center. Most of the research is about new materials and ways of use that can be used for building products, as well as the re-examination of traditional building materials, exploring the limits of the materials and robot, the most efficient use of the robot.

Smart Dynamic Casting, a research project between 2012-2015 with the collaboration of Gramazio & Kohler Research Center and ETH Zürich, produces complex concrete structures using robotic arms. The research is an attempt to test the limits of concrete production systems that exist today. The production of free-from designs is expensive due to the use of non-standard molds. Smart Dynamic Casting aims to eliminate the need for individually made molds for the construction of complex concrete structures (Fritschi, et al., 2017).

Figure 1.5. Smart Dynamic Casting, ETH Zürich, 2012-2015 (URL-23)

The Institute for Computational Design and Construction (ICD) at the University of Stuttgart is conducting advanced research on robotics production. ICD is an institute established to research the computational design and computer-aided manufacturing processes in architecture. Like Gramazio & Kohler, the structural systems and the use of traditional materials examined in ICD; however, researches in the performance of new materials investigated more intensively.

Figure 1.6. ICD-ITKE Research Pavilion, University of Stuttgart, 2016-17 (URL-24)

ICD / ITKE Research Pavilion, which built between 2016-2017, is a structural system produced by three different robots, two of which are robotic arm and one drone, with fiber composite materials. A large-scale and long-span structural system made of fiber composite material, which is lightweight and structural. The main subject of this research is the structural performance and material behavior of composite material that not used as building materials (Felbrich, et al., 2017).

Interdisciplinary environments for the new system and material researches are essential for transferring information from different disciplines. Comprehensive research is more difficult due to the high cost of materials and mechanisms and the need to work in an interdisciplinary environment. However, the architecture faculties of universities in various countries contribute to the robotics production literature by incorporating robotic arms. Providing education in this field, which is almost new for architecture, contributes to the development of construction and design practices. The students are informed about the design, engineering, and construction fields, and the way to improve the calculation processes in architecture opened. The combination of different disciplines ensures that their spatial, formal, and structural potentials emerge in the best possible way. Besides, parametric design, material performance, structure, such as

contributing to the development of each time on top of the issues, contributed to the development of these issues in each production to create a database with the information acquired.

RESEARCH TOPIC	PAPER TOPIC	INSTITUTION	YEAR(S)	MATERIAL	TOOL	RESEARCH IMAGE
ICD/ITKE Research Pavilion 2011	Machinic Morphospaces: Biomimetic Design Strategies for the Computational Exploration of Robot Constraint Spaces for Wood Fabrication	ICD / ITKE University of Stuttgart	2011	Plywood (6.5 mm)	Customized Milling Tool	
ICD/ITKE Research Pavilion 2013-14	Integrative Computational Design Methodologies for Modular Aarchitectural Fiber Composite Morphologies	ICD /ITKE University of Stuttgart	2013-2014	Fiber Composites	Two Sets of Frame	
ICD Aggregate Pavilion 2015	Graded Lightin Aggregate Structures Modulating the Daylight in Designed Granular Systems Using Online ControlledRoboticProcesse	ICD University of Stuttgart	2015	Recycled Plastics	Pneumatic Radial Gripper	
ICD/ITKE Research Pavilion 2015-16	Robotic Sewing A Textile Approach Towards the Computational Design and Fabrication of Lightweight Timber Shells	ICD / ITKE University of Stuttgart	2015-2016	Plywood (4 mm)	Adaptable Gripping Effector	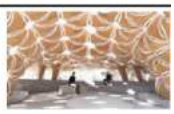
The Programmed Wall	The Informed Wall: applying additive digital fabrication techniques on architecture	ETH Zurich	2006	Brick	Gripper	
The Sequential Wall	Cultural Performance in Robotic Timber Construction	ETH Zurich	2008	Timber	Gripper	
Remote Material Deposition Installation	Remote Material Deposition Exploration of Reciprocall Digital and Material Computational Capacities	ETH Zurich	2014	Loam	Custom Engineered Launching Mechanism	
Robotic Wire Cutting	Spatial Wire Cutting Cooperative Robotic Cutting of Non-Ruled Surface Geometries for Bespoke Building Components	ETH Zurich	2015	EPS Foam	Two Sets of Hotwire Cutter	
Wave Pavilion	Robotic Rod-Bending Digital Drawing in Physical Space	University of Michigan Taubman College of Architecture and Urban Planning	2011	Extruded Steel Rod	Welded Steel Grippers	

Table 1.1. Table of the robotic fabrication research projects in architectural schools. Research projects are not limited by the table

2. METHODOLOGY

2.1. The Triply-Periodic Minimal Surfaces

A minimal surface is a zero-curvature surface that covers the minimum area within the boundaries of a pre-defined space (Sierra & Rodriguez, 2014; Rossi & Buratti, 2017; URL-24). Initial examples of minimal surfaces were introduced by German mathematician Hermann Schwarz in 1865. In 1883, Edvard Rudolf Neovius, who was Schwarz's student, extended the research on the minimal surfaces (Tenu, 2009; Weber & Wolf, 2011). In 1970, Alan Schoen published research that contains 17 periodic minimal surfaces. He illustrated, and modeled five known minimal surfaces and introduced twelve new ones (Sierra & Rodriguez, 2014; Schoen, 1970).

Since their discovery, minimal surfaces continuously catch the attention of a broad range of disciplines, from art and architecture to chemistry and engineering. In architecture, minimal surfaces mostly utilized in structural systems such as bridges, shells, and roof systems. Philips Pavilion (Figure 2.1), designed by Le Corbusier and Iannis Xenakis, is a well-known example of the use of minimal surface as an architectural element. Basento Viaduct (Figure 2.2) is a concrete shell bridge, designed by the Italian engineer and architect Sergio Musmeci. Frei Otto is another essential figure on the design-research studies of architectural minimal surfaces. He used soap films as the form-finding tools for his lightweight structure designs (Figure 2.1) (Tenu, 2009).

Figure 2.1. (a) Philips Pavilion designed by Le Corbusier and Iannis Xenakis. (b) Soap film form-finding experiment by Frie Otto. (c) German Pavilion, Expo in 1967 designed by Frei Otto (URL-1, URL-2, URL3)

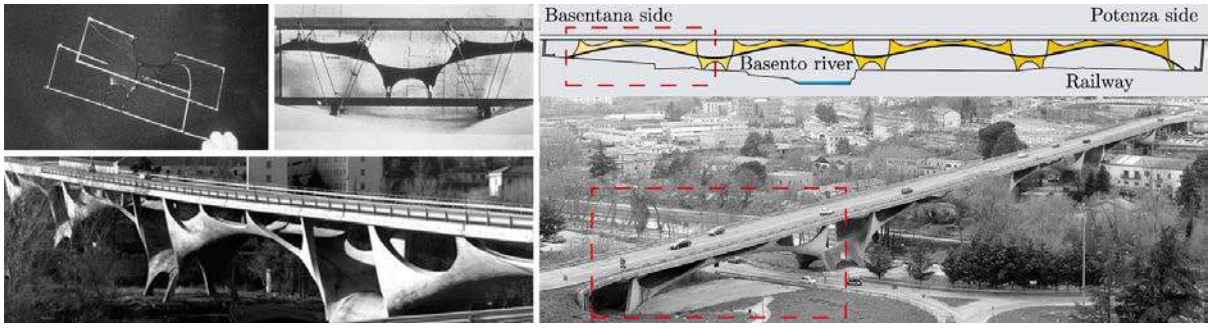

Figure 2.2. Basento Viaduct Bridge designed by Sergio Musmeci (URL-4, URL-5)

Triply periodic minimal surfaces (TPMS), also known as infinite periodic minimal surfaces, are a family of minimal surfaces, which have the quality of growing and extending in three directions. This is established by the symmetry transformations on fundamental units in cartesian space, without intersecting or interrupting each other. (Rossi & Buratti, 2017; Sierra & Rodriguez, 2014; Vamvakidis, 2007; URL-24) TPMS can be generated by rotation and mirror of a small piece, known as a “fundamental region”. Similar to the other minimal surfaces, TPMS attracts the attention of art and architecture because of its geometric sophistication. Artists such as Norman Carlberg, Vlan Tanu, and Carlo Sequin are studying and utilizing TPMS on their sculptures.

Figure 2.3. (a) A sculpture by Norman Carlberg in Northern Parkway Junior High School in 1971. (b) Scherk-Tower by Carlo H. Sequin in 2007. (c) Minimal Surfaces as Architectural Prototypes by Vlan Tanu in 2009 (URL-6, URL-7, URL-8)

Erwin Hauer is another influential artist who explored the geometric features of minimal surfaces. He is known as a "modular constructivist", who structured modules with infinite patterns of repetition (URL-27). His art is about exploring the modularity of infinite continuous surfaces (Figure 2.4) (URL-25).

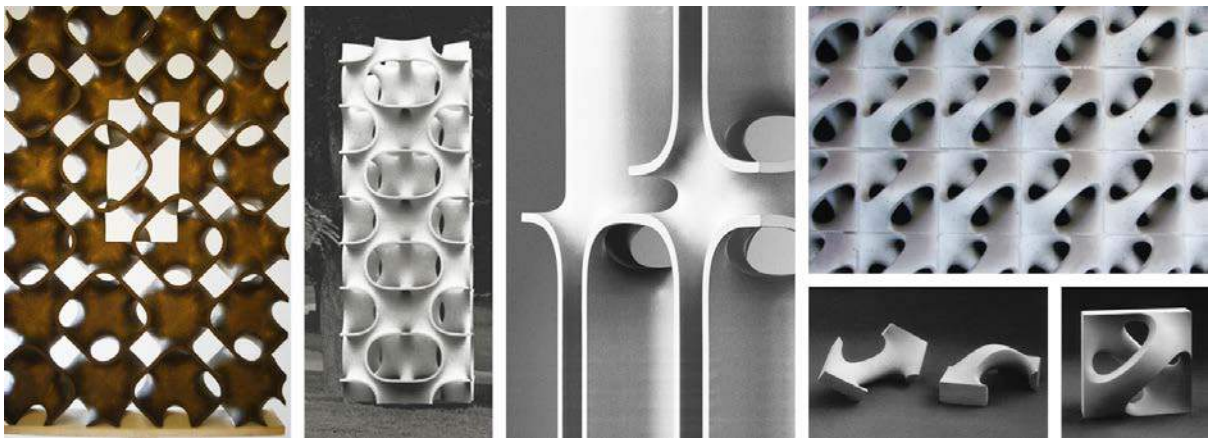

Figure 2.4.Sculpture installations designed by Erwin Hauer (URL-9, URL-10)

Another example in the intersection of art and architecture is the Commune-Action Walls installation designed by POTplus Design Research Group, founded by Funda Akiperk and Tuğrul Yazar within the Fourth International Antalya Architecture Biennial in 2017. Commune-Action Walls is the research of transforming TPMS to a building element by using traditional

building techniques. The structural system established with the permaculture system by planting edible plants to the slots on modules. Modules produced in a factory environment with the soil compaction method for precision with a mold in the form of the Gyroid fundamental unit. Gyroid geometry allowed producing the design form single module, which forms continuous surfaces by using 90-degrees rotated units (Figure 2.5) (Akipek, 2018).

Figure 2.5. Commune-Action Walls research design and production (URL-30)

TPMS are modular and repetitive, continuous, and variable, and their labyrinth-like surfaces can extend in all directions in space systematically (Sierra & Rodriguez, 2014; Tenu, 2009). These double-sided, continuous labyrinths create a unique spatial quality that mentioned in several architectural projects. In addition, the labyrinth system of TPMS opens new and original research fields in building physics with their potential performances in absorbing sound, acoustic, lighting, and temperature control. For this reason, it would be efficient to use these geometric systems in spaces that need sound diffusion, like theaters, auditoriums, or exhibition areas (Sierra & Rodriguez, 2014). Although there are potential benefits, TPMS not widely utilized in architectural design because of its specific formal characteristics. Taichung Metropolitan Opera House is the most relevant application of TPMS in architecture. Opera House, designed by Toyo Ito and Associates, is based on a deformation of P Schwarz's minimal surface (Sierra & Rodriguez, 2014), which consists of a rectangular prism with horizontal and vertical voids. The curved walls and voids generated by the approximation of the minimal surface and used for various functions such as circulation, theater, and atrium spaces. Because of the variability of the geometric system, the measurements of the spaces arranged as needed. Toyo Ito briefly explained the design process by saying, “The geometry came first, and then we forcibly introduced the theaters” (Ito, Grand Opera, 2016). The curved structural elements of

the building also function as the spatial separation elements. The geometrical system allows the optimal distribution of the loads (Aziz & El Sherif, 2016; Bognar, 2017).

Figure 2.6. (a)(b) The exterior of the Taichung Metropolitan Opera House. (c) Interior of the Taichung Metropolitan Opera House (d) Section drawing of the Taichung Metropolitan Opera House (URL-11, URL-12)

Minimal surfaces do not give priority to creating functional spaces in architecture. For this reason, it needed geometrical deformation and additional elements such as horizontal and/or vertical planes for spatial needs (Chen, 2016). Continuity can be sustained by deforming the minimal surface, but adding planar surfaces such as slabs, walls, and facade elements interrupt the spatial fluidity of the system. Due to this reason, the Taichung Metropolitan Opera House project is an important example of the intersection between mathematical and architectural domains in terms of the contrasts between the accuracy and geometric qualities of the TPMS, and the functional necessities of architecture. According to Bognar, this is the "...inherent paradox of the system" (Figure 2.6 and Figure 2.7).

Figure 2.7. (a)(b) The roof garden of the Taichung Metropolitan Opera House. (c)(d) Terraces of the Taichung Metropolitan Opera House (URL-13)

Other innovative architectural examples of minimal surfaces are Meditation Club and Double Negative projects, designed by Khoa Vu. In these two projects, geometric potentials of minimal

surfaces augmented by creating a fluid and continuous spaces that can modularly extend and vary by the scale and form of the modules (URL-14; URL-15). In Double Negative, the surfaces become the building by variation of the geometry as needed, without any interruption. This project presents a general spatial solution, suitable for functions like a gallery, museum, and library. It is conceptual and formal research aiming to uncover the potentials of using minimal surfaces with their unique spatial qualities (Figure 2.8) (URL-14).

Figure 2.8. Double Negative project designed by Khoa Vu (URL-14)

The Meditation Club project also presents a fluid and continuous public spaces. Within this fluidity, the designer focused on creating private spaces (URL-15). In this project, the concepts of structure, wall, ceiling, and stairs are conceptually “melted” and integrated, within the building itself (Figure 2.9).

Figure 2.9. The Meditation Club project designed by Khoa Vu (URL-15)

Another architectural research example designed in 2013 at The University of Hong Kong Master of Architecture studio named Groovy Tectonics, led by Tom Verebes with Paul Wintour. The main aim of the studio was researching curvature, mathematical concepts, tools for their spatial potentials. One of the final projects of the studio was named "Minimal Surfaces," designed by Kwok Hoi Lam Helen and Wong Yok Fai Arnold (Figure 2.10). In this project, designers researched modularity, continuity, and variability potentials of the minimal surfaces for continuous spaces and transformation of modules according to topographical change (URL-16).

These examples indicate that architects are increasingly using and researching minimal surfaces for form and structure solutions of their designs. It is still an open and promising research field of utilizing the formal qualities and generative potentials of minimal surfaces in the search for solutions to the new and challenging problems of architecture in the future.

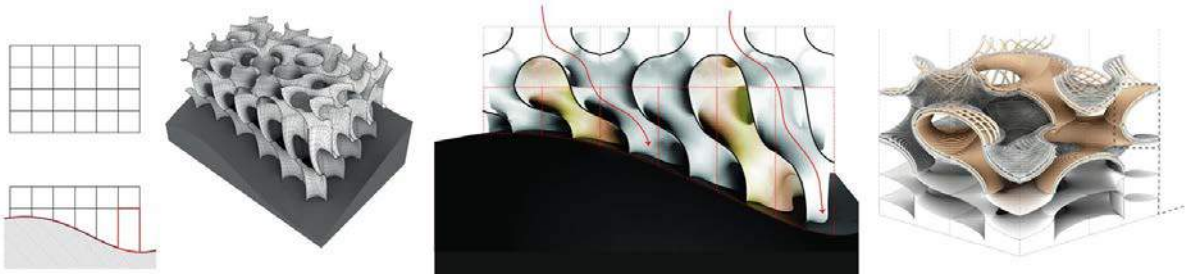

Figure 2.10. The Minimal Surfaces project designed by Kwok Hoi Lam Helen and Wong Yok Fai Arnold (URL-16)

2.2. Digital Fabrication Strategies and Material Computation

With the recent developments in Computer-aided Design (CAD) and Computer-aided Manufacturing (CAM) technologies, the cognitive layer between digital models and physical production disappears. Digital fabrication technologies enable designers to design and produce free-form geometries with mathematical accuracy and precision. There are various production approaches for free-form or double-curved architectural elements, including additive and subtractive manufacturing methods. In additive fabrication, like three-dimensional (3D) printing, the production material is cast layer-by-layer until the desired outcome achieved.

Subtractive fabrication based on removing the pre-defined volumes from solid materials or panels. Laser cutting and Computer Numerical Control (CNC) milling are the technologies based on subtraction. (Kaftan & Stravric, 2013; Rust, et al., 2016)

The generally accepted fabrication methods for free-form architectural geometry are 3D printing and CNC milling. However, depending on the geometric features of the design, the most economical and fastest fabrication approach usually involves subtraction. For example, hotwire of hot blade cutting of expanded Polystyrene foam (EPS) is one of such efficient techniques utilized in architectural design-researches extensively (Rust, et al., 2016). Hot-wire and hot blade cutters have different features. The most known use of a hotwire cutter tool includes a straight wire. It is one of the most practical tools for fabricating simple, non-double-curved geometries. The tool works by melting EPS foam, leaving a gap between the cut pieces, which is proportional to the heat of the wire. The wire should be durable enough to sustain the friction of the material while cutting. It should also be resistant to the deformation effects of the extreme heat. This is why, in general, thick and straight wires used in this technique. The straight wire limits the possible geometric outcomes of the process. Nevertheless, there are a few fabrication examples that used hotwire cutters for forming complex geometries by implementing a carving technique. Because of the possibility of giving shape to the cutting edge, hot blades or hot knives are generally more suitable for fabricating double-curved or complex geometries. In this research, a hotwire will be modified and used for cutting Gyroid-like geometries.

The main challenge to cut double-curved surfaces with non-linear hot-wire is to shaping the wire in the correct form and keeping the wire stable in the given form. In this research, the initial wire tests held with three different wires. In the initial cutting tests, thick nickel-chrome (NiCr) wires proved not useful in heating and cutting EPS. This is why thin shape-memory wires became an alternative solution. In this research, the initial wire tests held with three different wires. Two of them are nickel-chrome (NiCr) wires with 0.9 mm and 1.2 mm thicknesses. NiCr is the standard cutting wire used in industrial and hobby foam cutting practices. Because of the stability issues mentioned above, a shape memory wire with 1 mm thickness is also tested and proved to be useful.

The next step of the setup was to investigate tools that generally used in foam cutting applications. Hand-held hotwire or hot blade tools are usually small, light-weight, and compact tools that enable fast cutting results. There are two types of hand-operated tool systems, namely hand-held and table-top. To accurately cut any free-form geometry by using the hand-operated tools, the tool or the foam block should be fixed and referenced properly to avoid precision problems. It is also difficult to cut continuous and seamless surfaces by manual actuation. CNC hot-wire cutting, on the other hand, enables more complex geometries to be cut with precision. CNC can be regarded as a Cartesian robot; therefore, it can move in three orthogonal directions as X, Y, and a limited amount of Z, without orientation, angles A, B, or C. Some CNC systems include a turning table, which allows non-orthogonal motion paths. Industrial robots are more flexible than CNC. They can orientate any attached tool not only in six axes as X, Y, Z, but also rotation around those axes, as A, B, and C. Industrial robots can manipulate the material in any coordinate in space with the chosen tools attached to them (Ivanovskis, 2017). In this paper, the six-axis industrial robot manipulator KUKA KR-20 will be described with a more common short name, “robotic arm”.

Robotic arms are relatively fast, cheaper to work with, providing more working volume, and can perform more complex movements and various tasks than other digital fabrication systems (URL-28). With the robotic arms, designers can fabricate their designs by controlling the motion path and sequence, speed, approach, and other operational parameters. Two-dimensional subtractive fabrication systems like CNC milling and laser cutting also provide these parameters; however, their accessibility is limited.

Expanded Polystyrene (EPS) is recyclable, lightweight, low-cost, quick formable, and easy-to-assemble material (Jovanović, et al., 2017). Because of these features, EPS is a suitable material for design research and prototyping. Density is a distinctive feature of EPS foams. Particles of the low-density foam are bigger and easier to cut by heat. However, it has a lower resolution than foams that have more density. This is why, the precision of the outcome, especially the complex shapes such as double-curved surfaces is limited. High-density foam is heavier than low-density foam, yet, it has more resistance to pressure. There is a gap created, as the hotwire melts the material while cutting. This gap of the low-density foam is wider than higher density

foams that cut with the same wire and power. In addition to that, the fumes created by melting with the thermal cut is observed more with low-density foam. In this research, 20 kg/m3 and a less dense 60x60x60cm EPS foam blocks used for the experiments.

Thermal cutting tools are not only using in the construction industry. In recent years, they are also getting the attention of the design and fabrication related research fields. There are several robotic fabrication research examples aimed at exploring geometric performances, motion planning, or material performance of hotwire cutting systems.

Figure 2.11. Periscope Foam Tower designed by Matter Design Studio (URL-17)

Periscope Foam Tower, designed by Matter Design Studio, is one of the examples in design research with hotwire cutting. This project designed for a competition that required installation in less than 24 hours on a 10-ft-sq plot with a two-person team (Figure 2.11). Designers managed the requirements with the advantages of EPS as it is lightweight, easy to join, and easily formable with a hotwire cutter. The 50-ft long temporary installation fabricated by carving ruled

geometries from over 500 units of EPS blocks with a hotwire cutter that was attached to the seven-axis industrial robot. These blocks stacked into sub-assemblies, which are three-ft long. For stabilizing the sub-assemblies, plywood profiles placed at the bottom and top of each stack. The Tower was installed by adding fourteen sub-assemblies on top of each other and held down with the tension cables (FABLAB, 2017).

Figure 2.12. Case-Specific Robotic Fabrication of Foam Shell Structures researched by Marko Jovanovic, Marko Vucic, Dejan Mitov, Bojan Tepavčević, Vesna Stojakovic and Ivana Bajsanski (URL-18)

Another design research example based on constructing a vault-like thin shell structure with EPS, which was cut by a robotic controlled hotwire cutter. This project designed and manufactured for the European Research Night by Marko Jovanovic, Marko Vucic, Dejan Mitov, Bojan Tepavčević, Vesna Stojakovic, and Ivana Bajsanski. The overall form of the project was a distorted Igloo, designed with three entrances for visitors to move through. The shell was tessellated in hexagonal double-curved panels and fabricated from EPS blocks with a hotwire cutting tool in 40x40 cm size (Figure. 2.12). Two robotic arms collaboratively used in this research. A tool for holding the EPS foam was attached to one robot, while the other holds the hotwire cutter (Jovanović, et al., 2017).

A research focuses on Gyroid production with hot-wire cutter. In this example, the research aims to deconstruct Gyroid, Saddle tower, and Costa's minimal surface to analyze and to generate an analytical model. In line with this goal, it involves the identification of minimal surfaces and production with hot-wire cutting method. 5-axis CNC and 6-axis robot arm used for production. Minimal surfaces created by bringing together the basic units produced by the

Carving method. Saddle tower and Costa's surface manufactured with the robot arm, while 5-axis CNC used in Gyroid production (Figure 2.13) (Hua & Jia, 2018).

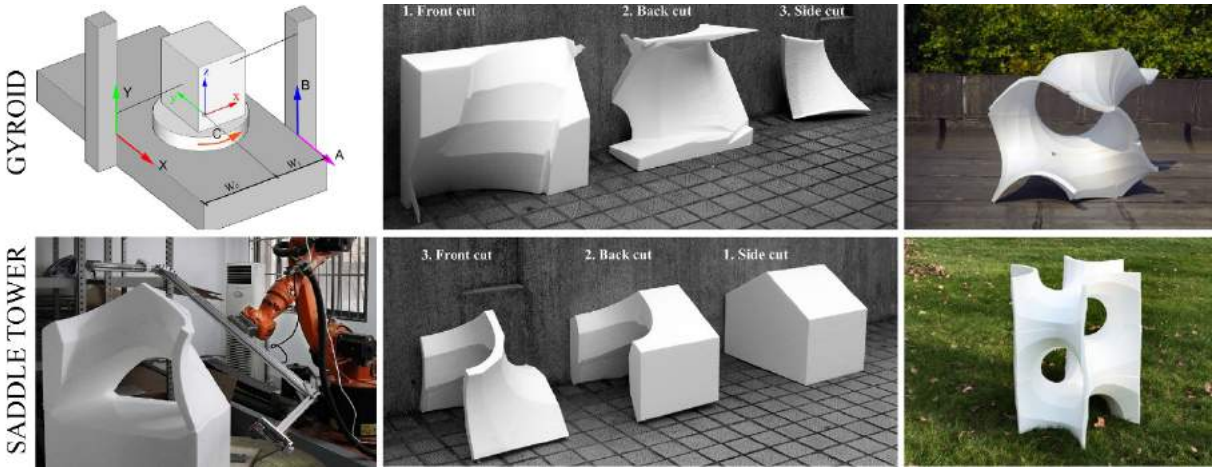

Figure 2.13. Gyroid and Saddle tower fabrication with hot-wire cutting method (URL-31)

2.3. Parametric Design and Coding Environments for Robotic Fabrication

The code to be prepared for the research should include the parametric design of the final product, as well as convert the code into robot language for the production of the units of the design. Parametric design is the design of the product with computer language. The motion of the robot can be controlled by computer programming systems. Parametric design and robot programming can be generated using much different software.

In this study, it aimed to control both parametric modeling and robot programming with the same code. Therefore, Rhino software and Grasshopper plug-in, which can be controlled by both systems, are preferred. In the early stages of the research, Millipede add-on used to create a mathematical surface from the equation, as well as Robots add-on, which simulated the robot and transformed the code into robot language throughout the research.

Grasshopper, an add-on program of Rhinoceros software, is used for parametric modeling. Unlike other coding programs, the commands used in the Grasshopper program placed with the visual units, not written, by establishing relationship networks. Although this system gives the

impression that Grasshopper has a structure that is more understandable and easy to relate to, it is quite complicated.

The mathematical surfaces created by the equation are varied by the range of numbers given to the equation or by changing the equation. The mathematical surface to be produced in the research must be selected among the others. For the selection to be made, all the mathematical surfaces need to remodel as a result of the changes made in the models, equations, and equations. Therefore, MathMod software used for selection. MathMod is mathematical modeling software for visualizing mathematical surfaces. The software includes mathematical surfaces, equations, and number ranges of equations. Variations of mathematical surfaces observed by changing equations and number range in the program.

2.4. Methods of Analysis and Evaluation

It aimed to establish the research between fabrication and feedback to reach the result by developing the information set obtained by experiments. Production will be made both digitally with computers and physically with the robot. The code prepared in the computer environment will be transferred to the robot to run. The code containing the new edits will be transferred to the robot and rearranged with the resulting information. In other words, the experiments consist of fabrication plans, fabrication, and feedback. Each experiment is an improved version of the previous one.

Following this system, five main experiments and numerous conducted intermediate experiments. The product fabricated in each trial is closer to the correct result than the previous one (Figure 2.13).

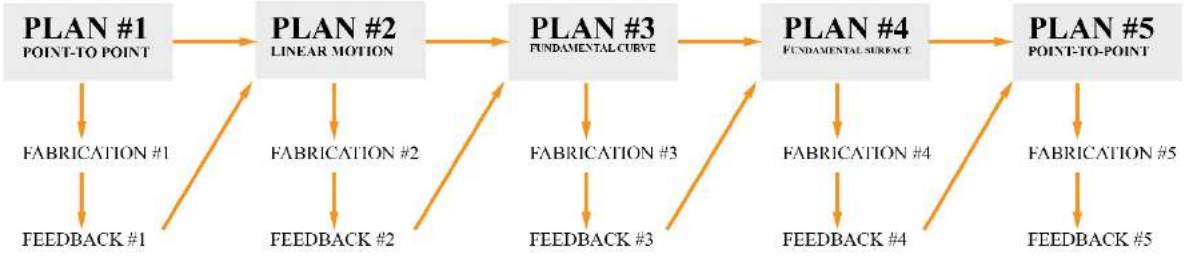

Figure 2.13. Analysis and evaluation methods of the research

3. CASE STUDY

The minimal surfaces to be researched in the scope of the case study selected according to four parameters. The parameters determined to highlight the architectural potential of the selected minimal surfaces are the volumetric potential, modularity, continuity, and variability. Considering the parameters, selection made among the minimal surfaces within the MathMod software. In the first place, four minimal surfaces selected as Gyroid, Diamand, Sherk, and Holes. The variation potentials of selected minimal surfaces have been researched and listed by changing in equations. As a result of the selection, Gyroid included in the case study due to the fundamental curve.

3.1. Digital Modeling

Computer Programs

The first stage of the case study is choosing minimal surfaces, which consist of the value ranges to be given to the equation in the computer program. Minimal surfaces that form by equations are variable and expandable systems. In this research, MathMod used as a visual program to understand variation and chose minimal surfaces.

Another issue is to choose the parametric modeling and robot control software. Parametric modeling and robot control preferred to be generated in the same software for avoiding the possible errors. The motion route created in the computer program must be converted to KRL code for the robot to understand. The selected computer program needs to be able to translate the design created in the digital environment into the language required for production. Rhinoceros is a software that provides the needs of the digital design in this research with the plug-ins and add-ons. Digital visualization, modeling, and fabrication processes parametrically programmed in Rhinoceros 3D software and Grasshopper plug-in. Robots used as an add-on program of the Grasshopper that can simulate the industrial robot in the program and convert

the motion path to the format language required for production. Creating surfaces with the equation is an important step in the research. For that, the Millipede add-on used.

Minimal Surface Variations in MathMod

TPMS are generating with mathematical equations. By varying the parameters contained in the equations, the surfaces are varied. There are two groups of variables in the equations. One is the unknown in the equation, such as x, y, and z, and the other is the Domain range of values given to those unknowns. The number range controls the number of units arranged. With the changes made in the unknowns of the equations, the unit size in X, Y, and Z-axis controlled.

The surface variations formed by the changes made in the equations and number ranges of the selected surfaces researched with the MathMod software and lists created for each minimal surface. Gyroid cubic unit cell generates when equation domains of the unknowns limited between -4 and 4. Limiting unknown domains between -1 and 1 generates a fundamental unit. Without making any changes in the equation, limiting each unknown domains in different range causes the minimal surface to extend. With the unknown X limited between -4 and 16, and unknowns Y and Z limited between -4 and 4, surface extends through X direction (Figure 3.1. (c)). Multiplying the Z unknown with 5 and defining with the same range creates a stretched surface (Figure 3.1(f)). Other variation lists created by using different minimal surfaces (Figure A.1., Figure A.2., Figure A.3.).

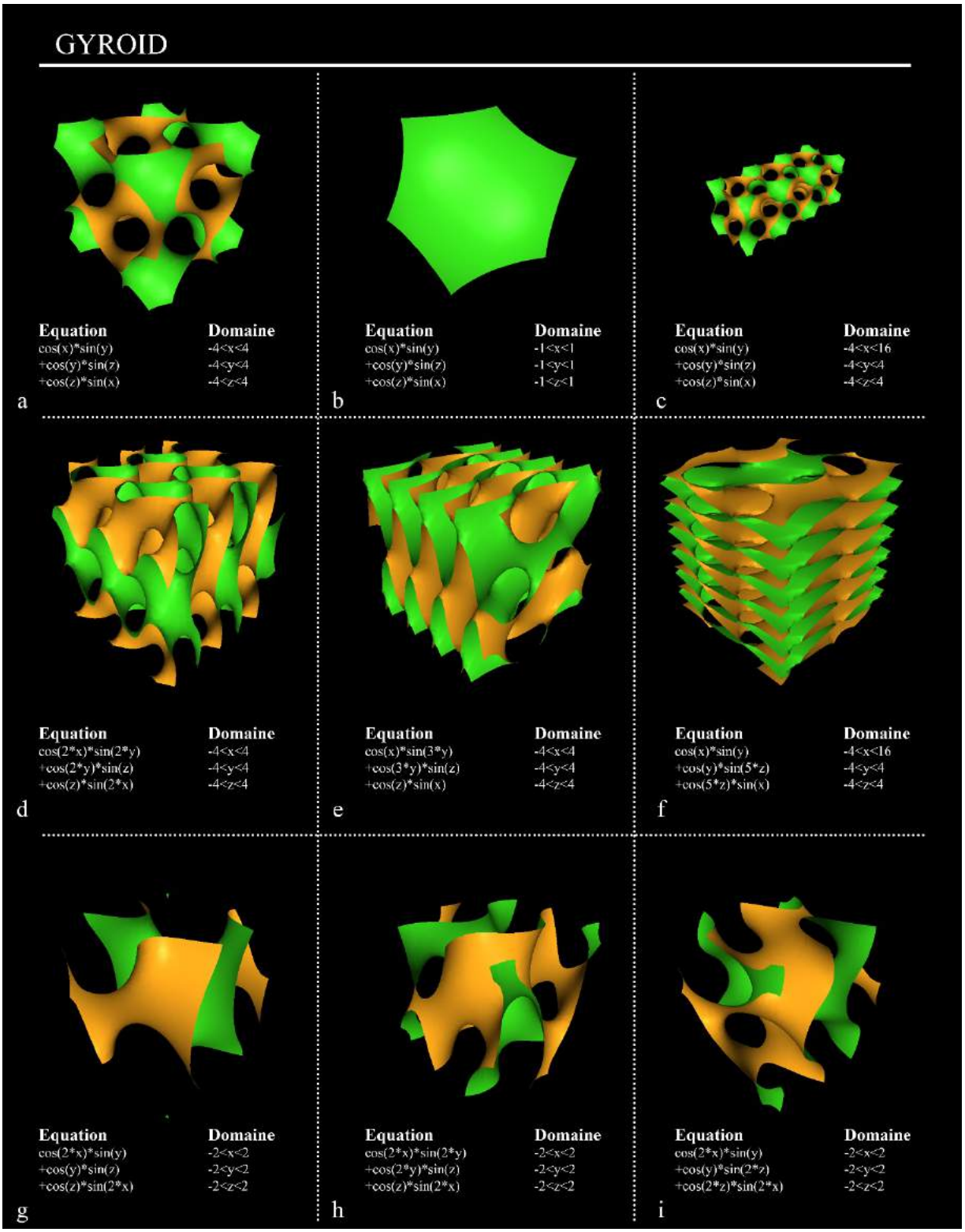

Figure 3.1. Variation of Gyroid minimal surface by changing the equation

Creating TPMS by Equation

The first definition of creating the minimal surfaces in grasshopper reference from diploma studio 10 at Westminster University School of Architecture website (URL-29). The definition was created by using **Iso Surface** from **Millipede** add-on.

Definition;

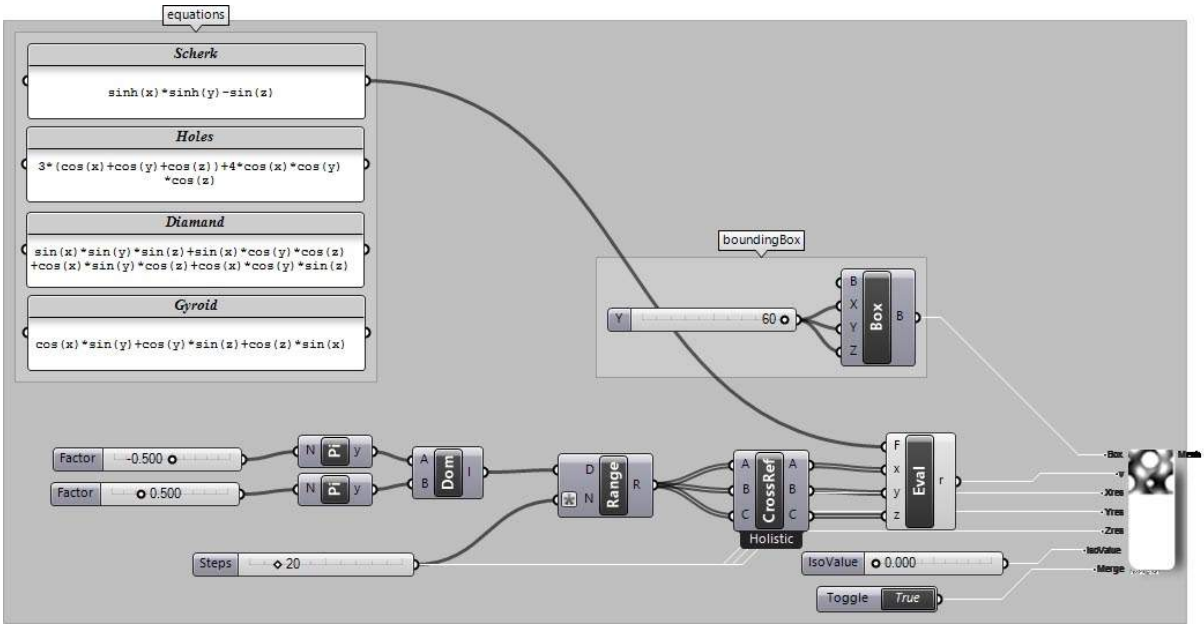

Figure 3.3. Minimal surface generation code by equation

Component Index and Parameters of the Definition

Panels used for texts of the equations of the minimal surfaces. Chosen minimal surface equations integrated into the file with panel components. They use the input value of the **Evaluation** components' **F** input.

Evaluate creates a list by placing the values assigned to the unknowns by **X**, **Y**, and **Z** inputs in the specified range in the equation.

The output of the **Evaluate** component, which is **R** (Result), connects with the **V** (Values) input of the **Iso Surface** component.
The output of the **Range** component converted into three separate lists with **Cross Reference** as **A**, **B,** and **C** and connected with the **X**, **Y,** and **Z** inputs of the **Evaluate** component.

To define the bounding box of the minimal surface **Domain Box** component used. A number slider connected to the **X**, **Y**, and **Z** inputs to specify the edge values of the box. The output of the **Domain Box** (B) connected with the **B** input of the **Iso Surface** component, which is in **Millipede**.

The range component used for placing the defined number of points with the **N** (Steps) input in equal intervals in specified limits. **Expression** of the **N** input needed to be changed as **x-1**. To specify the limits, **Domain** component used. **A** and **B** inputs of the **Domain** component specify the limits of the unknowns in the equation, for example -1.00*pi < x,y,z < 1.00*pi

The three-dimensional grid resolution defined with the **Xres**, **Yres,** and **Zres** inputs of the **Iso Surface. N** (Number) input of the **Range** component connected with the **Xres**, **Yres,** and **Zres** inputs for containing the minimal surface incorrect form to create the three-dimensional grid.

The minimal surface created by triangles and the resolution of them defined with **Iso Value** input of the **Iso Surface** by a slide.

Minimal Surface Variations in Grasshopper

Ex.1. Domain defined between -1 and 1;

- -1<x,y and z<1
- Contains in 30x30x30 cm^3 bounding box.
- The surface resolution is 20.
- IsoValue is 0.

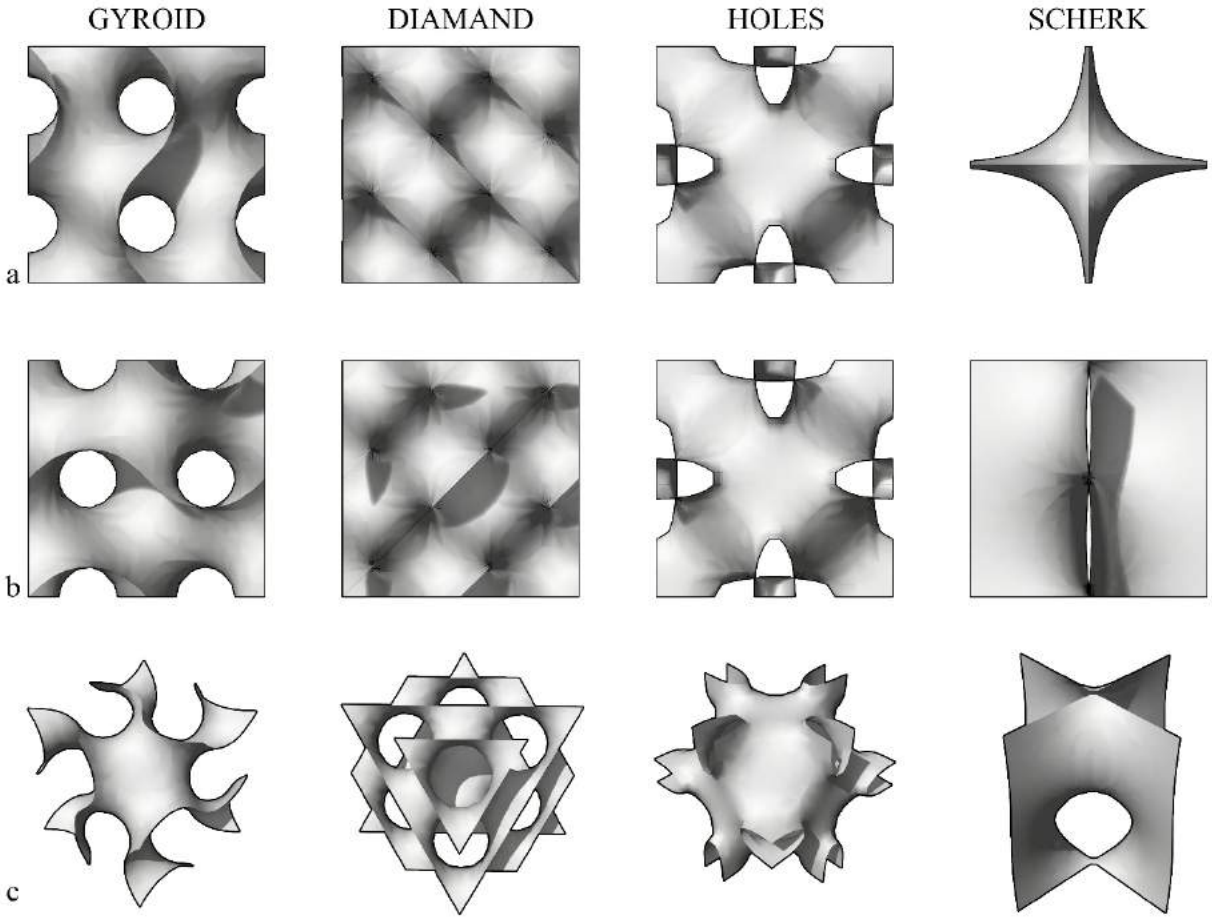

Figure 3.4. The outcome of the ex.1; generating minimal surface cubic unit cells in Grasshopper; **(a)** Top view **(b)** Front view **(c)** Perspective view

Ex.2. Domain defined between -0.5 and 0.5;

- $-0.5 < x,y \text{ and } z < 0.5$
- Contains in 30x30x30 cm^3 bounding box.
- The surface resolution is 50.
- IsoValue is 0.

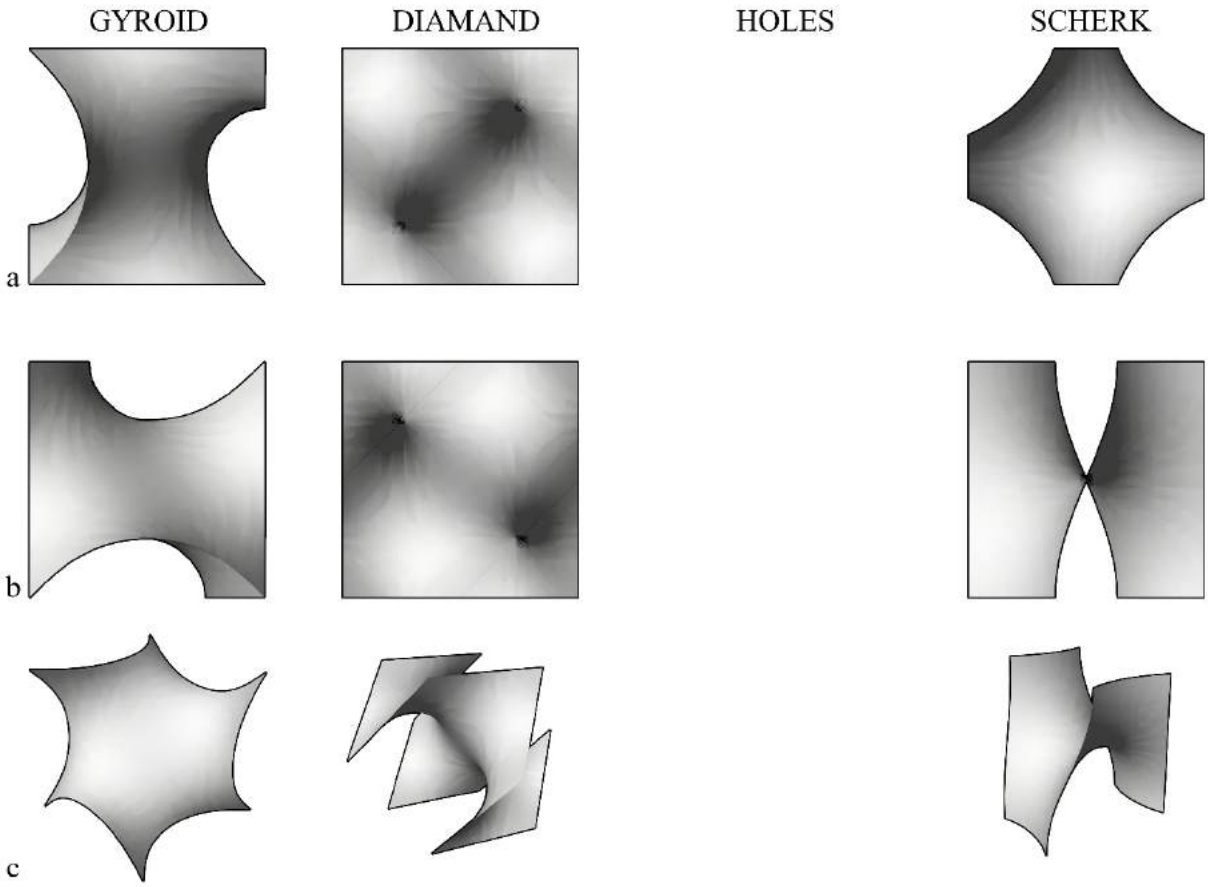

Figure 3.5. The outcome of the ex.2; generating minimal surface fundamental patches in Grasshopper; **(a)** Top view **(b)** Front view **(c)** Perspective view

Robot and Running System

The digital fabrication robots have tools that do the primary job, such as the laser beam part of the laser cutter or the tip of the three-dimensional printer that puts the material on the counter. The movement of those robots controlled with defining a movement path and the tool center of the robot follows the path that the designer arranged for fabrication. In laser cut, the product divided into sections and placed on a representative plane as lines, which are movement paths of the laser beam. The same logic works on the CNC with a mill and 3D printers with the tip that material flows. Fabrication with the three-dimensional printer, it is necessary to determine the path that the tip follow. However, the three-dimensional form to be produced should be

divided into sections that connected and become a loop/ spiral and production made by following this loop.

Industrial robots have the same logic in three-dimensional space. However, the tool attached to the end-effector of the robot arm can be changed according to work. Therefore, unlike other robots, there is no fixed center point. The center of each tool must be calibrated before production with the robot arm, and the movement line should be drawn according to the tool. The tool center point of the robot arm is called Tool Center Point (TCP). The movement route of the robotic arm determined by the points that TCP will go through, the operations it will perform at these points, and the movement between points. The line of action can be created by teaching and programming. The movements of the robot arm can be simulated in a computer environment with the plug-ins of the Rhino program, Grasshopper, and Robots. At the same time, the movement line created in this program can be translated into the language that the robot will run.

In the research to be conducted in this thesis, the movement route will be formed in Rhino software with Grasshopper plug-in and simulated by Robots add-on. Istanbul Bilgi University laboratory consists of a KUKA KR 20 industrial robot as a robotic fabrication system.

KR 20 model designed as 6-axis jointed-arm kinematic systems and lift 20kg payload. It has 6 axes, and end-effectors are attached to the sixth axis (A6) (Figure 3.6. (a)) (URL-26). Robotic arms can work in a spherical area. Reaching dimensions of the KUKA KR20 robotic arm shown in Figure 3.6. (b) and (c).

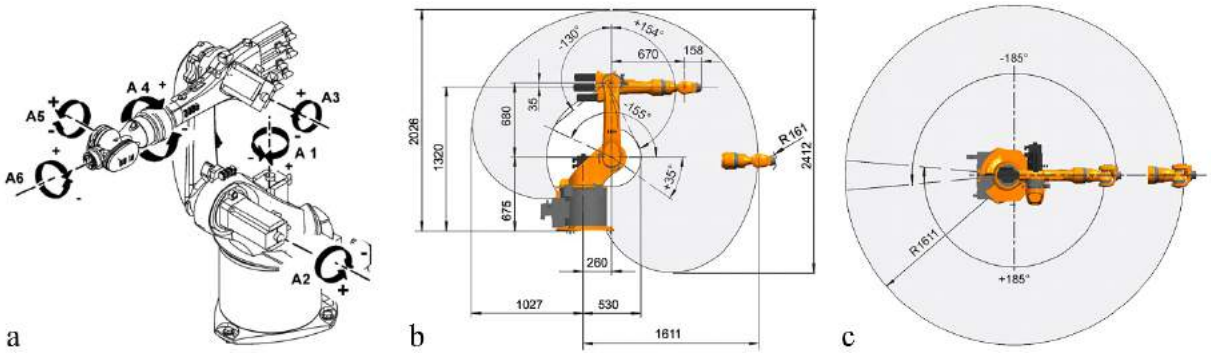

Figure 3.6. **(a)** The direction of rotation of the KUKA KR20 industrial robotic arm **(b)** Work envelope, side view. **(c)** Work envelop, top view. Dimensions are in mm (URL-28)

3.2. The Geometric Structure of Gyroid

The Gyroid is a TPMS that can extend infinitely without self-intersection. (Schoen, 1970) The Gyroid cubic unit cell has three subunits, and the smallest can form the other two. Each of these subunits is on different scales, and all three can be used for Gyroid production. A combination of two "fundamental regions" (Figure 3.7.d) creates a "fundamental patch" (Figure 3.7.c), and six fundamental patches combination create a "fundamental unit" (Figure 3.7.b). Eight fundamental units create a Gyroid cubic unit cell. The fundamental region of Gyroid is 1/96 of the cubic unit cell of it. (Gandy & Klinowski, 2000; Schoen, 1970) In this research, the expected outcome of the case study is understanding the generating logic of a Gyroid composition called "unit cell" (Figure 3.7.a) and variation of it.

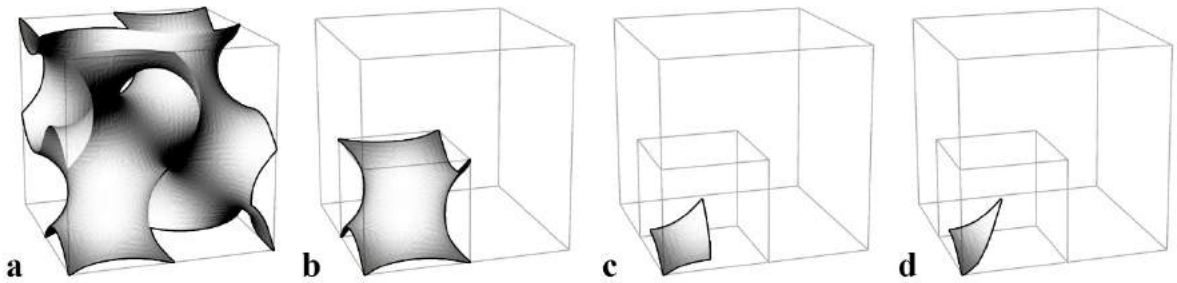

Figure 3.7. (a) The cubic unit cell of the Gyroid surface. (b) The fundamental unit. (c) The fundamental patch (d) The fundamental region

Triply periodic minimal surfaces generally have symmetry axes as their three-dimensional extending system. According to Schoen, Gyroid does not contain linear and planar symmetry axes. It does not have mirror reflections either. (Schoen, 1970) Some rotation sequences that generate the Gyroid surface. However, because of its geometry, after the rotation, several units become mirror reflections of each other.

The cubical unit cell of Gyroid can be obtained by four different rotations of the fundamental unit. If one of the rotated fundamental surfaces selected as the reference surface, the other three needs to rotate three different axes and angles. Rotating the fundamental surfaces can be complicated. Therefore, a three-directional line system added to the fundamental unit for

navigating the rotating units. With a three-directional line system, positions, rotating angles, and axes are better understandable.

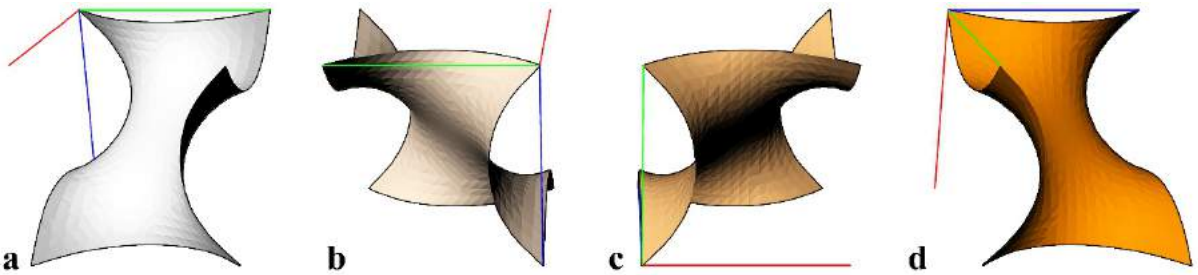

Figure 3.8. Rotations of the fundamental units in the Gyroid cubic unit cell. (a) The reference fundamental surface for rotating; G. (b) G1 (c) G2 (d) G3

There is no strict evolution system for creating a Gyroid surface. In this research, these four rotated fundamental surfaces used for the evolution of the Gyroid cubic unit cell. They also can be used for three-dimensional extrusion.

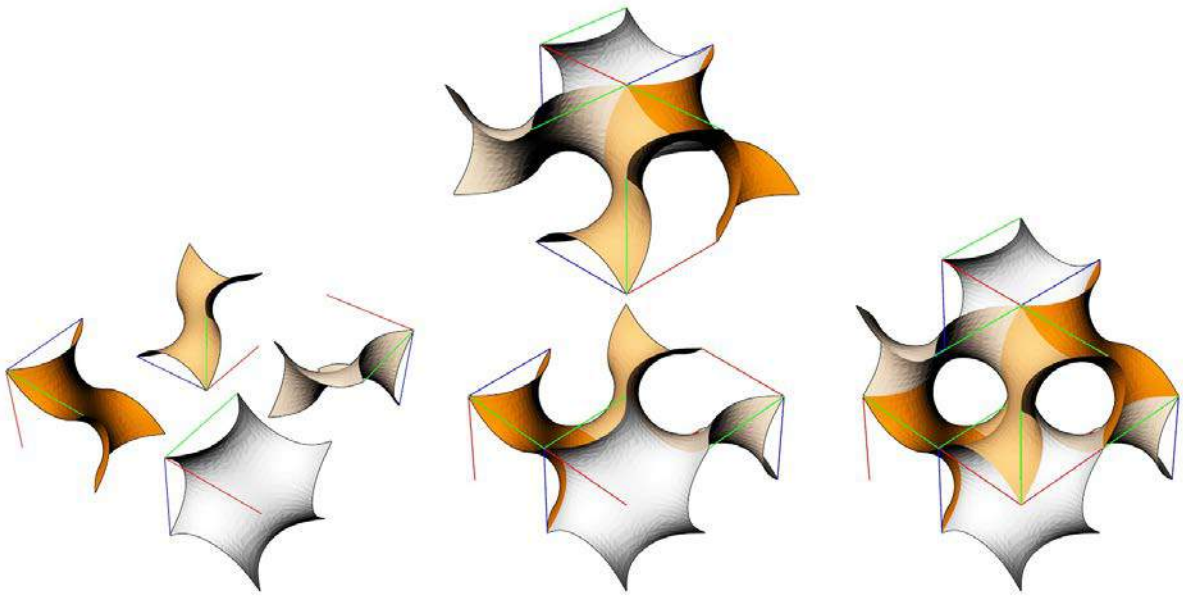

Figure 3.9. Evolution of the Gyroid cubic unit cell

TPMS split their boundary volume into several spaces generally called “labyrinths”. The Gyroid cubic unit cell has two independent, non-intersecting labyrinths, which are mirror-symmetric to

each other. (Schoen, 1970) The volumetric module in this research is created from the Gyroid cubic unit cell surface to split the solid bounding box into two systems.

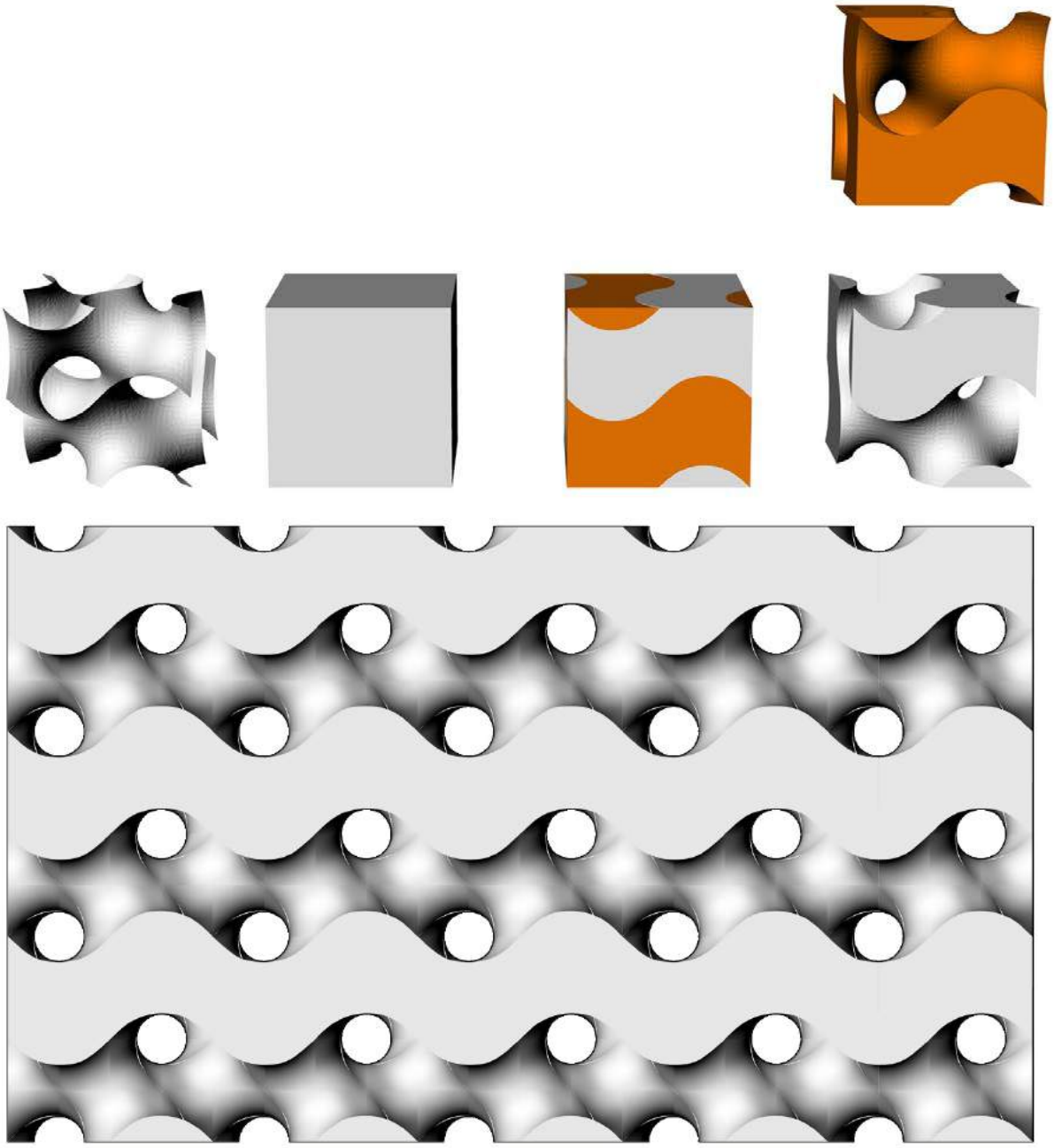

Figure 3.10. Splitting a cube with the cubic unit cell surface of the Gyroid and generating a wall

3.3. Parameters of the Cutting Wire

Form to be Cut

Gyroid can be generated in various ways, as mentioned above. In order to cut the Gyroid with a straight wire, multiple carving movements are required. In the case study, the unit intended to be cut with a single cutting motion. Fabricating Gyroid fundamental unit is not seem possible without carving. Because of two fundamental regions creates a fundamental unit, fabricating a fundamental region would be repeating the same movement twice. Therefore it is decided to fabricate the fundamental unit of the Gyroid.

Wire Form

If a straight wire used for cutting, as shown in (Figure 3.11), the cutting route followed by lines not touching the surface of the unit to be cut. Since it is not possible to cut with straight wire in one movement, cutting with curved wire is considered. It predicted that the curve which will form the hotwire cutter should be the Gyroid fundamental curve.

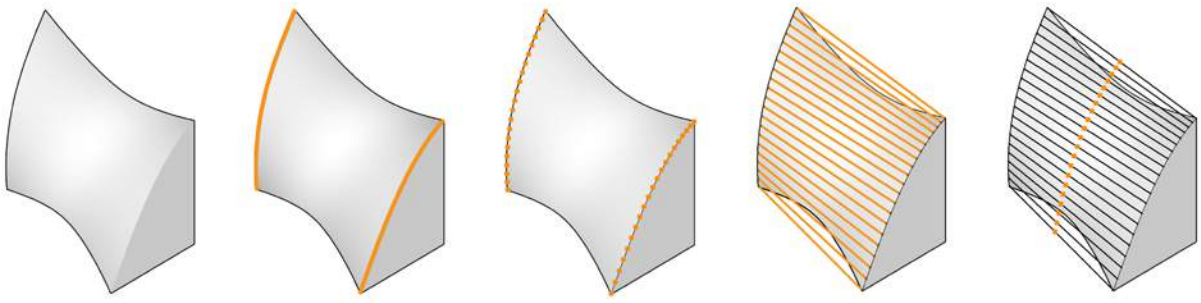

Figure 3.11. Motion path generation of the Gyroid surface fabrication with straight wire

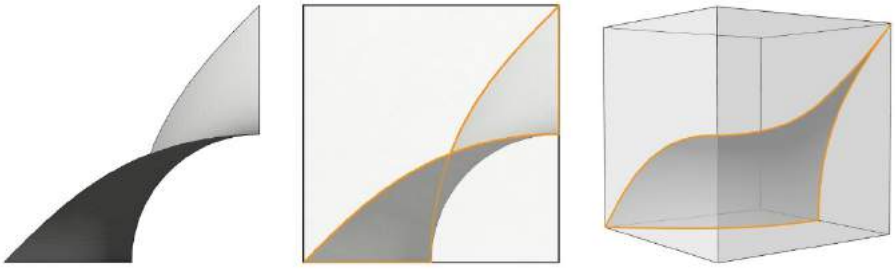

Figure 3.12. Edge curves of the Gyroid fundamental patch

Each edge of the Gyroid patch is the same curve in different positions as a curve, a mirror of the curve, and rotation of them. Preparing a wire with a fundamental curve and mirror of it is necessary to fabricate Gyroid.

Figure 3.13. Wire form

Figure 3.14. The active section of the wire moves from point 1 to point 2

The active cut section of the wire changes at every moment of movement. The active cut section starts at between the starting point and the middle point of the wire and proceeds through the central point and the endpoint of the wire.

In case of attaching the hotwire cutting tool to the robot arm, the center of the active cutting section should be defined as TCP. However, the active cutting section of the wire needs to be changed during the cut. In other words, the active section of the wire should be uncertain; therefore, the center and length of the active section on the wire constantly change. Two

different cutting methods can be followed in the scenario of attaching the hotwire cutter tool to the robotic arm. The first is to make TCP moveable during the cut. It would be hard to control, not precise, and complicated, but it is not impossible to do. The second is to fix TCP to the center of the wire and control the movement with reference points outside the material. That is to say, in the simulation prepared for the cut, the movement path of the TCP must extend beyond the EPS block. Since it is not possible to see the product in the simulation in rhino and grasshopper programs in this stage, it thought that it might confuse the definition.

Apart from attaching the hotwire tool to the robotic arm, creating a tool for attaching the EPS block to the robot. TCP can be defined as a fixed point if the material is attached to the robot in this scenario. By controlling the movement of the robot, it is possible to change the active cutting part of the wire, which would be fixed on the ground. In this case, the movement of the TCP can be ignored. It sufficient that the TCP is correctly identified on the surface of the material and that the path of the material designed according to the reference points to be placed around the wire. Because of these reasons, it decided to attach the EPS block to the robotic arm.

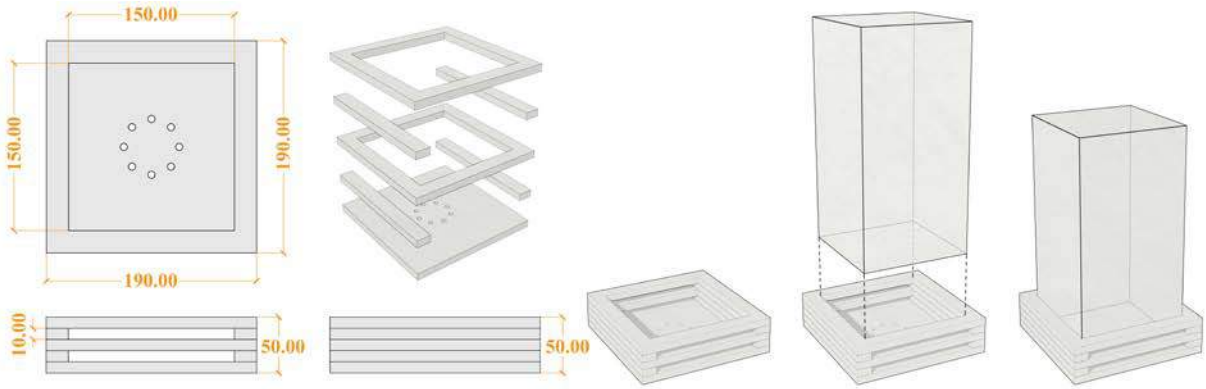

Figure 3.15. EPS holding tool dimensions in mm

The tool designed to attach the foam to the robotic arm. The foam and the unit holding the foam defined as a tool in the Grasshopper file. In this way, TCP can be defined at every point of the foam and changed as desired.

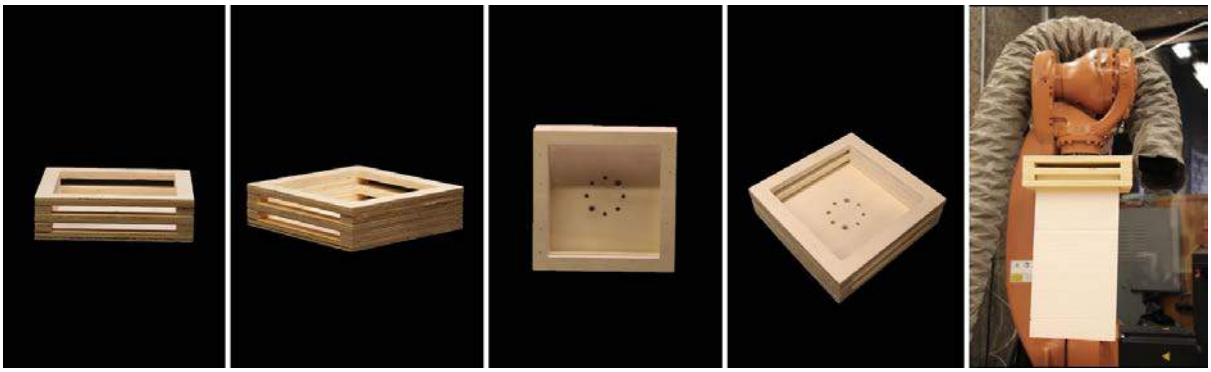

Figure 3.16. EPS holding tool attached to the robot

The Size of the Unit

The Foam units will be produced by cutting 60 cubes. The distance between the start and endpoints of the wire to be cut must be twice the length of the edge of the unit cube to which the fundamental unit is to be cut. When the distance increases, the deformation rate of the wire increases. Considering the cube size and the length of the wire, fabricating the fundamental unit from a 15 cm cube was decided. In this way, the entire 60 cubic styrofoam cube can be used, and there will be no remaining material. Every 15 cubes will be cut to fabricate a fundamental unit and a mirror. In this case, if the cuts made correctly, it is possible to cut 64 Gyroid fundamental units and 64 mirror units from the cube of 60.
The Gyroid fundamental unit fits into the 15-cube. Cutting with 15 cubes can damage the tool or wire attached to the robot. Therefore, the foam units will be cut and used in size 30x15x15.

Correct positioning of the base is essential for cutting 60cm cubes of EPS. The slope of the surface on which the 60cm cubes will be placed must be known in the code to be written for each unit to be the same dimensions.

Units were consisting of prisms of 15x15x30 cm^3 cut from cubes of 60x60x60 cm^3. 32 units obtained by cutting the cube to the specified dimensions.

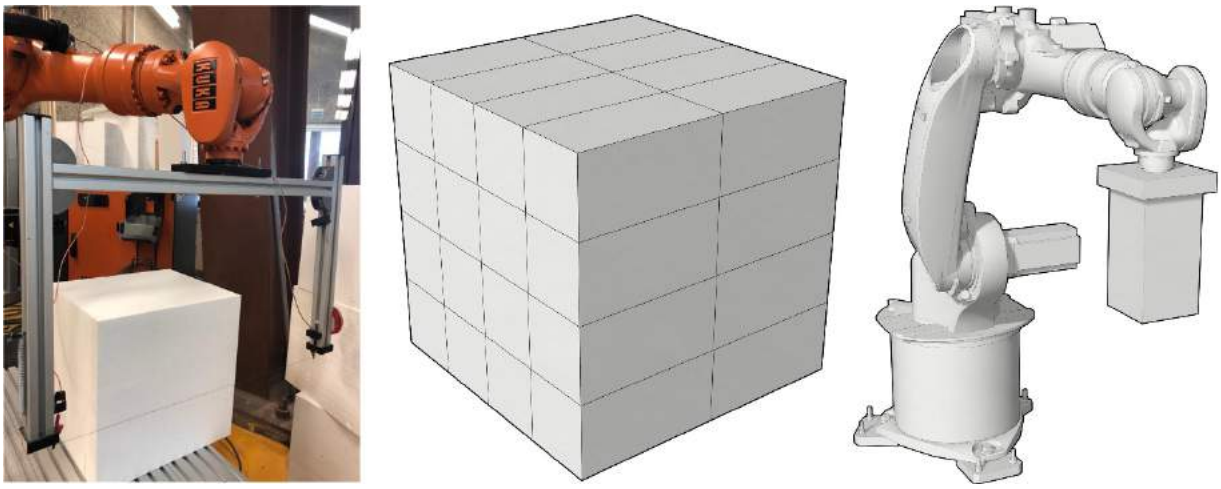

Figure 3.17. EPS unit blocks

The dimensions of the units are a few mm less than 15x15x30 due to the melting of the foam while cutting with the hot wire cutter.

3.4. Initial Tests of Robotic Hot-wire Cutting

Before cutting Gyroid with the robotic arm, several wire and material experiments have been made. The experiments prepared to decide the density of the EPS foam, the thickness of the wire, and the value of the power supply for heating the wire.
EPS foam will be used as a material. The foam will be cut in the form of the fundamental unit by the curved hot wire by melting. Because of the heat and the thickness of the wire, there will be a melting range. EPS foam should be in the ideal density to minimize the melting range.

Wire thickness is an important parameter for cutting. It needs to be in the ideal thickness for the melting range, steady, and heating. The EPS foam is going to be cut by the wire, which is heated by current electricity. The wire should be shaped in the Gyroid fundamental curve while cutting and not deform while heating and cutting the EPS foam.

For thickness and density experiments, a simple mechanism set up. In the first place, the thickness of two-wire and two EPS densities tested manually. After deciding wire and material,

speed and heat experiments have been done with the industrial robotic arm. The power supply used for the mechanisms is the one available in the fabrication laboratory, which has values of 30 Volts and 10 Amps maximum.

The thickness and Density Experiments

Two different types of wires and EPS foams tested in this phase. For the wire, a non-magnetic alloy of nickel and chrome, which called Nichrome wire, used in different thicknesses as 2 mm and 0,9 mm. Nichrome wire has a high resistance to oxidation at high temperatures.

The mechanism set up for the experiments, made by a woodblock and wire. The cutting wire is 36 cm long and 2 mm thick. When the 2 mm thick nickel-chrome resistance wire is attached power supply, the power supply's power is 12.7 V 10.1A at maximum. In the first test with 2mm diameter Nickel-Chrome wire, two foams with different densities cut. The cutting speeds of the foams, the resistance to the wire, and the melting rate of the material are different for different EPS witch have different densities.

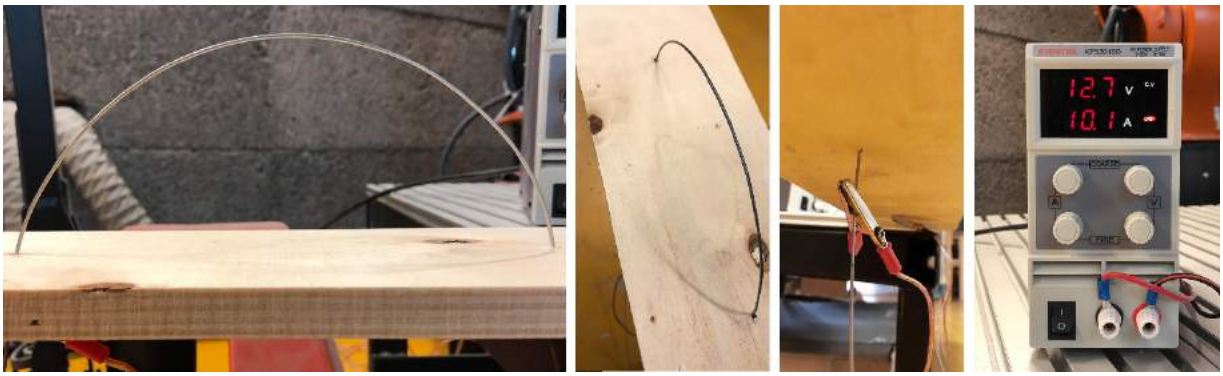

Figure 3.18. Experiment tool for wire and power supply

For the EPS foam, two different foam used in different densities which are 20 kg/m^3 and 13 kg/m^3. Between them, particles of the low-density foam are bigger and easy to cut by hand. High-density foam is heavier than low-density foam, yet, it has more resistance to pressure. The melting thickness of the low-density foam was recorded 2 mm more than high-density foam as

5mm to 3 mm. In addition to that, the fumes exiting by melting with the heated cut is observed more with low-density foam. Therefore, it decided to use more dense EPS foams for fabrication.

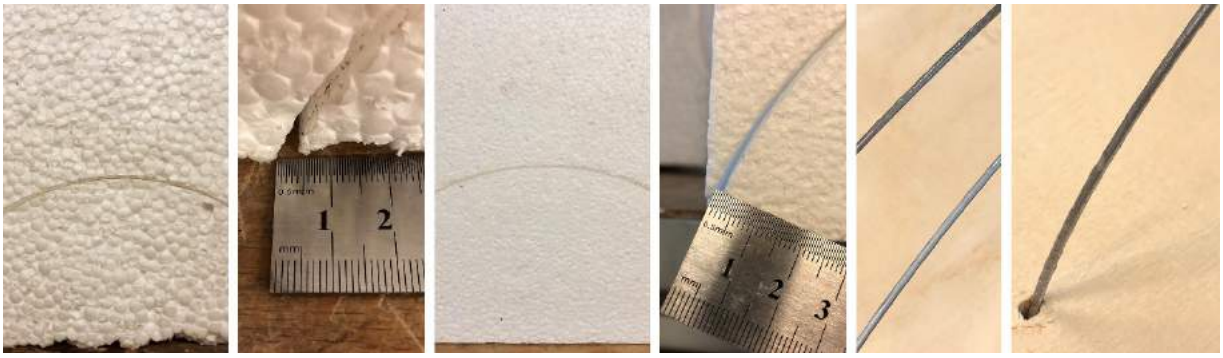

Figure 3.19. Wire and EPS density experiment

The foam melted during cutting remains on the wire as a layer (Figure 3.19). After a few cuts, the thickening layer can lead to sensitivity problems with the wire. In order to reduce the melting rate of the foam in the cutting, it necessary to increase the cutting speed or reduce the heat at a constant speed. It projected that increasing the speed in the section where the form of the wire remains intact will damage the wire. For this reason, it will be more accurate to increase the temperature for cutting with 2 mm thick wire. In order to increase the temperature of the wire, a high power supply required. However, the increase in heat is also a factor that will increase the melting rate of the foam. Increasing the melting rate may prevent the final product from being fabricated correctly.

0.9 mm thick Nichrome wire can be used for cutting with less melting. It observed that the thinner wire compared to the previous test did not deform during cutting but bent according to the speed of movement of the material. The correct speed and heat ratio must be defined in order to complete the cut without deformation.

Speed and Heat Experiments

Another hot-wire cutter tool made for speed and heat experiments with the industrial robotic arm. After the tool set up, the new hot-wire cutting tool model made in the Rhino file for creating

the movement path in grasshopper. The material was attached to the robot arm for cutting speed tests.

Figure 3.20. Experiment tool for speed and heat

For this experiment, support units prepared to stay fixed on the table placed in front of the robot to hold the wire. The supports are round 2 cm thick wooden bars. The wire placed in the holes drilled in the centers of the rods bends 5 cm higher than the centers to form a Gyroid curve. For heating the wire, the conductors of the power supply connected to both sides of the 2 mm thick wire.

The length of the wire is one of the parameters of the heating speed and deforming against externally applied forces. Since the fundamental patch intended to be cut from 15 cm cubes, the projection of the wire should be 30 cm. If 5 cm units wanted to be cut, the projection length of the wire would be 10 cm.

Figure 3.21. First experiment and result

Wire heating problems occurred in the cutting experiments. The 10 A power of the power supply was not sufficient for the 2mm thick wire to heat up quickly. Due to the force applied by the foam block moving through the wire, the wire is deformed, and the foam removed from the tool after it has been damaged. To reach the desired heat, 2mm thick and 36 cm long wire, a new power supply with higher amperes needed. With the stronger power supply, the 2mm thick wire can be heated more, and the EPS can melt on the wire without applying force. If 2mm thick wire used in the tool, which arranged to melt the styrofoam quickly, the melting rate will be quite high.

For 0.9 mm thick wire experiments, the rearrangement made. The wire with a smaller radius will heat up more and faster with the available power supply. Thus, the styrofoam will melt without applying force to the wire, and the deformation problem of the wire will be eliminated. In the cut made with 0.9mm thick wire, it observed that the styrofoam melting range is about 2 mm.

When speed defined 100 in Grasshopper, it observed to running robot arm in 10% and 30% speed more suitable for cutting tests. In order to run the robot at 100% speed, the speed in the grasshopper file must be defined as 30%.

Tests performed with two different powers as 8.40 A and 10.1 A, and it found that 8.40A were sufficient for cutting. If the speed increased, the power will also have to be increased. It decided to use 0.9 mm thick Nichrome wire for heating with a 10A power supply.

3.5. Robot Setup and Tools

Shape Memory Wire

The main challenge to cut double-curved surfaces is to have a heated cutting wire that is adequately formed and stabilized in place. In the initial cutting tests, thick nickel-chrome (NiCr) wires proved not useful in heating and cutting EPS. Therefore thin shape-memory wires became

an alternative solution. In this research, the initial wire tests held with three different wires. Two of them are nickel-chrome (NiCr) wires with 0.9mm. and 1.2mm. thicknesses. NiCr is the standard cutting wire used in industrial and hobby foam cutting practices. Because of the stability issues mentioned above, a shape memory wire with 1 mm thickness is also tested and proved to be useful.

Shape Memory Alloys, also known as SMAs, can memorize a shape and retain it by activating factors like heat or electricity. (Jani, Leary, Subic, & Gibson, 2014) Nitinol wire is an alloy metal wire which belongs to a class of shape memory alloy.

The shape training based on the transition between the high-temperature austenite phase and the low-temperature martensite phase. The phase change causes shape and dimension variance in the material. Nitinol wire can both re-shape and train by heating with an outside source or by electrical current. (Dönmez, Özkan, & Kadıoğlu, 2010) The wire should be stable in the desired shape for training. After fixing the form, it needs to be heated for a while and put into the cold water immediately because of the quick phase change. After training, the wire would memory the shape of the mold. When it gets heated, the wire will go back to the trained form.

Figure 3.22. The first try of the Nitinol wire training

For research, a mold made in the shape of the wire should be while cutting, which is two mirrored fundamental curves that connected to each other. The first try of training the Nitinol wire made with a flame gun. Wire fixed in the mold and heated with the flame gun. However, the flame gun heat was not enough for the wire to be trained (Figure 3.22). The second try made with a ceramic oven, which can heat 3000 degrees. Mold with the wire put into the oven and heated gradually 510 degrees in one and a half hours and stayed in 510 degrees for half an hour. After the heating phase, mold put into the cold water (Figure 3.24). Wire re-heated with electric current for cut (Figure 3.25).

Figure 3.23. The second try of the Nitinol wire training

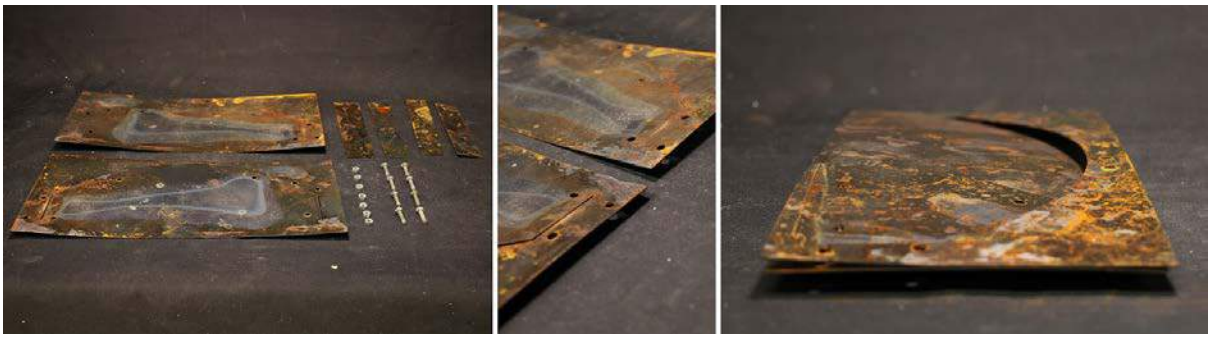

Figure 3.24. Nitinol wire mold pieces

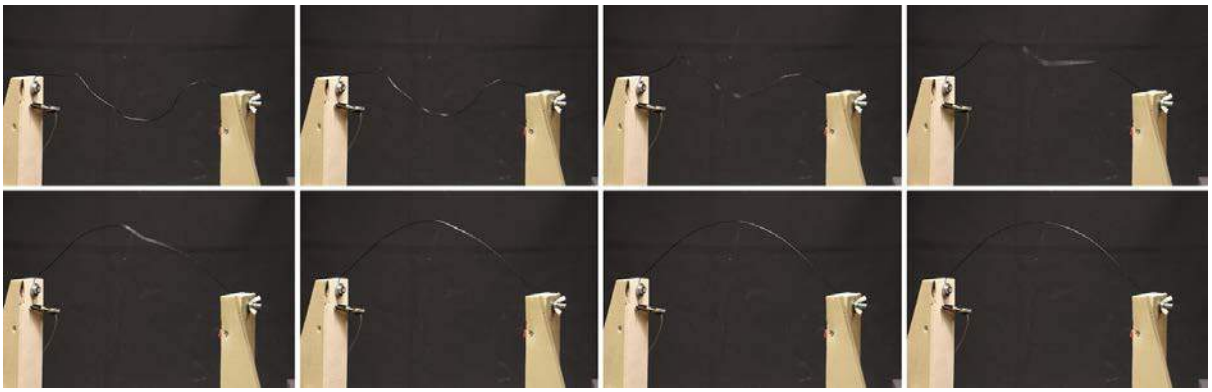

Figure 3.25. Re-heating the Nitinol wire with the electric current after deformation

The Hot-wire Cutter Tool Frame

After the speed, heat, thickness, and density test, it observed that the tool with 2 cm thick wooden supports are not structural enough for keeping the wire stable. That is why more structural tool frames made for the case study. The new hotwire cutter tool will be fixed on the table in front of the robotic arm, which is available in the fabrication laboratory.

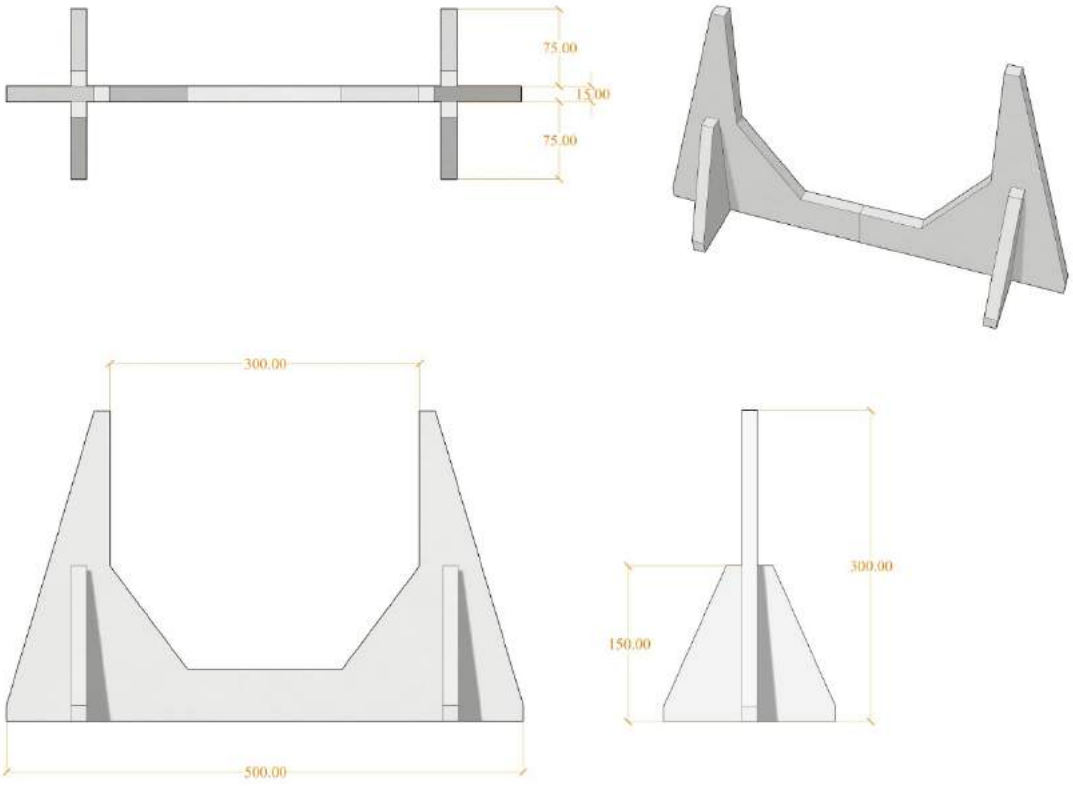

Figure 3.26. Hot-wire cutter tool frame dimensions

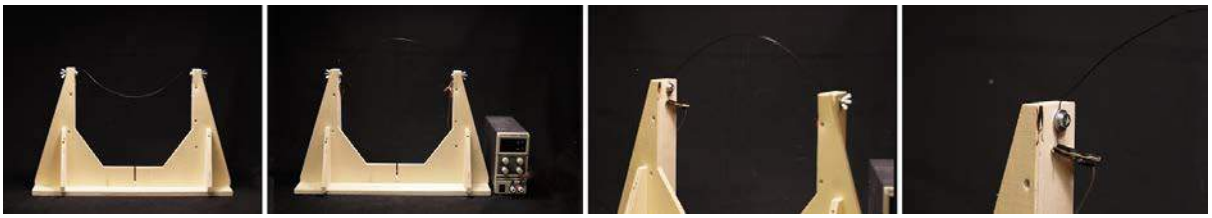

Figure 3.27. Hotwire cutter tool frame and power supply

Base and Tool Calibration

Tool

The tool designed for cutting needs to be modeled in exact dimensions and position in order to create the movement path correctly in grasshopper. In this way, it aimed to minimize the errors that may occur by transferring information from the physical environment to the digital environment. The physical model's information needed to be translated into the digital model for producing a more precise hot-wire cutter tool. The coordinate information of the corner points of the base can be learned with the robotic arm by the actual position information. For spotting the coordinates with actual position information, the pointer tool must be attached to the robotic arm. The coordinates of the points where the wire placed spotted with the pointer tool and actual position information in the robotic arms smart Pad.

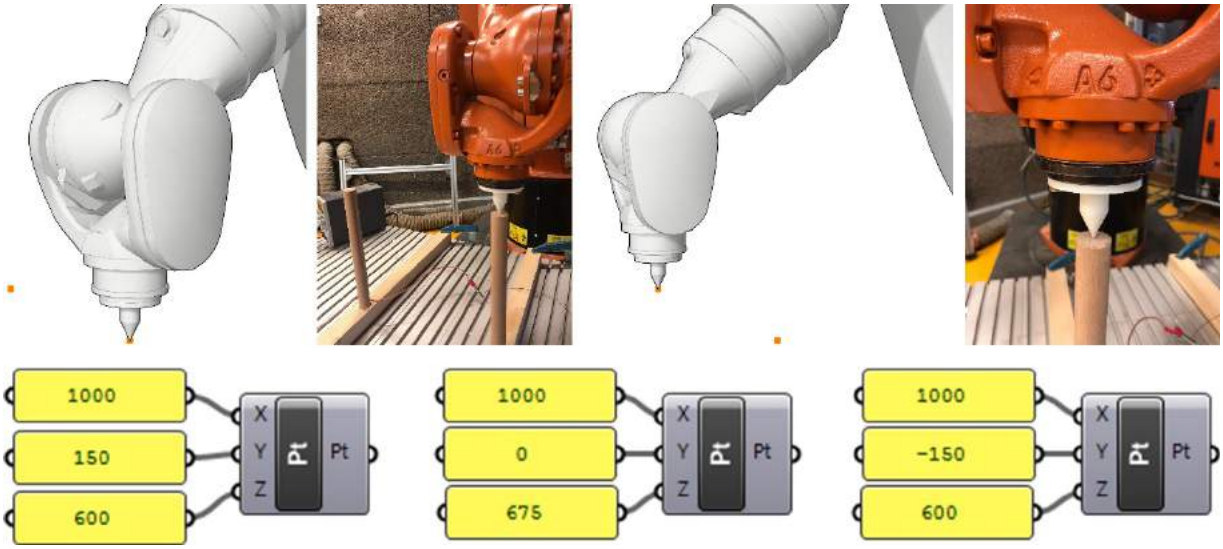

Figure 3.28. TCP position information for tool calibration

The hot wire cutter tool modeled in the grasshopper file with the coordination data. With this information, the physical model of the tool placed in a more precise position.

Base

The ground of the fabrication lab may not be flat. Therefore, coordinate information of the base that the hot-wire cutter tool be fixed needed for physical and digital information to be the same. The industrial robotic arm will also be used to cut the EPS units evenly. It important for the units to be at the same sizes as each other for the Gyroid form that they will create together would be seamless and accurate. The inclination of the base, which the wire to be fixed on it, causes problems in the cutting of the units.

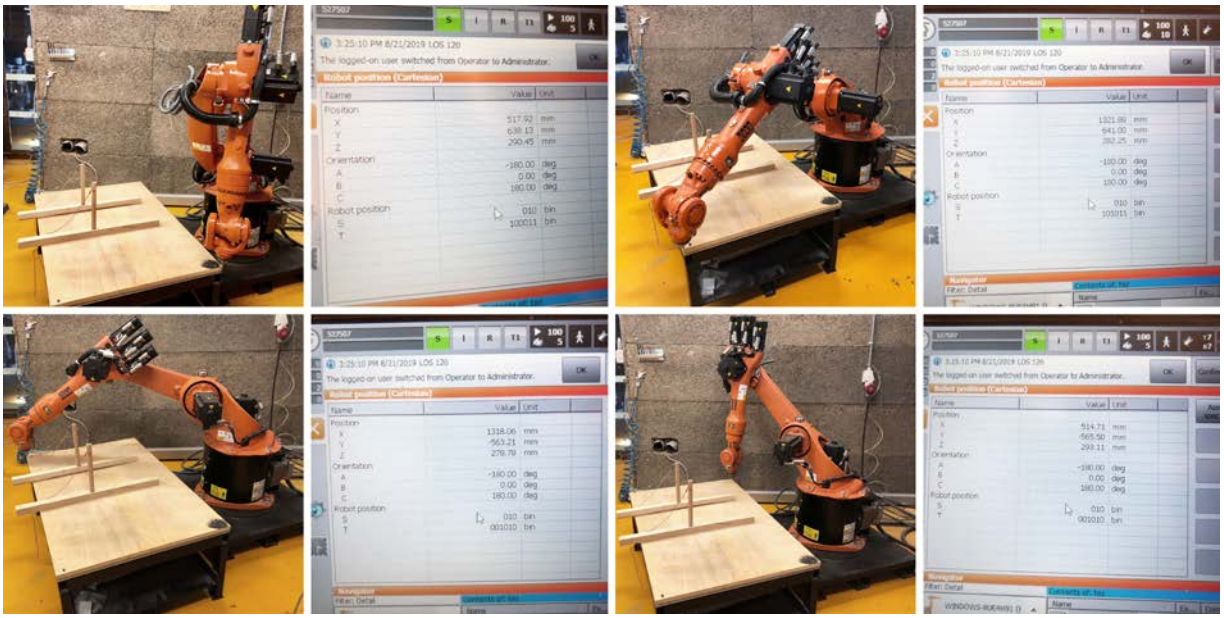

Figure 3.29. The base recreated in Rhino with the coordinate information

Programming the Movement Path in Grasshopper

There are some predictions about how cutting should be done before start. It decided to cut the fundamental patch with the curved wire. The front and back edges of the fundamental unit

mirrored, and 90 degrees rotated curves of each other. That is why the wire's shape is going to be the connection of the fundamental curve and the mirror of it.

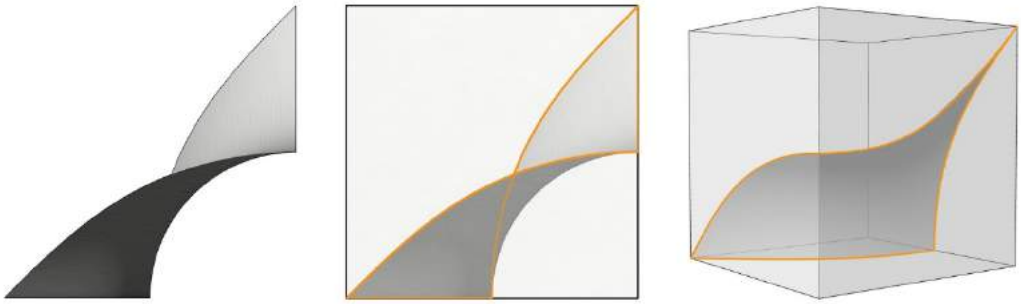

Figure 3.30. Gyroid fundamental patch edge geometries

Because the first half of the wire is the mirror of the second half, the front and back curves of the Gyroid can be cut into the correct form. In the first movement of the cutting, the first half of the wire should be the active cutting area. Furthermore, for the last movement, the second half of the wire should be the active cutting area. There should also be a 90-degree difference between the first and last movements. Therefore, it considered that there should be a 90-degree angle difference between the first and the last movement of the robotic arm movement path, which going to be defined in grasshopper.

4. ROBOTIC FABRICATION EXPERIMENTS

4.1. The General Strategy of the Experiments

In order to control the movement of the foam, references needed for placing the planes that TCP will travel. The reference curves were created by copying the wire to the front and back of the existing wire as much as the edge length of the unit. In this way, it is contemplated that reference curves can determine the position of the unit in front of and behind the wire. For this tool and fabrication system, the length decided as 15 cm. The motion route would be arranged between these two reference curves.

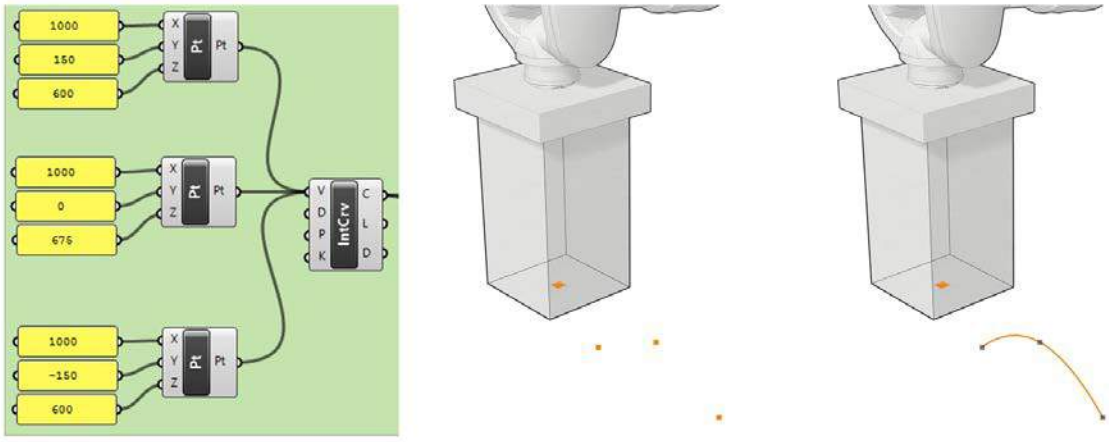

Figure 4.1. Generation of the wire representation

The start and end of the wire have 30 cm between and the midpoint 7,5 cm above from the projection of the wire. Three main points of the wire, which are the start, center, and endpoints, positions used for calibration coordinates of the hotwire cutter tool. A curve is drawn with three calibration coordinates for the representation of the wire in the simulation with the **Interpolate Curve** component (Figure 4.1).

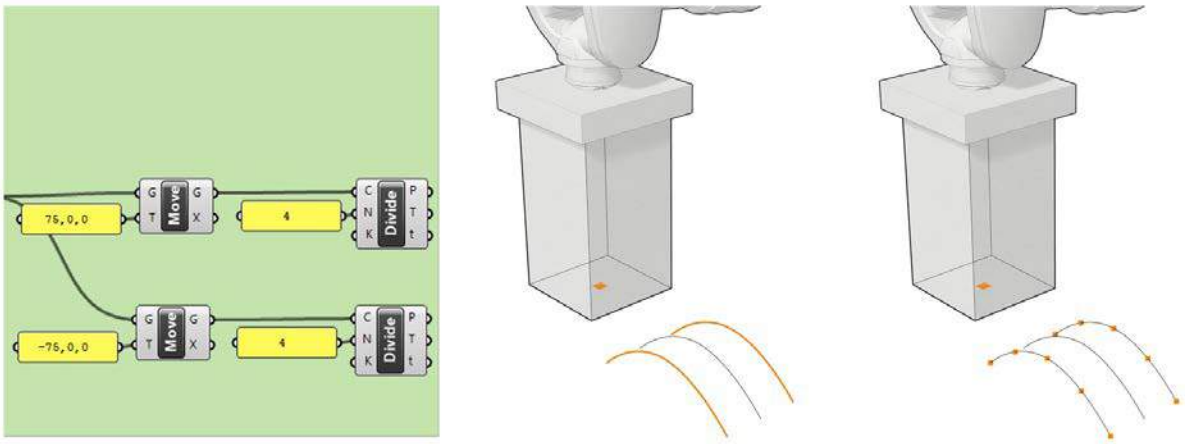

Figure 4.2. Generation of the references

The reference curves required for the controlled movement of the TCP copied at a distance of 7.5 cm front and back of the representative wire. The distance between the two reference points is the distance of one edge of the bounding box of the Gyroid to be produced, which is 15 cm in this research. The hotwire cutter located in the middle of the reference curves (Figure 4.2).

Hotwire cutter can damage the EPS block if the first movement of the cut is on the reference curve. Therefore, new points generated as the start and end points of the movement path, which are 5 cm away from the first and last movement points so that the wire does not damage the foam.

4.2. Experiment #1: Point-to-Point Motion Path

Since the center of the active section of the wire must be shifted during the cut, the first movement of the first experiment defined in the center of the first half of the curve. The first plane placed on 1/4 of the reference curve on the front and the last plane of the movement situated on 3/4 of the other reference curve. The first experiment made with two planes defined at these two points. The first and last plane is placed tangential to the wire in order to make the rotational movement, and two planes are the mirror of each other (Figure 4.3, Figure 4.4).

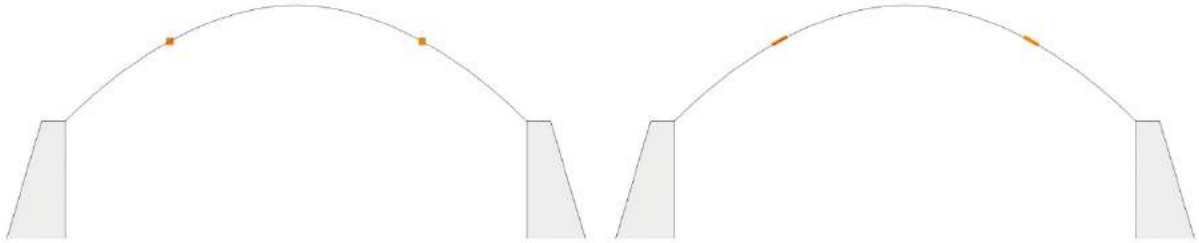

Figure 4.3. Plane positions on the references

Robot movement between defined planes has different types like linear and point-to-point. Linear motion, allows the robot to move linearly between two points. The point-to-point movement provides the most comfortable movement of the robot between two points. In this experiment, the movement path coded as point-to-point move.

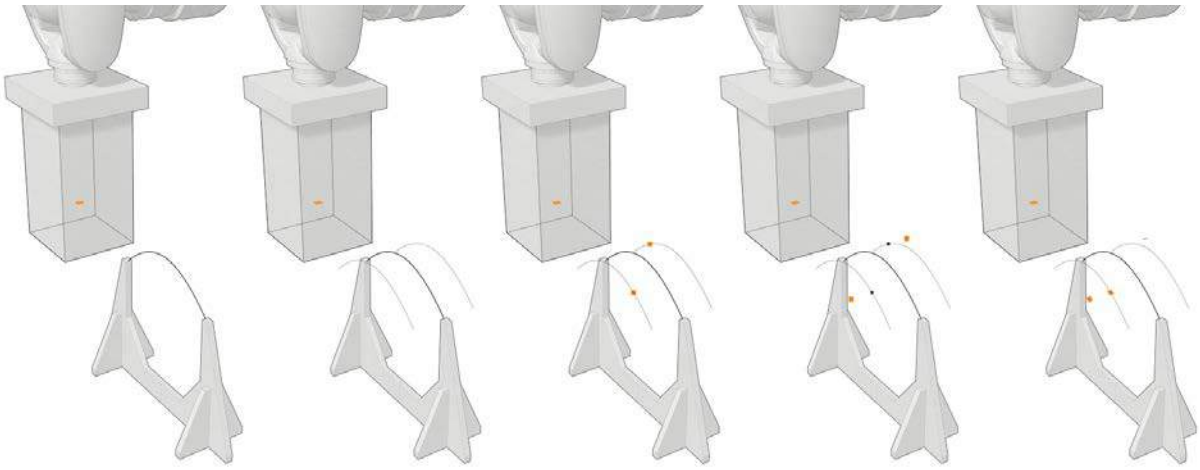

Figure 4.4. Generation of the experiment#1 motion path

TCP located 22,5 cm below from the EPS holder tool and on the center axes, which is 7,5 cm offset from the edges. This distance is equal to the distance between the reference curve and the wire. In this way, when the TCP reaches the reference point, the foam will touch the wire (Figure 4.5).

Figure 4.5. TCP position of the experiment#1. Dimensions are in mm

Cutting

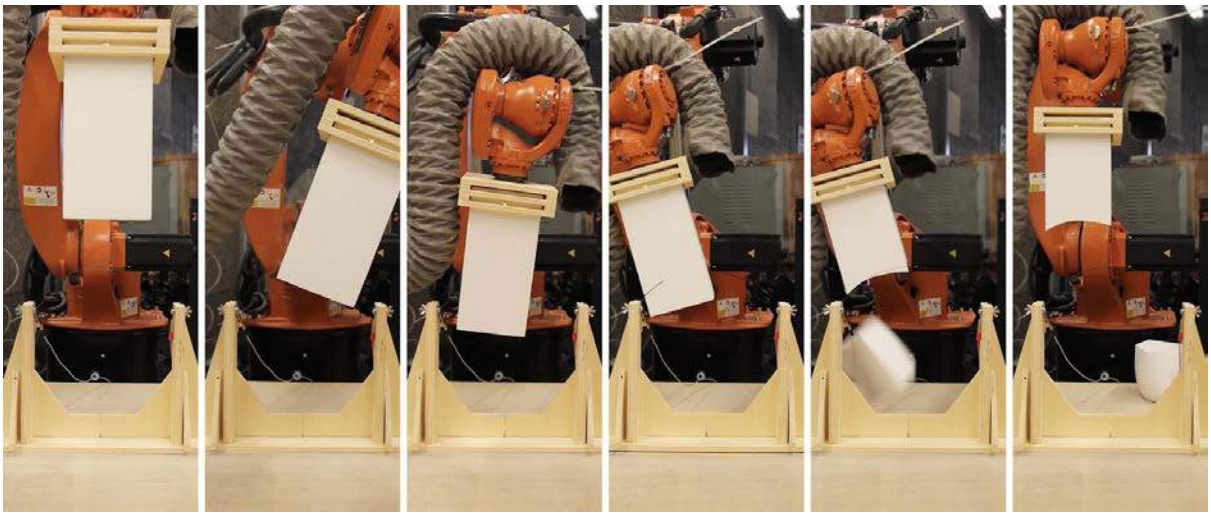

Figure 4.7. Cutting photos of the experiment#1

Definition

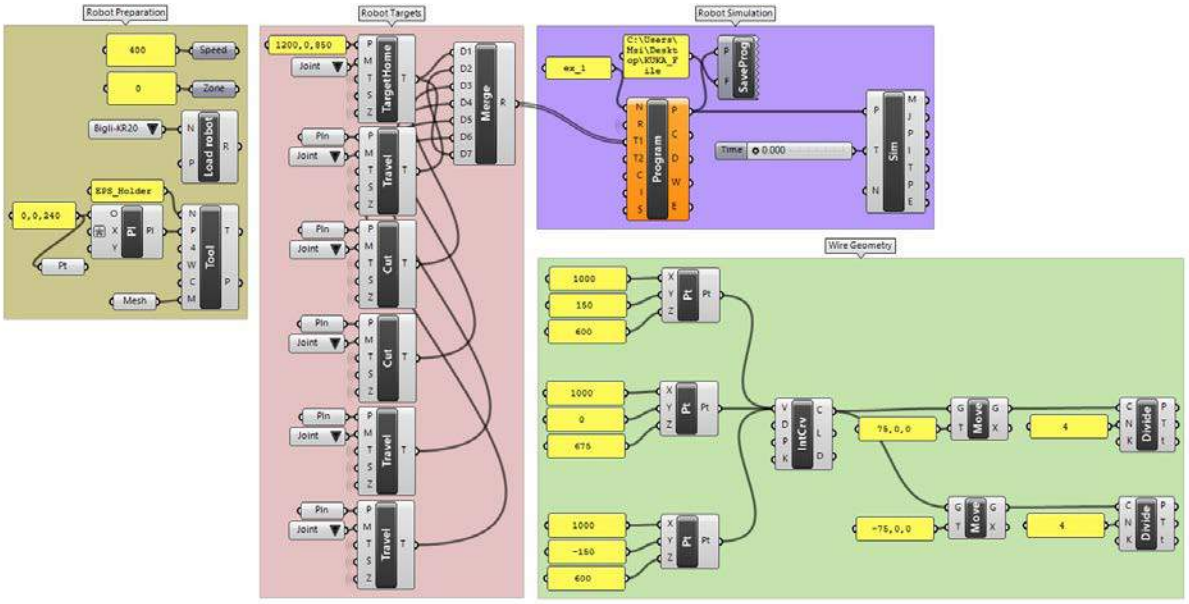

Figure 4.6. Grasshopper definition of the experiment#1

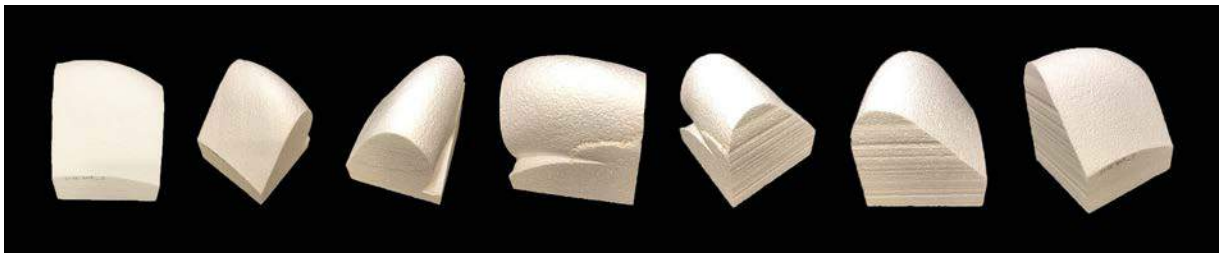

Figure 4.8. Cut geometry of the experiment#1

Outcomes of the Experiment#1

The cut form was not even close to the Gyroid patch geometry. It thought that the positions of the planes are correct. However, tangentially oriented, the planes cause incorrect resold for 90-degree rotation. In order for the foam to be cut in the form of Gyroid fundamental curves, in the first movement, one side of the foam needs to be parallel to the projection of the wire and rotate exactly 90-degree.

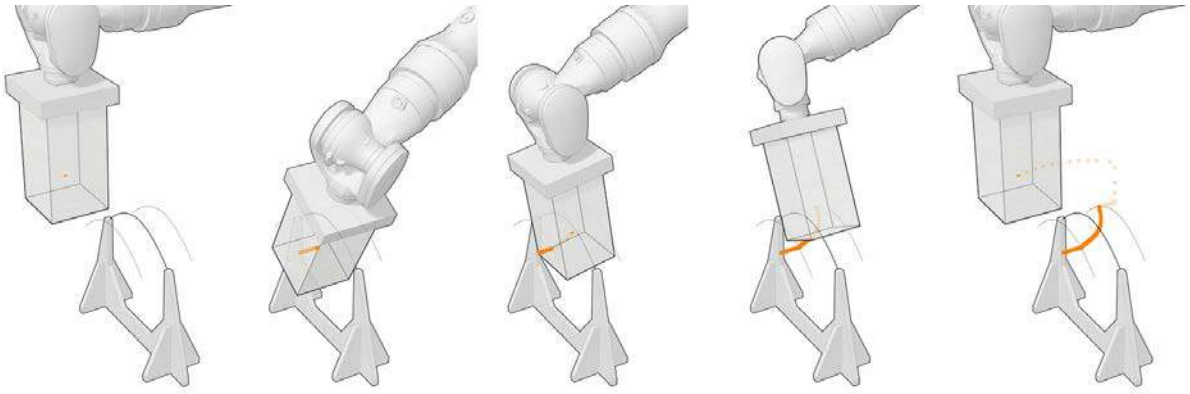

Figure 4.9. Point-to-point movement path of the experiment#1

The movement between the two planes followed a path that does not intersect with the center point of the wire. The motion path must pass through the center of the wire (Figure 4.9, Figure 4.10). The fact that the path generated with two points may be the reason for the incorrect cut. Does increasing the number of points at which the path defined could be the reason for accurate cutting?

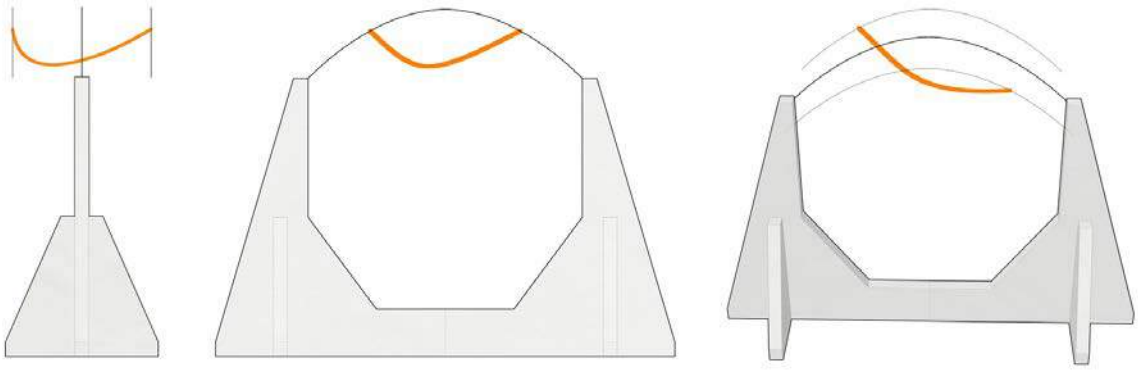

Figure 4.10. Point-to-point movement path of the experiment#1

4.3. Experiment #2: Linear Motion Path

In this experiment, problems like the diagonal movement of the cutting route and the 90-degree rotation of the foam block during cut tried to solved without error. The defined motion path is diagonal like in the previous experiment and formed by a curve that starts and ends at the same two reference points and passes the center of the wire. Curve divided equally, and planes placed on those points with rotating 90-degree slightly from the beginning through the end (Figure 4.11). Therefore, the Gyroid curves cut on the surfaces where the wire touches the foam first and last will be in the correct position.

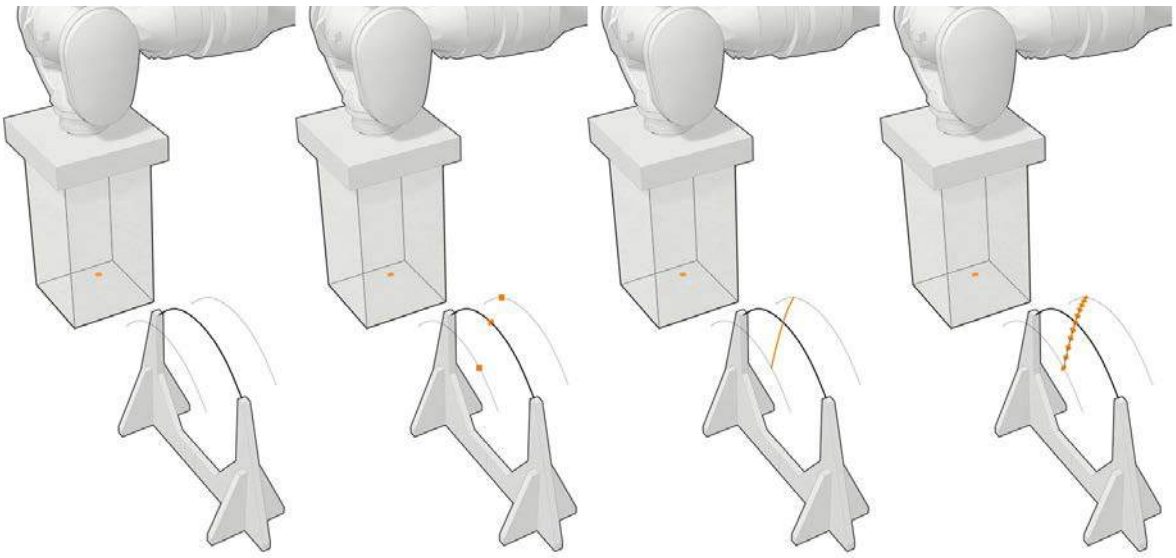

Figure 4.11. Generation of the experiment#2 motion path

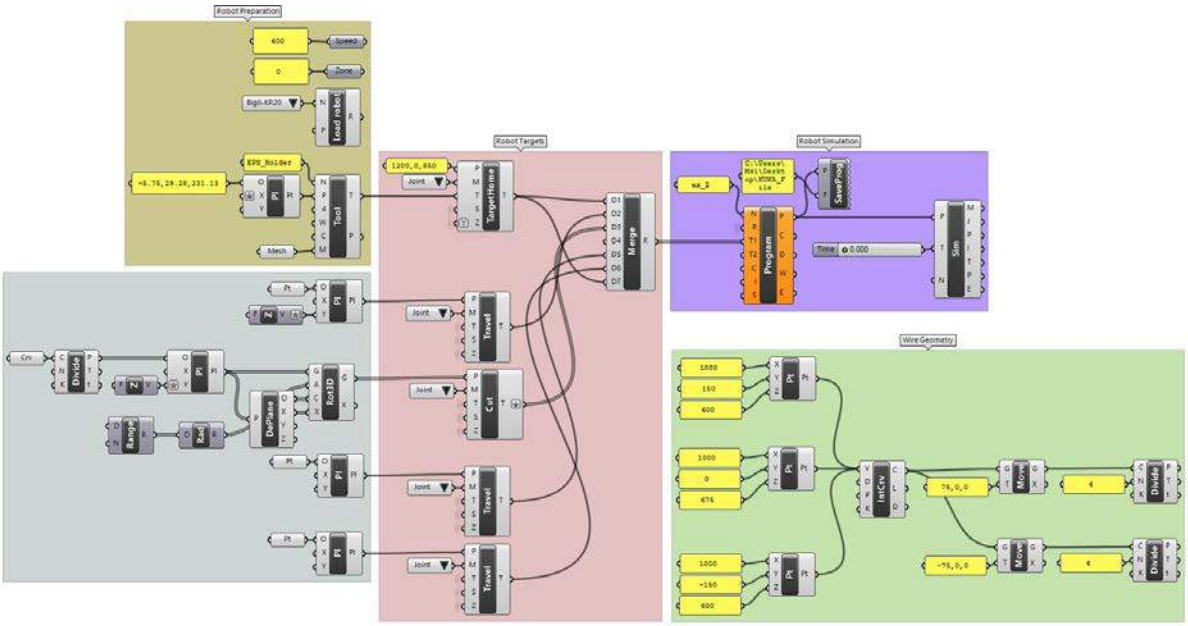

Figure 4.12. Grasshopper definition of the experiment#2

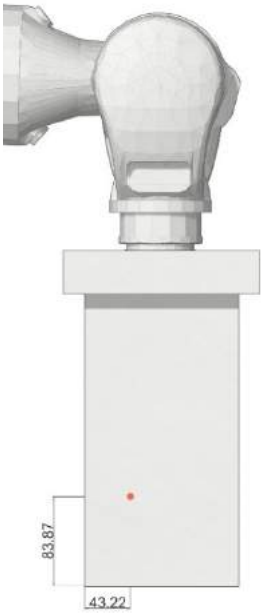

Figure 4.13. TCP position of the experiment#2. Dimensions are in mm

TCP repositioned according to the correct position of the foam block in the first cut, which is the first half of the wire and the middle point of it. In order to ensure that the foam is in the correct position when starting and finishing the cut, TCP is moved from the base of the foam up as much as 1/4 of the wire in the Z-direction and X-direction.

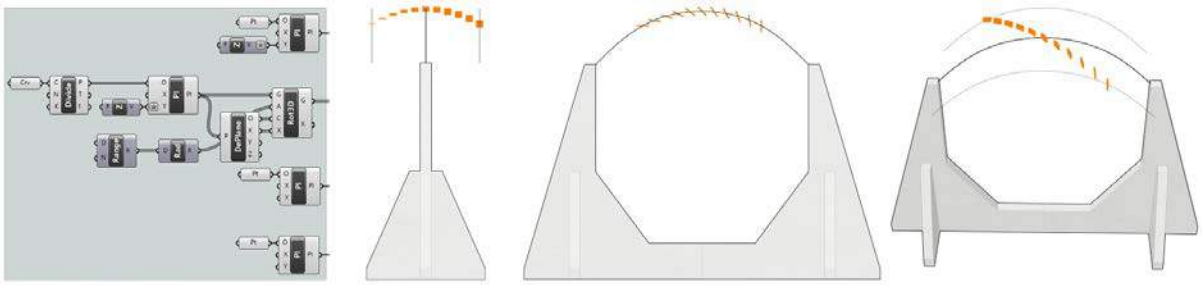

Figure 4.14. The movement path of the experiment#2

The most challenging part of the grasshopper code was 90-degree rotation because of the insufficient knowledge of the grasshopper. In the first experiment, rotation for motion path planes placed manually. In this experiment, the rotation of the planes parametrically coded. Through the cut, the Y-axis of the planes needed to rotate 90-degree from the Y-axis to the Z-axis (Figure 4.14).

Cutting

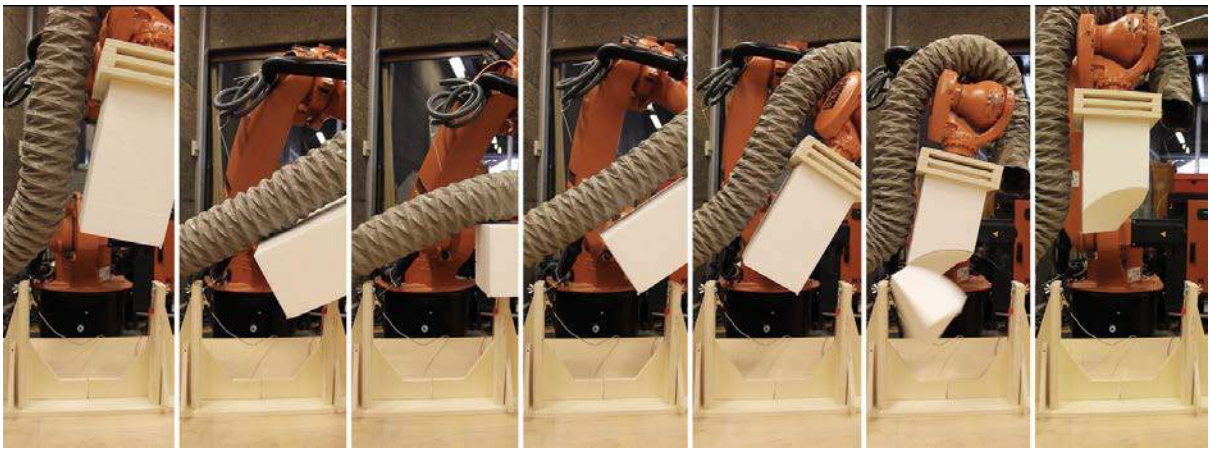

Figure 4.15. Cutting photos of the experiment#2

With the changes made for the second experiment, the correct curve cut for the front and back surfaces of the styrofoam.

In the first run of the experiment with the same code, it observed that the robot arm began to rotate before contact with the hot wire cutter. The robot was run several times to re-understand and reproduce geometry. It observed that the styrofoam block had started earlier than required

in the course of motion. Coordinates were retrieved, and new cuts were made to correct this error. The same problem observed in the new cut tests. In order to solve such problems, it is necessary to make a tool that is placed later in specific coordinates in space.

Outcomes of the Experiment#2

As a result of the incorrect cut experiment, it decided that the TCP and the motion path positioned incorrectly. Defining TCP according to the height of the first quarter of the wire in the foam causes the foam to have an incorrect height in the last quarter of the wire. The difference in the height of the TCP between the beginning and the end of the cut is a result of the 90-degree rotation. Can this error be solved by defining TCP in the base center of the foam? Another reason for the error could be the beginning of the motion path in the first quarter and ending in the last quarter of the wire. The front and back edges of the geometry cut correctly because the form of the wire is the fundamental curve and 90-degree rotation. However, the side edges cut as straight diagonal lines. Could this be the cause of the motion path that does not refer to the Gyroid? Can the correct cutting be performed with the motion path that created with the reference of the Gyroid curve?

4.4. Experiment #3: Motion Path Based on the Fundamental Curve

Before starting the cut, the hotwire cutter has been repositioned. The coordinates of the hotwire cutter tool in the previous experiment rearranged to fit the central axis of the robot. All mistakes of the hotwire cutter have been corrected in the simulation and the tool. The coordinates of the start point and endpoint of the wire must be positioned correctly.

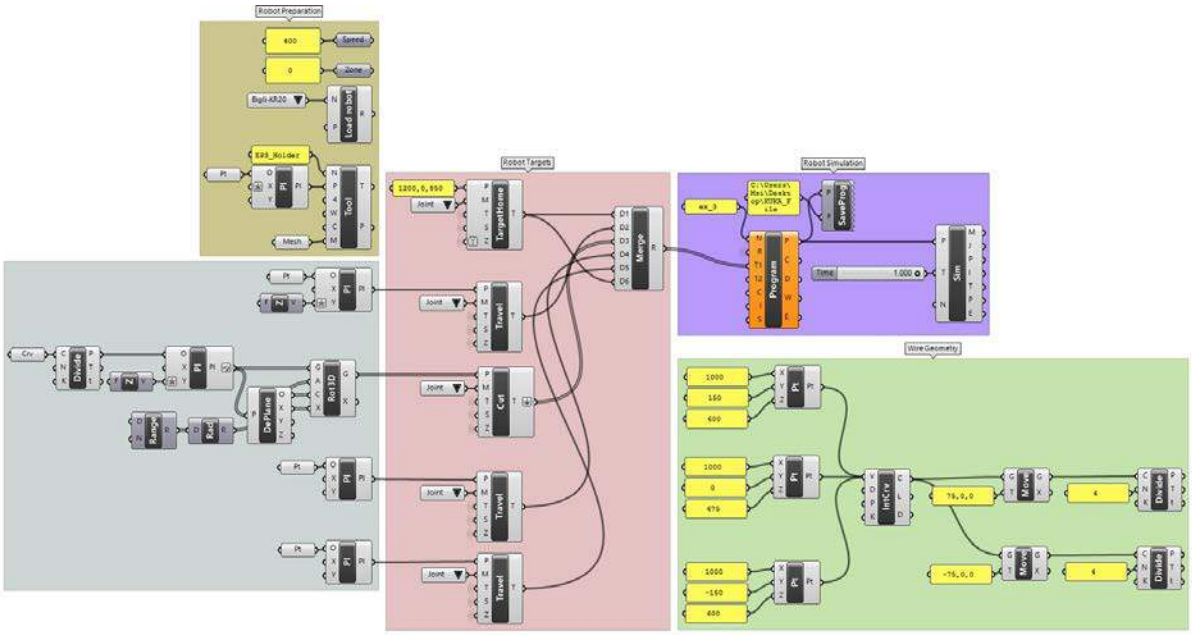

Figure 4.17. Grasshopper definition of the experiment#3

Figure 4.18. TCP position of the experiment#3. Dimensions are in mm

The motion path starts at the center point of the first reference line. The foam block is rotated 90-degree before beginning the cutting for the long edge of the block to be parallel to the projection of the wire (Figure 4.19). Preventing the foam from being damaged by the wooden supports holding the wire during the cutting movement is necessary.

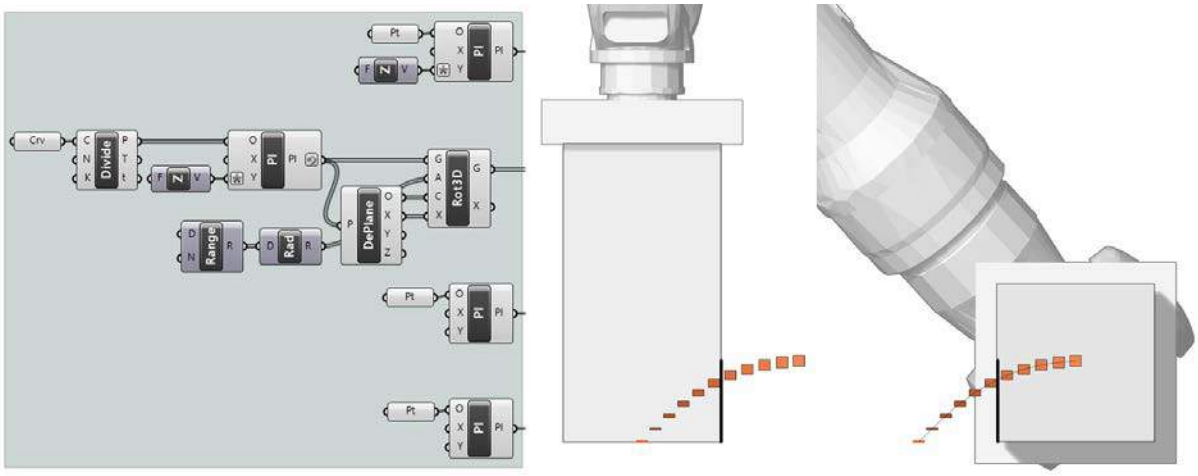

Figure 4.19. Side view of the TCP movement during the cut

It considered that the movement path between the start and endpoints to have a defined form. The length of the diagonally placed Gyroid fundamental curve was shorter than the distance between the beginning and the endpoints of the path. Therefore, Gyroid fundamental curve used as the reference for the movement path. The movement path formed by the projection of the Gyroid fundamental curve that placed between the two reference wire curves on a surface drawn between the starting and ending points of the movement (Figure 4.20).

The movement path that follows a diagonal curve makes it possible to shift the active cutting center. The first point of the motion path is at the center of the first reference line. The last reference point in the new cutting route is the same as the previous quarter-points projection. Between these two points, a diagonal surface generated. Y-axis of the TCP moves 90-degree from Z-axis to Y-axis through the movement (Figure 4.20).

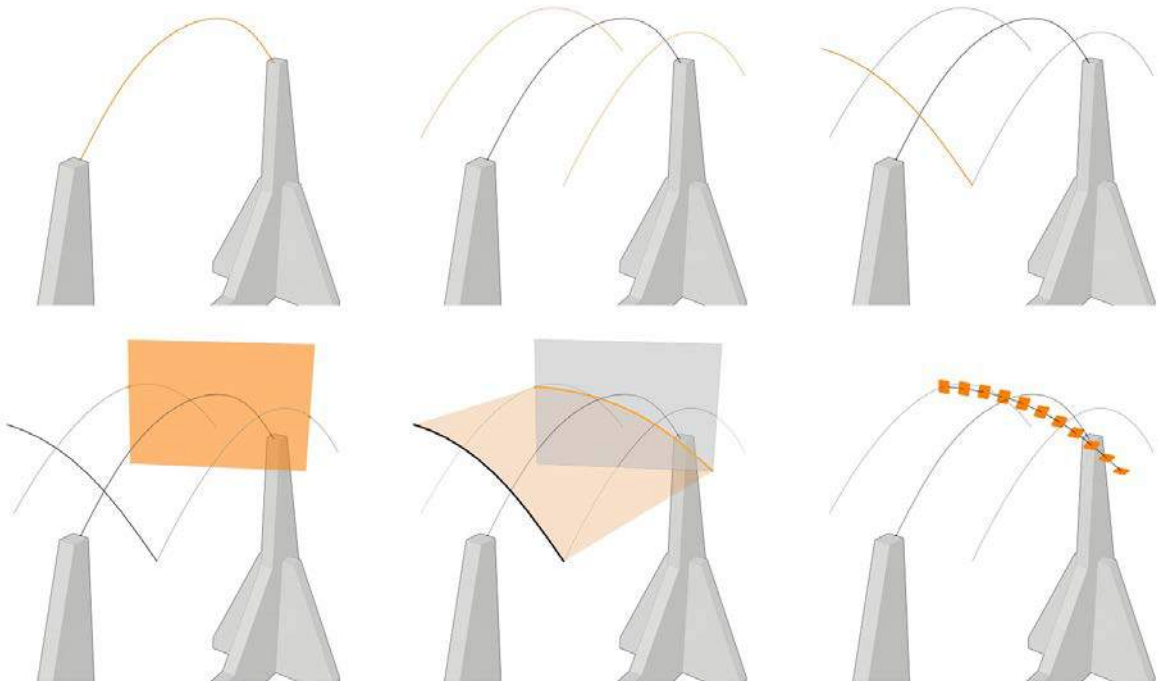

Figure 4.20. Generation of the experiment#3 motion path

Cutting

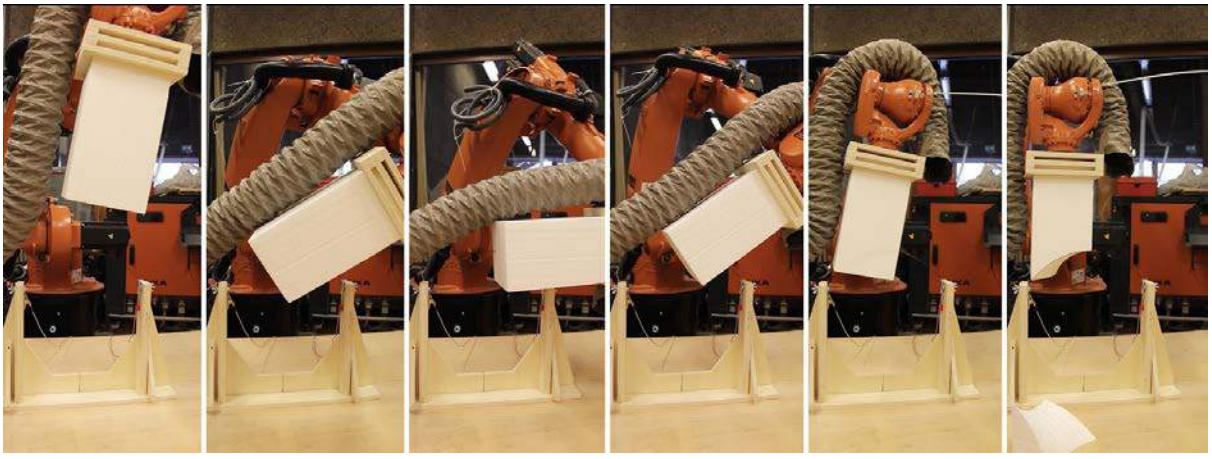

Figure 4.21. Cutting photos of the experiment#3

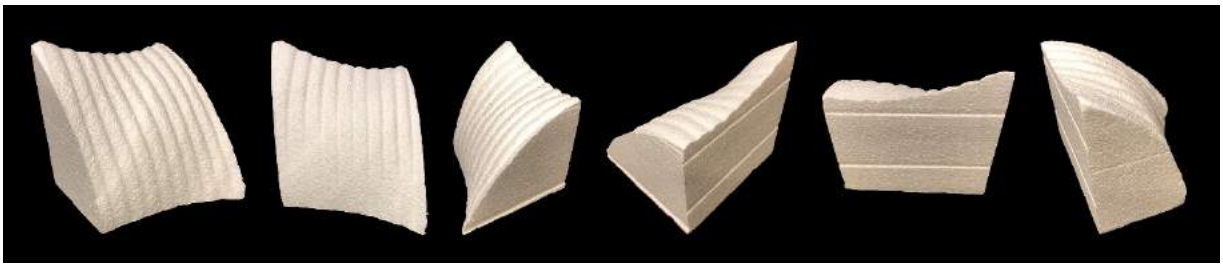

Figure 4.22. Cut geometry of the experiment#3

The fabricated form of experiment#3 is very close to the Gyroid fundamental patch. The dimensions and positions of the curves on the foam block surfaces are almost correct. The curves on the surfaces, where the wire cuts with the first and last movements, cut in the correct position. The other two curves are very close to the Gyroid fundamental curve due to the form of the movement path and 90-degree rotation. However, the Gyroid surface is not correct. The movement path used in this experiment caused the wrong cut of the surface even if the edge curves cut correctly. The movement path must be reconsidered in order to produce the Gyroid fundamental patch with the required precision. Can this error be solved with the cutting route drawn with reference to the surface itself?

It observed that the problem of not producing smooth surfaces continued. This problem must be solved when re-creating the movement path.

4.5. Experiment #4: Motion Path Based on the Fundamental Surface

The previous experiment did not result successfully because the movement path was not suitable for the cut. Is it not sufficient to choose the Gyroid fundamental curve as a reference for the success of the unit cutting? Is referencing the Gyroid fundamental patch a solution for the correct cut? Because of these questions, it thought that the movement path of the new experiment should be tested with reference to the surface of the fundamental patch.

The Gyroid fundamental patch was modeled in the Grasshopper code for a new movement path to form on it. Gyroid fundamental patch generated parametrically with Millipede add-on. The

code which Millipede used for the Gyroid cubic unit cell creation changed to obtain the patch by giving different domains and ranges.

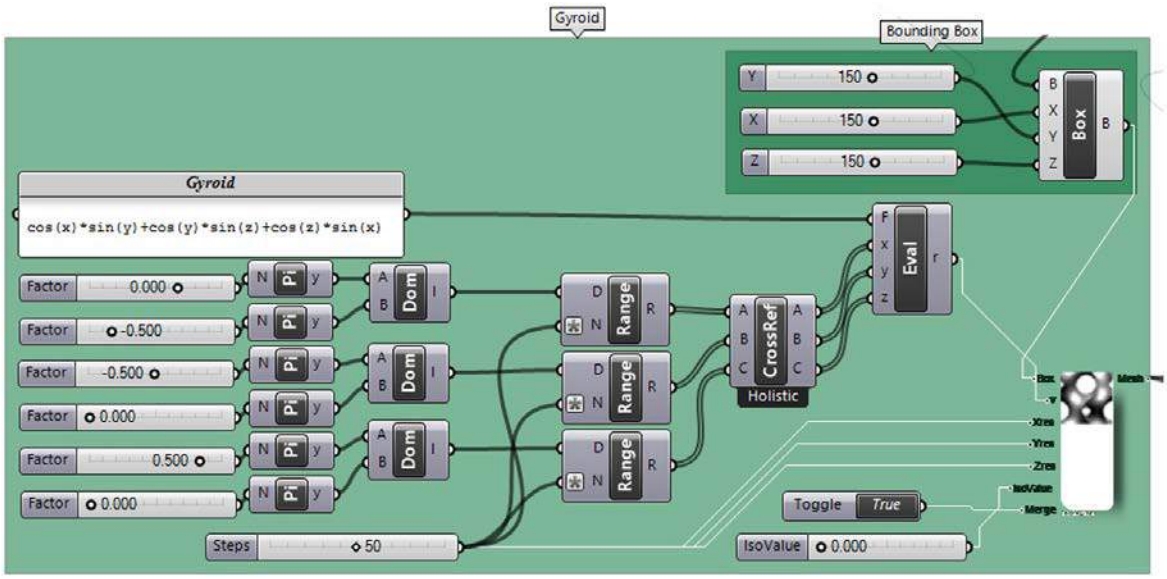

Figure 4.23. Gyroid fundamental patch generation code

The output of the Gyroid fundamental patch used for placing contour curves and points in the Path group (Figure 4.25). The new movement path formed with curves drawn at specified intervals using the contour command on the surface. Each generated curve divided into equal parts by the curve number. One of the points determined according to the order of the lines. For example, the third of the points on line three selected. Plane placed on each of the selected points. There should be a 90-degree difference between the first and the last plane in the movement path to rotate the foam. All planes in-between arranged as their angles increase at equal intervals.

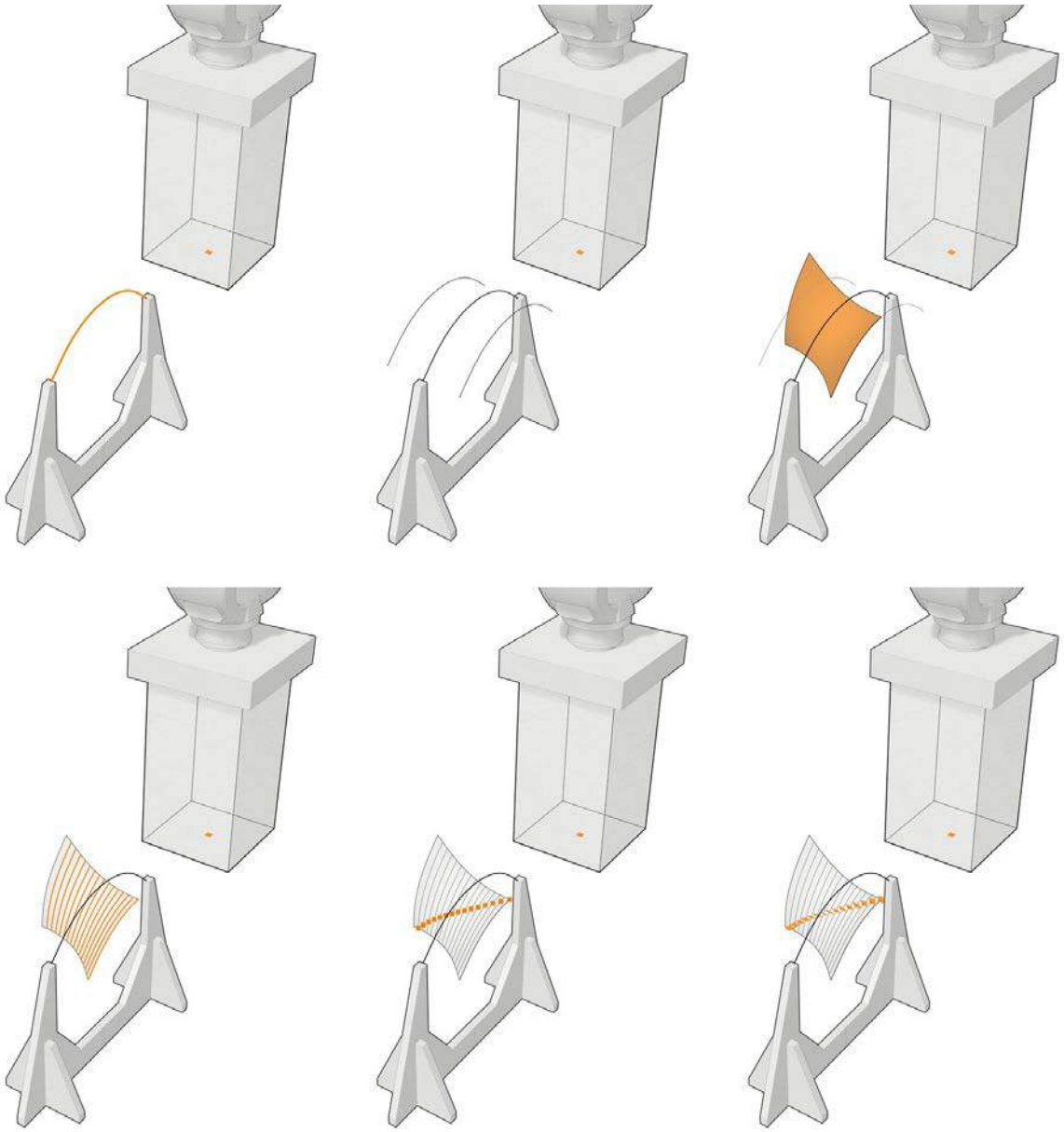

Figure 4.24. Generation of the experiment#4 motion path

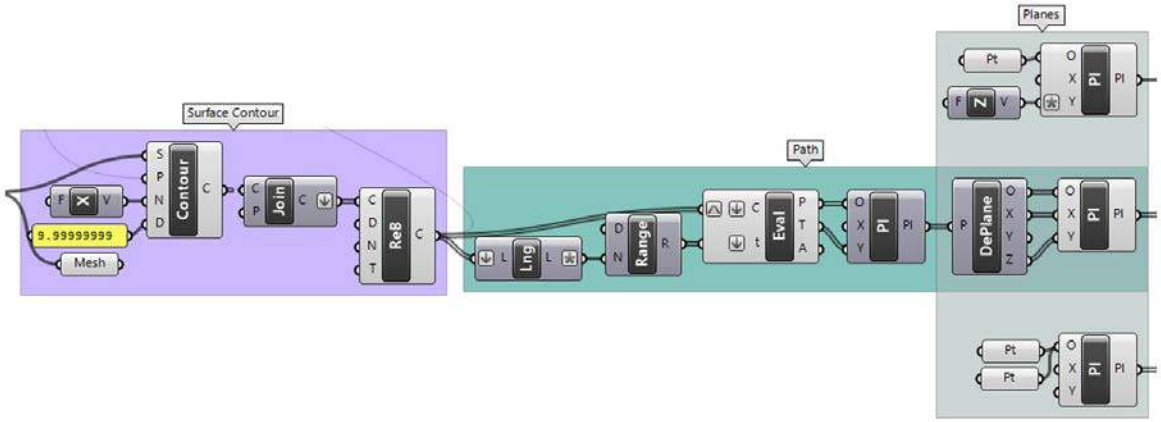

Figure 4.25. Contour and plane generation of the experiment#4 for the motion path

For fabricating the correct form, every change in the code must be tested. For minimizing the unnecessary experiments, simulation added to the Grasshopper code that simulates the side edges of the form to be cut. This issue is important for time and material use and doing less incorrect experiments.

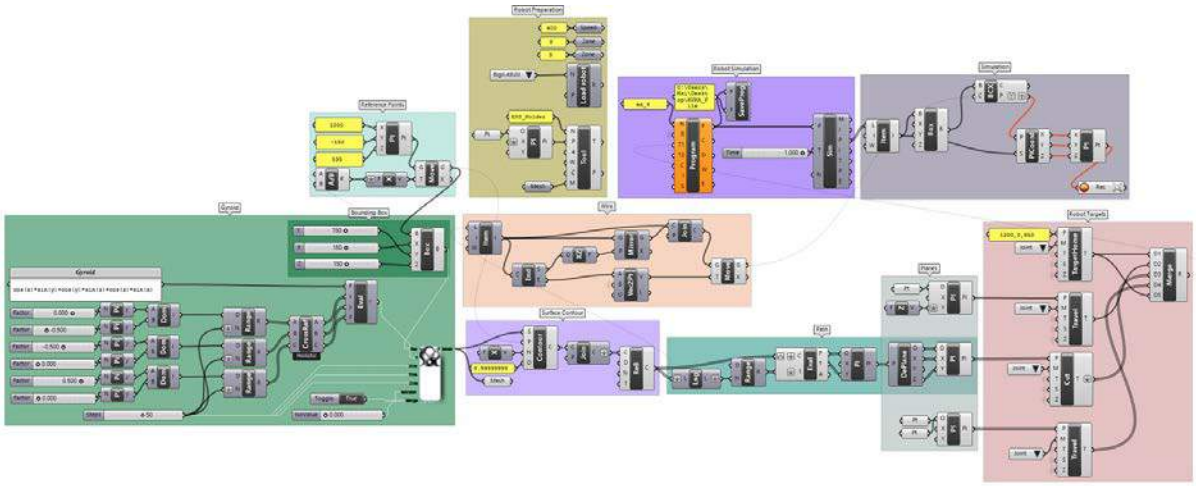

Figure 4.26. Grasshopper definition of the experiment#4

TCP position defined on the center point of the bottom surface of the block, which is the same as the experiment#3.

Figure 4.27. TCP position of the experiment#4. Dimensions are in mm

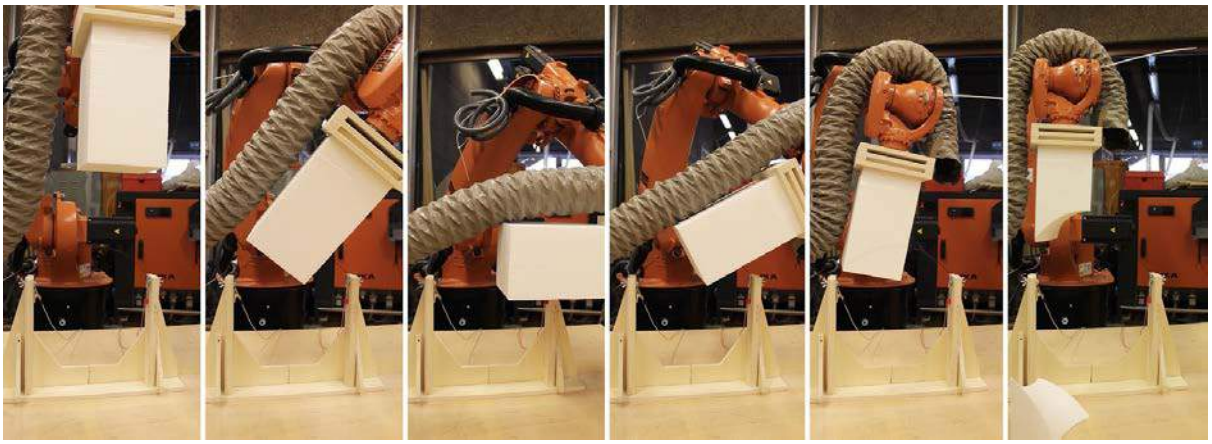

Figure 4.28. Cutting photos of the experiment#3

The outcome of the experiment#4

The dimensions and positions of the curves cut in the first and last movements are correct. However, two curves formed on the other edges are incorrectly cut. This error does not occur from the positioning of the first and last planes in the section. It occurs from the wrong movement between them.

The form of the cut surface is also incorrect, and this is more important than focusing on the accurate cutting of the edge curves.

Could be the reason for the surface cut incorrectly, is not the cutting path, but the form of the wire? Because the Gyroid fundamental curve has more than one curvature, the active cutting center changes while the geometry of the active cutting part of the wire changes during the movement. The wire that changes through the cut may be the reason that the surface formed on the foam is not the surface of the Gyroid fundamental patch. Is the reason why the Gyroid fundamental curve incorrectly cut on the side edges is that the curve geometry is not a single curvature?

Because of these questions, doing a new experiment decided in which the form of the wire rearranged without changing the logic of forming the movement path in the experiment#4. Is the result of the cut would be correct as the curvature of the wire will remain constant during the change of the active cutting center, in case of cutting with a single curvature wire like an arch? With this question, it decided to combine a single curvature geometry with the Gyroid cut logic used in previous experiments. The curve on each side of the form to be cut with a single curvature wire will be the same curve positioned in different ways as in the Gyroid.

Simulation Experiment of the Arch Wire

In order to achieve the correct result, every change in the code tested by cutting, which results in time and material waste. Therefore, in this experiment, instead of cutting, errors were observed with simulation.

A new experiment carried out by changing the form of the curve without disturbing the logic of the movement path that prepared with reference to the Gyroid fundamental patch. Since the four sides of the patch and the two halves of the wire are the same curve, only one curve changes are sufficient to rearrange the entire system. In the new experiment, a new arc has drawn without changing the height and width dimensions of the Gyroid fundamental curve. The width of the arch is 15 cm, and the height is 7.5 cm. In this way, it thought that a single curvature surface can be cut without changing the tool and cutting logic.

It is not necessary to use the equation in the experiment without using the Gyroid fundamental curve. Therefore, the Grasshopper code has been rearranged. Since geometry no longer produced from the equation in grasshopper, there is no need to use millipede.

The outcome of the Simulation Experiment

Previous error continued in the result of the simulation made with the arch curve. The dimensions and positions of the cut geometries at the beginning and end of the movement path are correct. However, the curves forming on the other two sides of the form have the wrong geometry rather than the defined arch. With this error, it understood that both the sides of the cut and the cut surface are wrong, and so the path of the cutting route is not correct for cutting the intended form. With this experiment, it tested that the Gyroid fundamental curve is not the reason for the Gyroid fundamental patch cannot cut correctly.

The error reasoned from the division of the curves formed on the surface into an equal number of parts. In the cutting simulation, it noticed that the lengths of the lines drawn on the surface were different from each other. Because the curves of various lengths divided into equal numbers, the point spacing of each curve is different. Therefore, the spacing of the points forming the movement path is also different from each other. In other words, the length of the movement of the second point to the third point is different from the length of the movement of the third point to the fourth point. So the distances between the planes on the movement path are different. Therefore, incorrect production made as a result of the cuts.

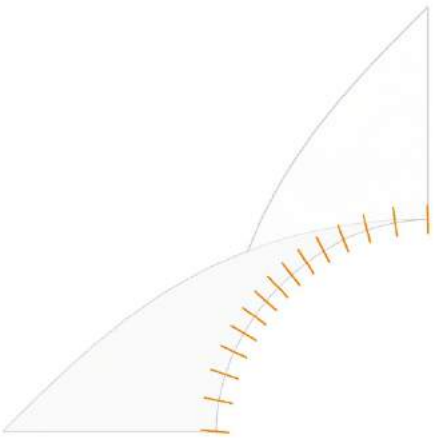

Figure 4.29. Experiment#4 motion path and Gyroid fundamental curve front view

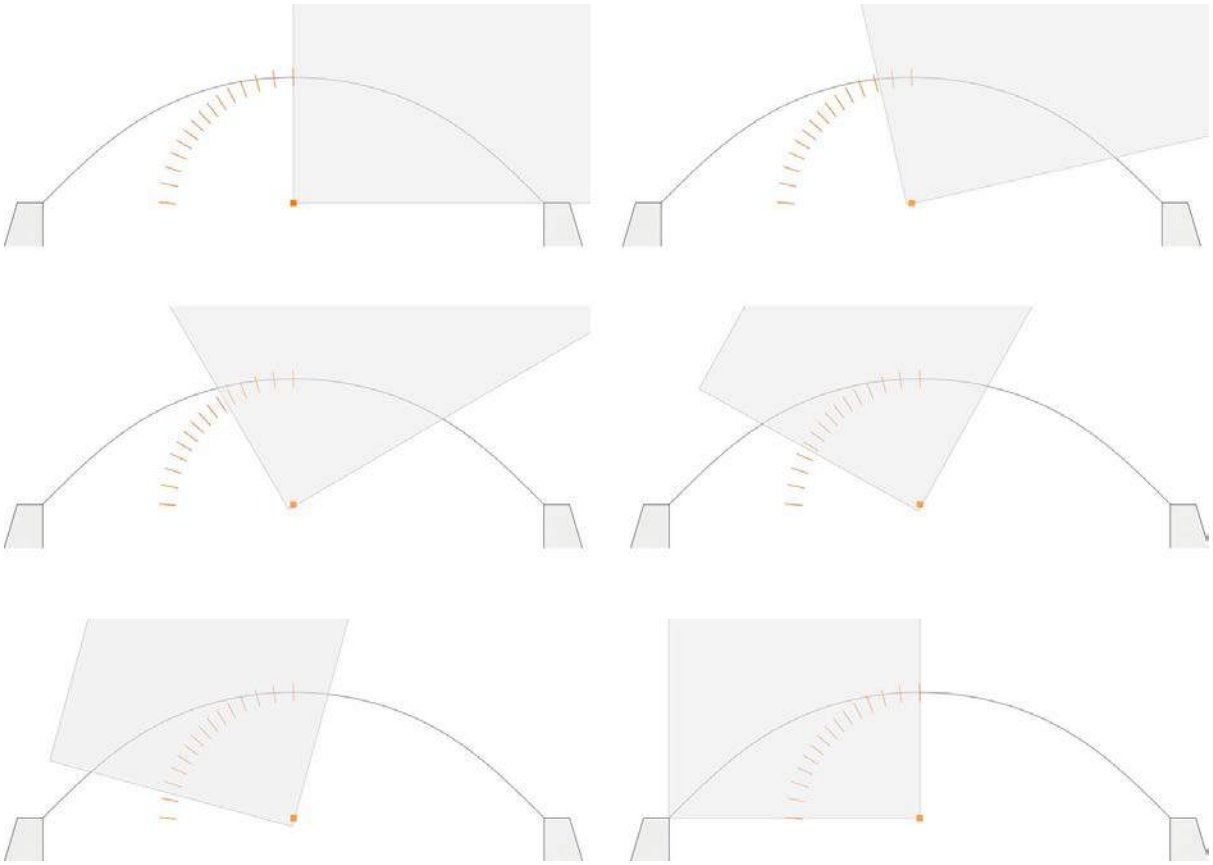

Figure 4.30. Experiment#4 motion of the EPS block and Gyroid fundamental curve front view

When investigating the solution of the error, the movement observed from the front view. It has been found that the foam does not remain constant on the axle on which it rotates 90 degrees and does not follow a regular axle (fig. 4.30). The reason for this found to be a PTP movement between planes. That is the reason for the same path is not followed during the movement between them, even if the locations of the points are on the right path. It is not possible to reach the right result with the cut made by the PTP movement between the planes.

After this error, it understood that the axle from which the foam rotates is important for cutting. Is it possible to make a successful cutting by forming the cutting line on this axis?

4.6. Experiment #5: Final Motion Path

In the fifth experiment, the main challenge was to program the TPC to follow a straight axis path while rotating 90-degree. To do that, the logic of the first experiment, which was creating the movement path with two planes only, retried with the knowledge that learned through experiments. Unlike the first experiment, everything that needed to be in the definition added parametrically.

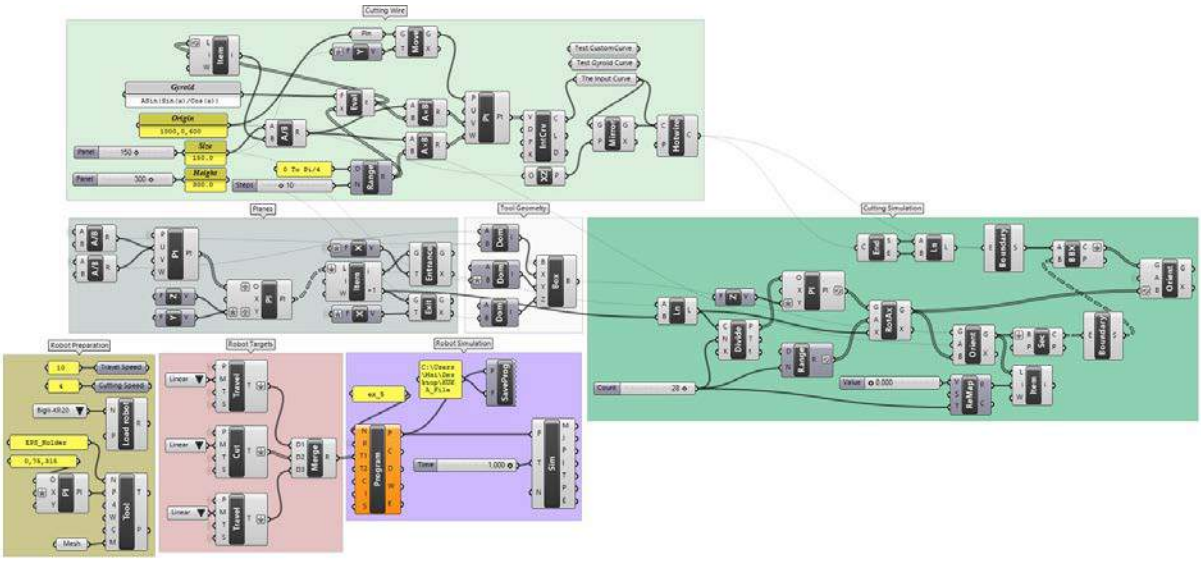

Figure 4.31. Grasshopper definition of the experiment#5

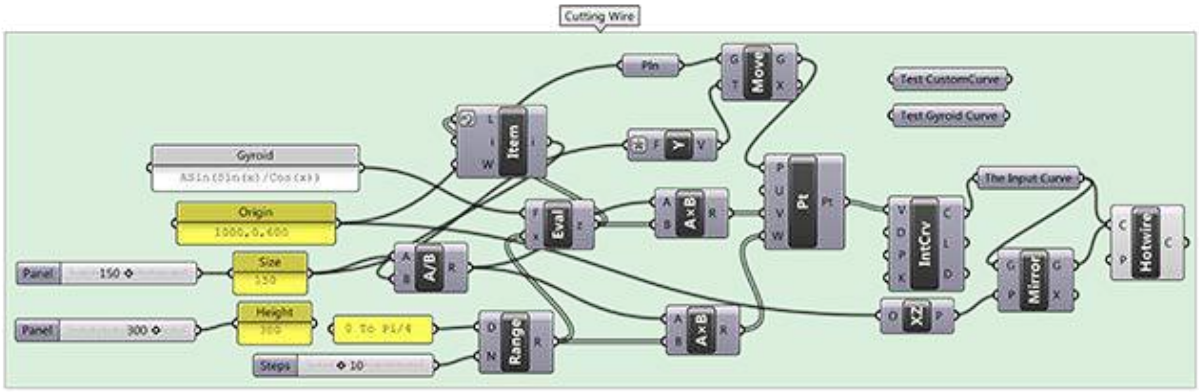

Figure 4.32. Grasshopper definition of the experiment#5 cutting wire representation

Making robotic fabrication with the definition of the experiment#5 can be different from Gyroid. The wire geometry of the hotwire cutter parametrically added to the code. The parametrically controlled wire form is important to not only control the wire form itself but also controlling movement path and simulating the final geometry.

Figure 4.33. TCP position of the experiment#5. Dimensions are in mm

The location of the TCP has been rearranged due to the change of the movement path. TCP, defined at the center of the base surface of the block, moved to the center of the edge, which will move on the axle.

The movement path consists of planes placed only at four points. Two of these placed before and after cutting to prevent the foam from being damaged by the wire. The other two planes are the starting and ending point of the active cutting path of the movement. The distance between the start and the endpoints must be in the width of the bounding box of the Gyroid fundamental patch created in. For this experiment, the distance between the two planes is 15 cm. Therefore, planes that obtain the active cutting movement path placed 7,5 cm away from the front and back of the midpoint projection of the wire.

There is a 90-degree difference between two planes. The plane at the starting point of the motion is parallel to the projection of the wire, and the plane at the endpoint is perpendicular to it. Therefore, the EPS block will rotate 90-degree by following these two planes. Between the two defined planes, there are no other planes, and the robot arm will make linear movement between these two points.

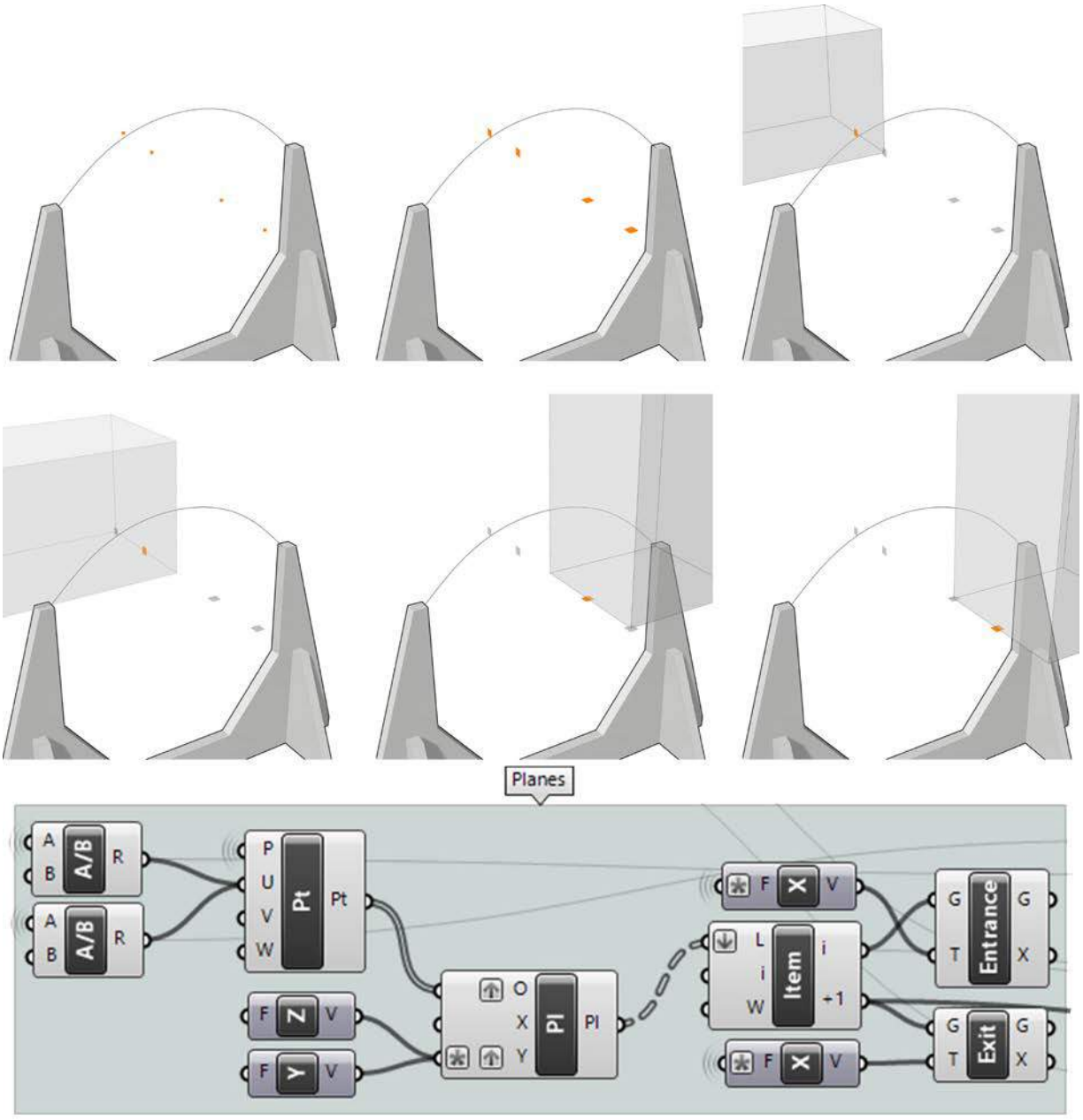

Figure 4.34. Generation of the experiment#5 motion path

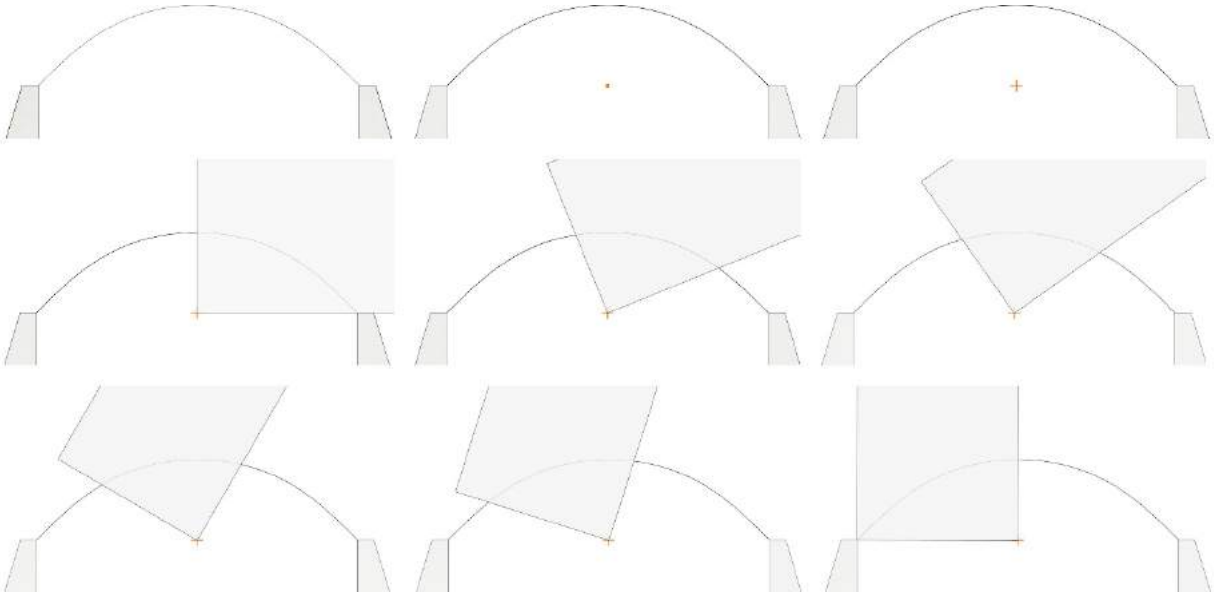

Figure 4.35. Experiment#5 motion of the EPS block and Gyroid fundamental curve wire front view

It possible to see the edge of the block on the center axis and rotates around that point from the front view. With this achievement, a smooth Gyroid surface could be fabricated.

Simulation code also added to see the result of the movement path. The simulation code basically visualizes the result of the intersection of the moving block with the wire. If the parameters in which the Gyroid dimensions determined in the code change, the dimensions in the simulation change simultaneously.

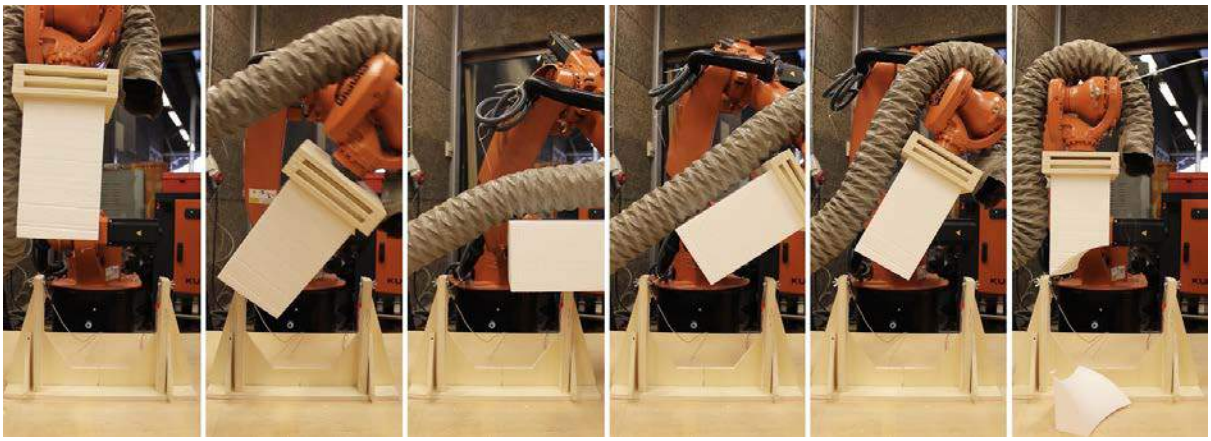

Figure 4.36. Cutting photos of the experiment#5

4.7. Experiment #5 Mirror

To create a volumetric Gyroid fundamental unit, a fundamental patch and a mirror of it needed. Therefore, a code prepared for the mirror of the experiment#5. Movement patch and plane rotation are basically the same as the experiment#5. The main differences are the directions of the planes on the path and TCP position. TCP moved to the mirrored edge middle point of the EPS block.

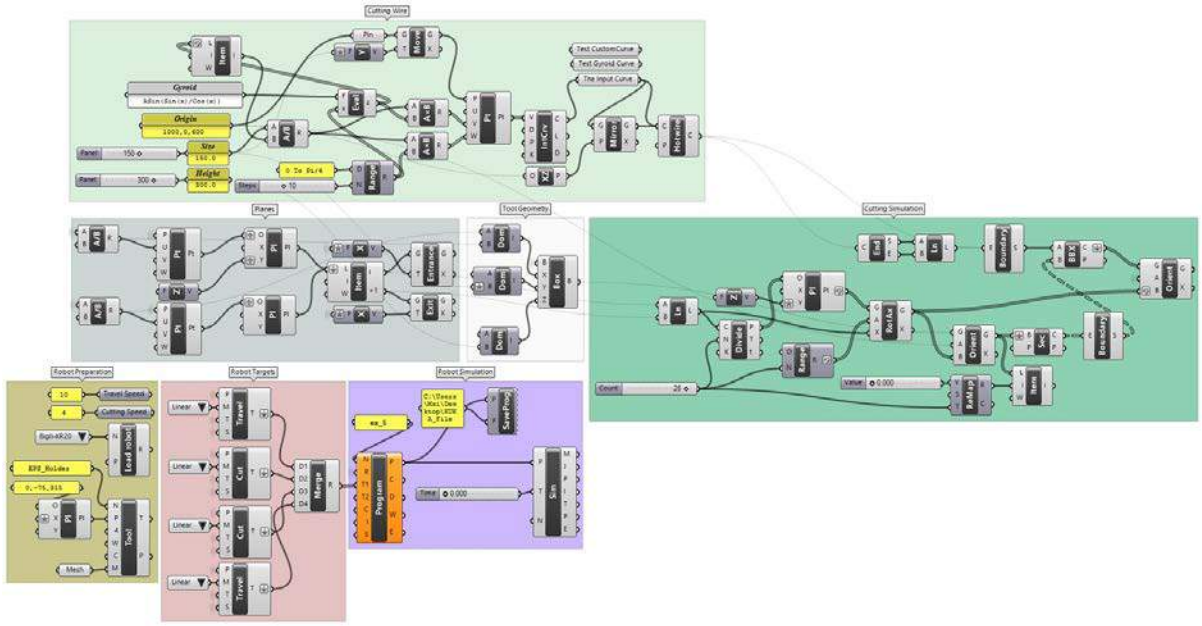

Figure 4.37. Definition of the experiment#5 mirror

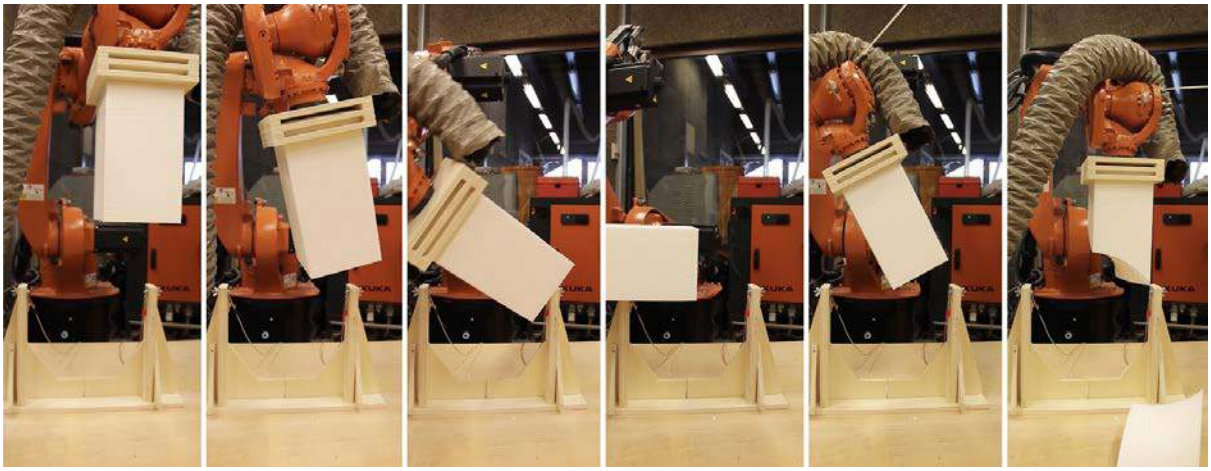

Figure 4.39. Cutting photos of the experiment#5 mirror

Figure 4.38. TCP position of the experiment#5 mirror. Dimensions are in mm

4.7. Final Fabrication and the Outcomes

In experiments, a solid block cut in fundamental patch geometry and split the block in two that have the same geometric surface as negative and positive patches. Negative patches are the ones that cut and fallen from the block at the end of the cut. Positive patches are the ones that formed on the block.

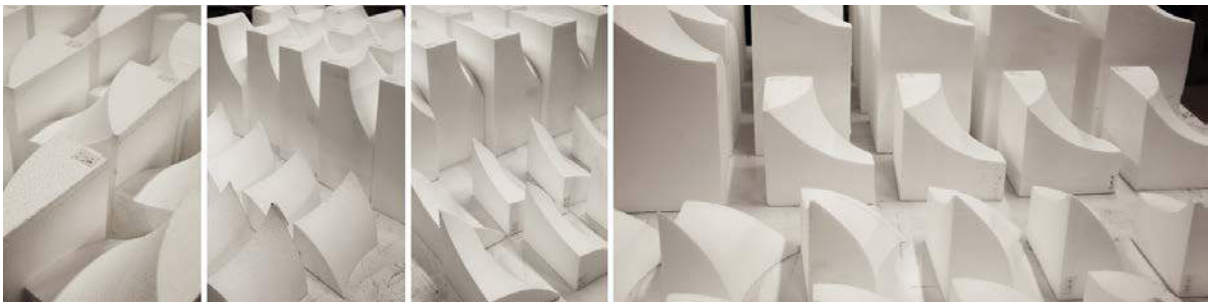

Figure 4.40. Gyroid fundamental patches cut from EPS blocks

Three of the two geometries that mirror each other needed to build a fundamental unit. Furthermore, for constructing a solid-void balanced Gyroid, one of the mirror geometries had to be negative and the other one positive patch.

The cut geometries named in groups as A and B. Group A and group B mirrored to each other. Four patches can create various geometric components with the same patch and the other three. There are several combinations of connecting the patches. Aggregation lists created for each of them. The combination of patch A at positions 1 and 2 with patches A, A', B, and B' shown in Figure 4.41.

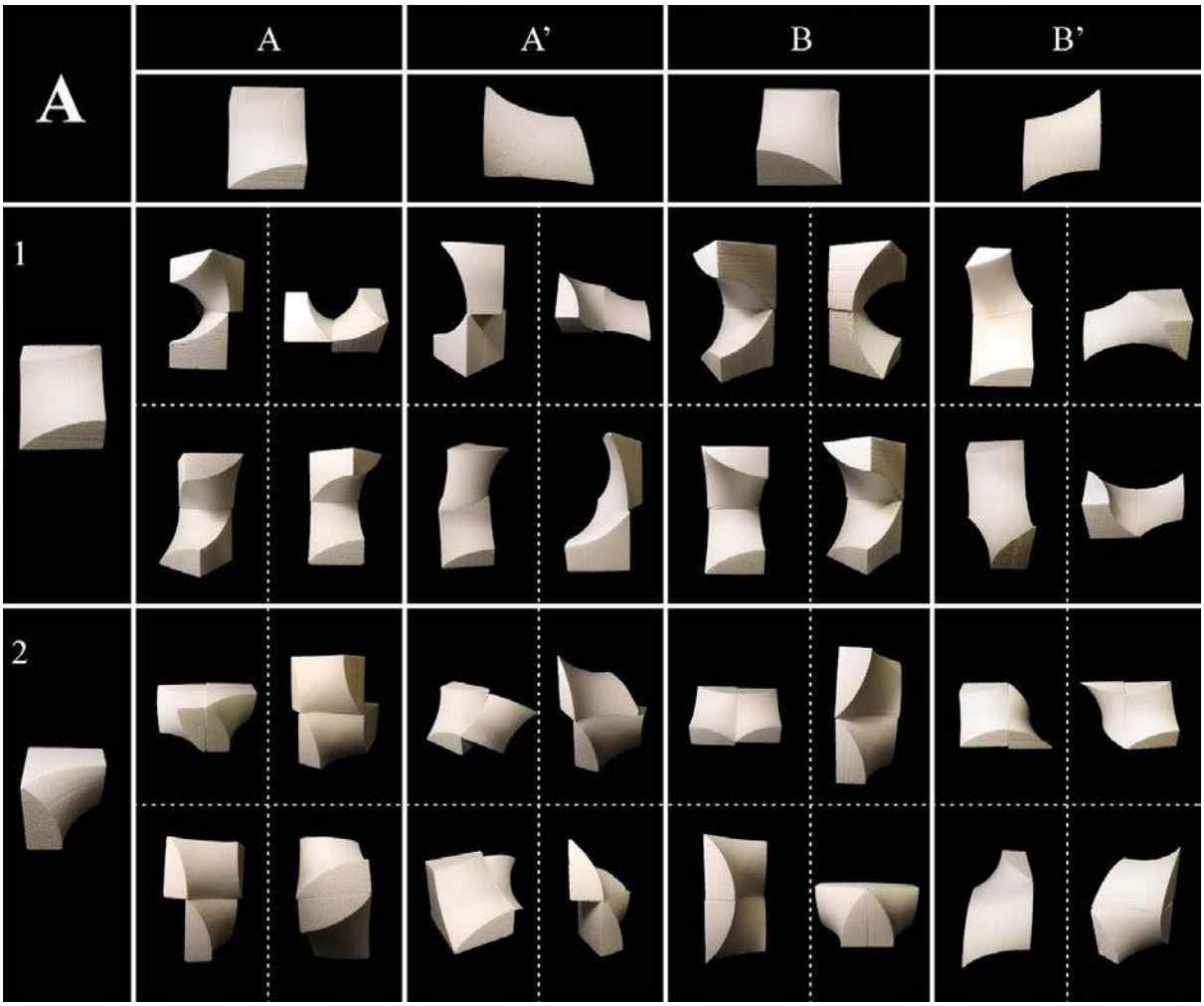

Figure 4.41. Connection combination list of A fundamental patch

Lists of A’, B, and B’ patches created with the same method used in the list of A. Thus, the emerged forms at the combination of each patch with others examined. Binary combination variations of the patches shown with prepared lists. Such lists can extend by increasing the patch numbers included in the combinations (Figure B.1.; Figure B.2.; Figure B.3.).

A combination of six identical fundamental patch surfaces generates a Gyroid fundamental unit surface. In order to create a volumetric fundamental unit, three sets of negative and positive patches should be used. To be more specific, a fundamental unit can be built with three of the negative patch of group B which named B’, and three of the positive patch of group A, which named A (Figure 4.45.).

Figure 4.45. A18, A19, A20, B’23, B’24, B’25

With the same logic, A’ and B unit generates a mirror of the fundamental unit in Figure 4.45. Therefore, fabrication without waste material made within the scope of this research.

Figure 4.46. A’5, B3, B2

Due to the units combining from different directions ability, various components generated. This allows creating flexible extension systems with patches. In this thesis, emerged components formed by using combination flexibility investigated (Figure 4.46; Appendix-C)

5. EVALUATIONS

5.1. The complexity of Parametric Models

Evolution of the Code

Before starting to generate the Grasshopper code, there was an initial assumption about how to produce Gyroid fundamental patch with the industrial robot. Cut needed to start from half of the wire and end with the other half by rotating 90-degree. This logic used in all experiments. For

the first experiment, a code prepared with two basic positions with this logic. At the end of all the experiments, the most accurate logic was the first experiment, but the surfaces created for the movement were wrong. Therefore, in the last experiment, logic in the first experiment was used, but a much more parametric code produced.

A straightforward code prepared for the first experiment and code gradually become more complex and parametric through the last experiment. The first code has more manually added components in the Rhino file, and the previous has none.

Experiment #1:

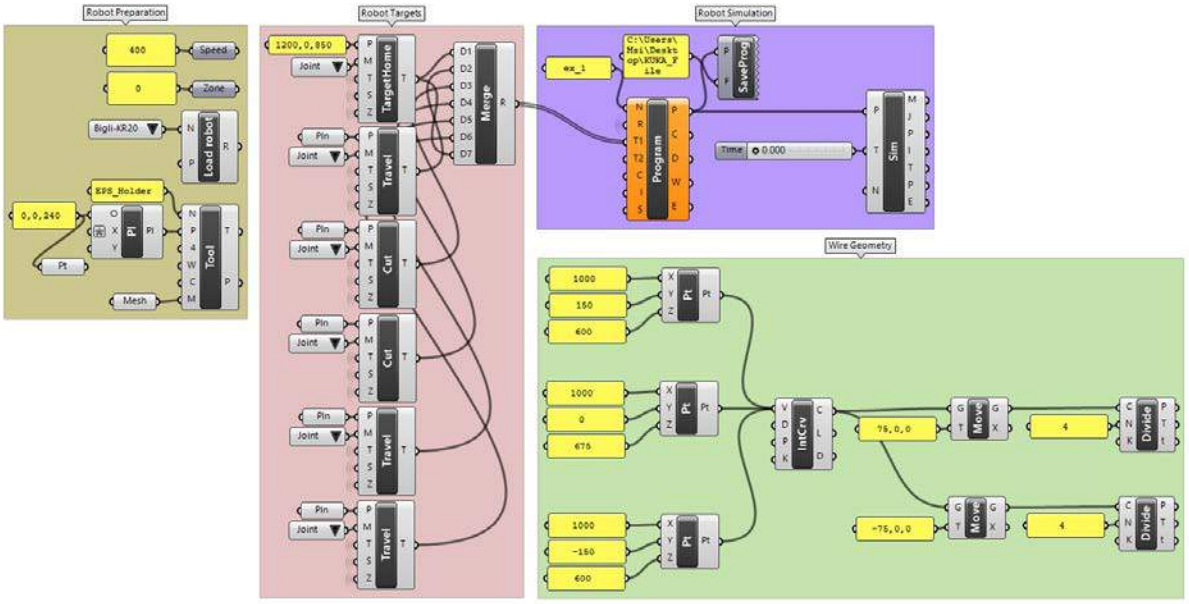

Figure 5.1. Grasshopper definition of the experiment#1

Experiment#1, based on two mirror planes, placed tangential to the wire in order to make the rotational movement. Planes are defined manually with reference curves and points and wire and references defined with the main commands. TCP defined on the center axes and 22,5 cm below from the EPS holder tool, which is 7,5 cm above from the bottom surface of the block. Grasshopper code has basic components for parametric robot control grouped in four main fragments: Robot preparation, Robot simulation, Robot target, and Wire geometry as an addition. Robots' work information components are in the robot preparation group, such as a

tool, TCP, robot load, speed, and zone. The robot simulation group has simulation and information transformation components. The program component which merges all components simulates the robot movement and saves the code in KRL language is in the Robot Simulation group. Robot target group contain the movement planes and merge components to order them. Wire size, geometry, and references included in the wire geometry component.

Experiment#2:

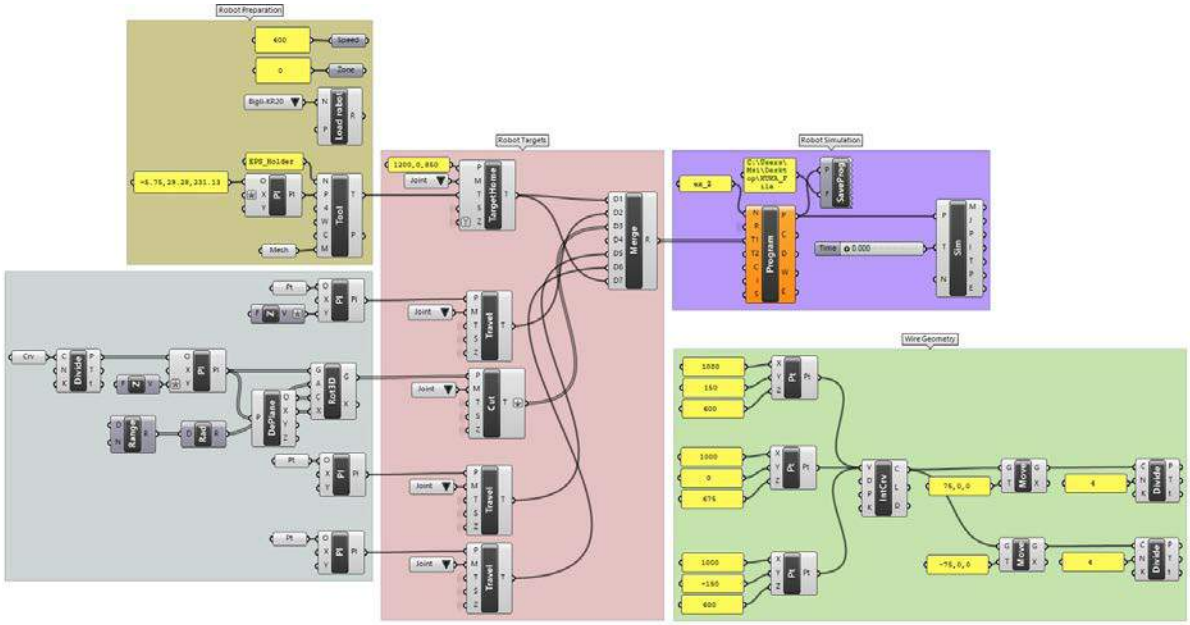

Figure 5.2. Grasshopper definition of the experiment#2

Grasshopper code in experiment#2 has five main groups. An additional group is for planes for robotic motion control placed parametrically and rotates 90-degree through the end; however, the curve that defines planes added to the code manually. TCP repositioned according to the reference point and the height of the wire to keep the Gyroid curves on the surfaces accurate.

Experiment#3:

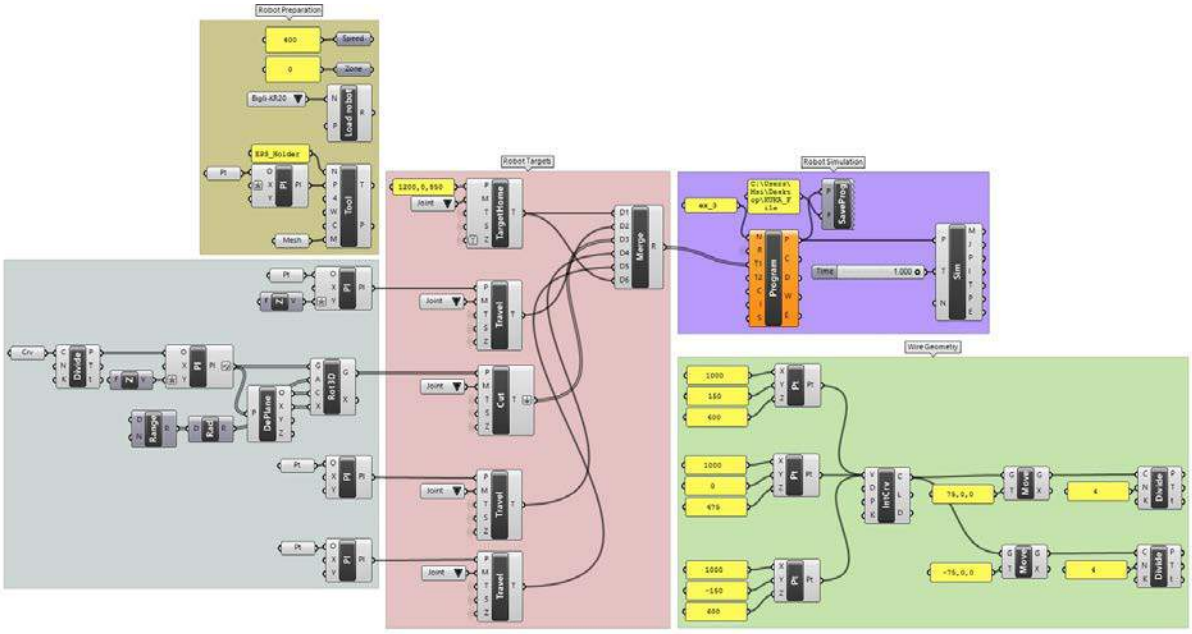

Figure 5.3. Grasshopper definition of the experiment#3

The third experiment has five main groups in the code that are not very different from the second. However, the motion path of the robot has changed according to the outcome. Cutting logic of the second experiment, which is programming the path with a curve maintains. A different curve used for the path and did not drawn parametrically. TCP replaced with a point in the code placed on the center of the EPS blocks bottom surface This Grasshopper code gives better performance than the previous experiments, but the cut form is not still a Gyroid fundamental patch.

Experiment#4:

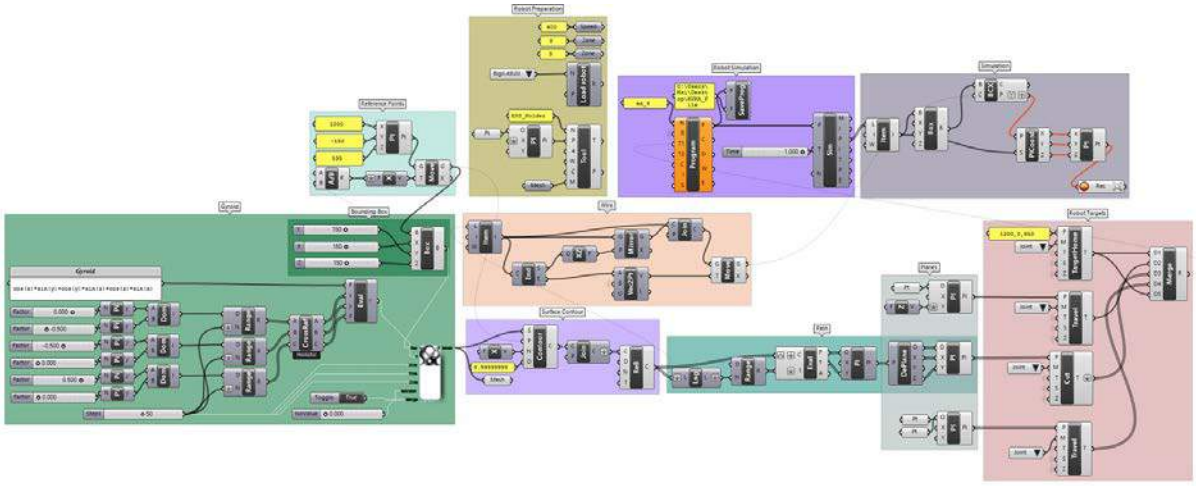

Figure 5.4. Grasshopper definition of the experiment#4

The Grasshopper code in the fourth experiment changes considerably. It becomes more parametric and complex than previous codes. It has the same logic with the second and third experiments; however, in this one, curve not drawn manually, it obtained with the reference of the Gyroid fundamental patch. Minimal surface generated parametrically to use as a reference for the movement path. Contour curves generated on the surface and divided into the same number. A list created in the code with the contour lines and points obtained by division and planes placed on the point that specifically chosen. The more important addition of this code is the simulation of the form of the side edges. With this addition, it is possible to make less incorrect cuts and to save up time and material use.

Experiment#5:

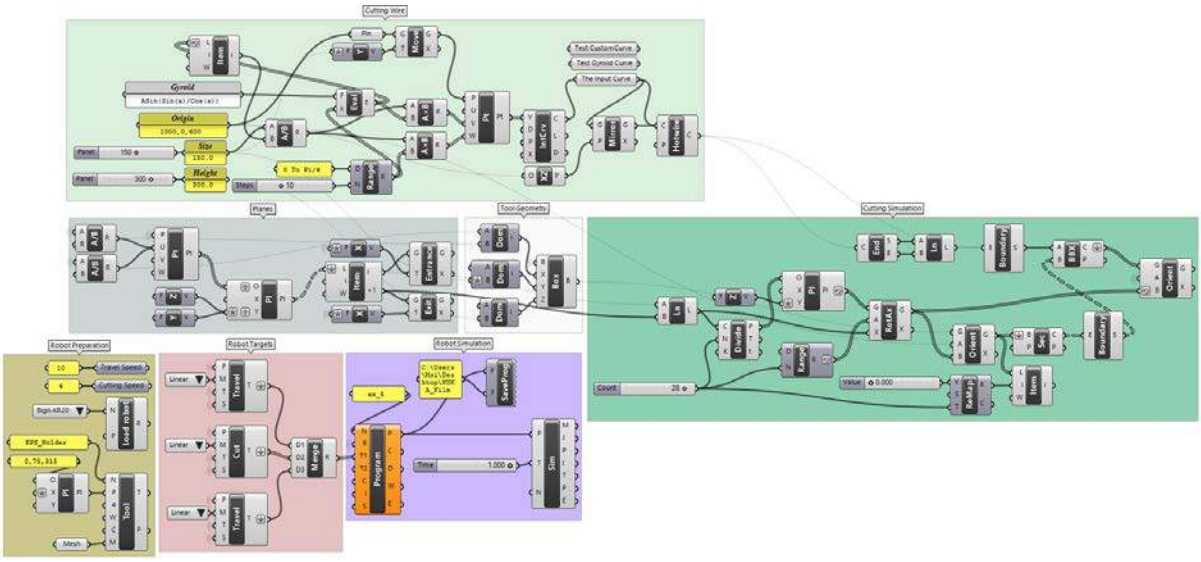

Figure 5.5. Grasshopper definition of the experiment#5

In the fifth experiment, the most straightforward logic among previous experiments used with the most complex and parametric code between them. Creating the movement path with two planes with 90-degree rotation retried with the knowledge learned through the experiments. Movement path is as simple as two planes on a 15 cm long line. However, the code itself complicated because every component that needed for robot programming and the Gyroid fundamental patch generated parametrically. With the **Input Curve** component or by changing the equation, other geometries than Gyroid can cut by using Gyroid cutting logic.

With the Cutting Simulation group, the reconstructed form of the wire and the form to be cut can be simulated. Simulation the sequence arrangement of the intersection geometries of the representative foam block, which is the Box component in the Tool Geometry group, and the wire, which is the last component of the Cutting Wire group.

Because of the wire parametrically added to the code, it is possible to use and another shape than Gyroid fundamental curve. A new curve should be defined to the **Input Curve** component or changing the equation, which is half of the wire, to cut with any other curve. The

reconstructed form of the wire and the shape of the cut can be simulated. With the prepared code, the cutting motion path can be obtained by defining the equation for the curve or any curve. In this way, a surface can be created from any curve using Gyroid cutting logic.

In order to construct the Gyroid fundamental curve, Z values in the equation rearranged to be 0. By changing the size and height parameters in the code, hotwire cutter tool dimensions are changing synchronously. Therefore Gyroid production can be made at any size by using a hotwire cutter in new dimensions.

The code completed by adding components that enable the conversion of the whole system to the robot language. The Robot Preparation group includes tool information, TCP point information, movement speeds, and components that enable the robot to run in the grasshopper program. The speed settings arranged according to the operation of the robot in automatic mode. There are two different speed values in the code. The speed of movement between reference planes and cutting planes is 12. Since the speed of the robot should be slower at the time of cutting, the speed between the cutting planes is 4. The Robot Simulation group includes components that allow the robot program to run, save the KRL code to the file, and simulate the robot arm.

Experiment#5 Mirror:

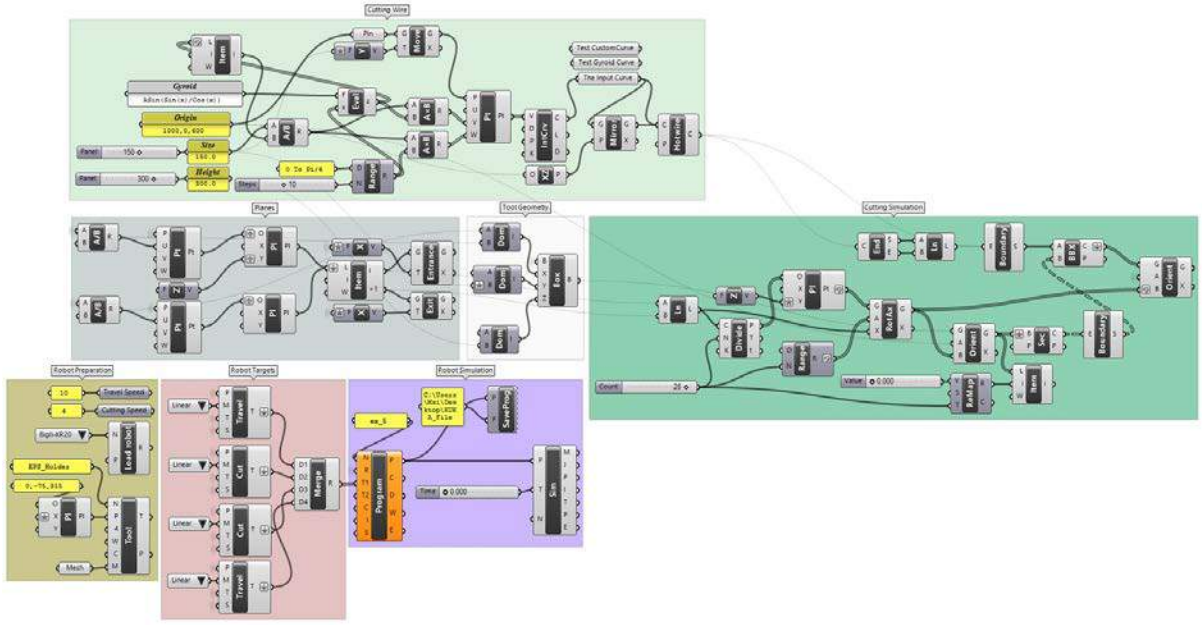

Figure 5.6. Grasshopper definition of experiment #5 mirror

The experiment#5 mirror is for cutting the mirror geometry of the Gyroid Fundamental patch. It basically for the robot to move the mirror of experiment#5. That is why they are slightly different from each other.

Differences between experiment#5 and #5 mirror:

Placing the planes have the same logic. However, mirror geometries' definitions have more components.

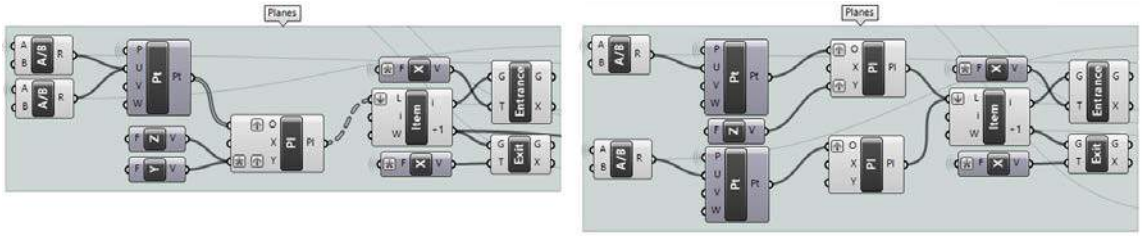

Figure 5.7. Plane difference between experiment#5 and #5 mirror Grasshopper definition. Left; Movement control planes of experiment #5; Right; Movement control planes of experiment #5 mirror

For rotating movement, path planes Construct Point and Construct Plane components added to the Grasshopper code. Because one plane added to the code, another Cut component had to be added to the Robot Targets group. The output of the added plane component connected with the input of the Cut component.

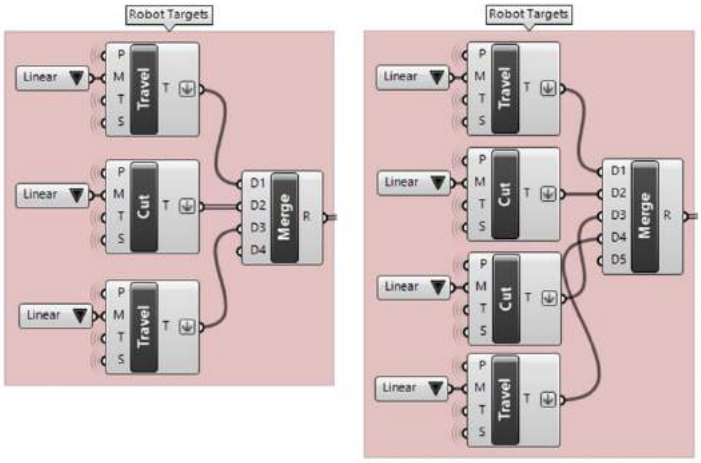

Figure 5.8. Robot motion target difference between experiment#5 and #5 mirror Grasshopper definition. Left; Robot motion targets of experiment#5; Right; Robot motion targets of experiment#5 mirror

TCP position had to be rearranged because of the movement path planes changed. In experiment#5, TCP defined on one of the edges of the bottom surface. Because the movement mirrored, TCP had to reposition to the mirror edge according to the Y-axis.

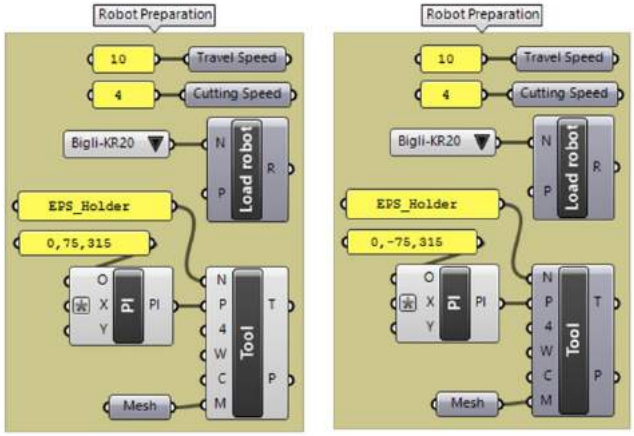

Figure 5.9. TCP position difference between experiment#5 and #5 mirror Grasshopper definition. Left; TCP position of experiment#5; Right; TCP position of experiment#5 mirror

TCP Positions

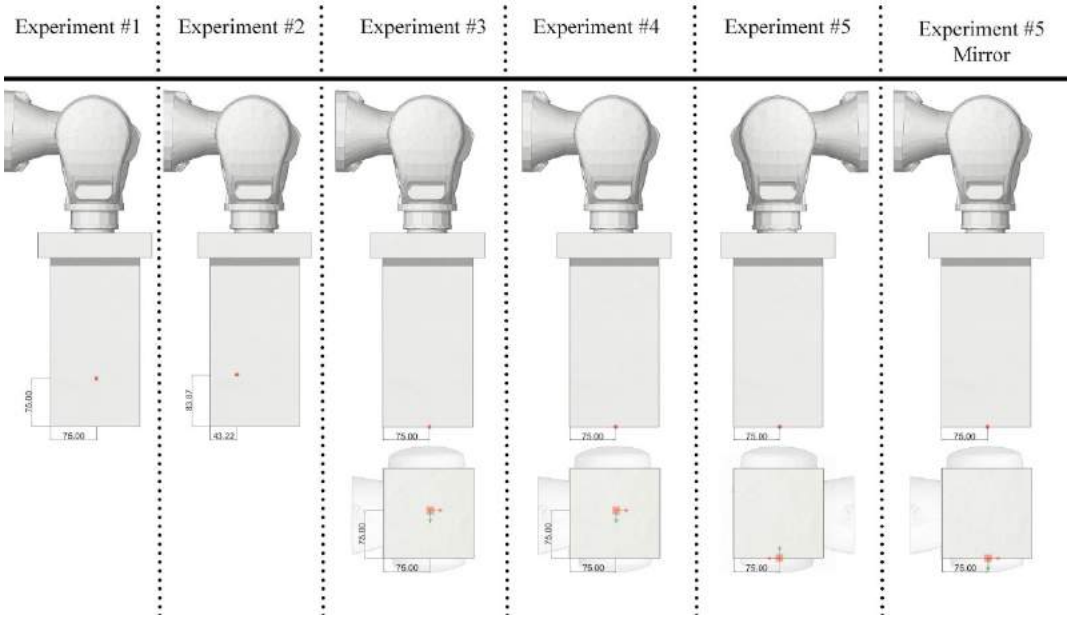

Figure 5.10. TCP positions cooperation

	Component Group Number	Component Number	Motion Number	Motion Path Plane Number	Motion Time
Experiment 1	4	58 (20 of them are panels)	7	7	149,7 sec
Experiment 2	5	65 (20 of them are planes)	6	16	164,1 sec
Experiment 3	5	65 (19 of them are planes)	6	16	151,2 sec
Experiment 4	10	96 (10 of them are planes)	5	20	147,5 sec
Experiment 5	7	82(10 of them are planes)	3	4	63,7 sec
Experiment 5 Mirror	7	85(10 of them are planes)	4	4	63,7 sec

Table 5.1. The difference in the Grasshopper codes between the six experiments. The significant difference is the motion time of experiments 5 and 5 mirror and others. The reason behind that difference is in experiment#5 and #5 mirror, robot arm does not go back to the home position after the cut is done.

5.2. Mathematical Precision and Accuracy

Simulating the motion of the robot allows minimizing the errors that may occur, as well as creating the most efficient way to experiment with the robot. Due to the simulation, the movement of the robot can be coded by minimizing the possibility of damaging the robot itself, material, or the objects around it.

Simulating only the movement of the robot would be enough for fabricating with a specified code. However, on some occasions, simulation of the fabricated product needed either. For researching with industrial robots, simulating only robot movement is inefficient for material, time, and energy use.

Some parametric robot control programs include the simulation of the robot movement and the product. In Robots add-on, robot movement can be simulated, but the product that fabricated with the robot cannot. Therefore, in this research, several product simulation systems added to the Grasshopper code. The first attempt was in experiment #4.

Simulation in Experiment #4

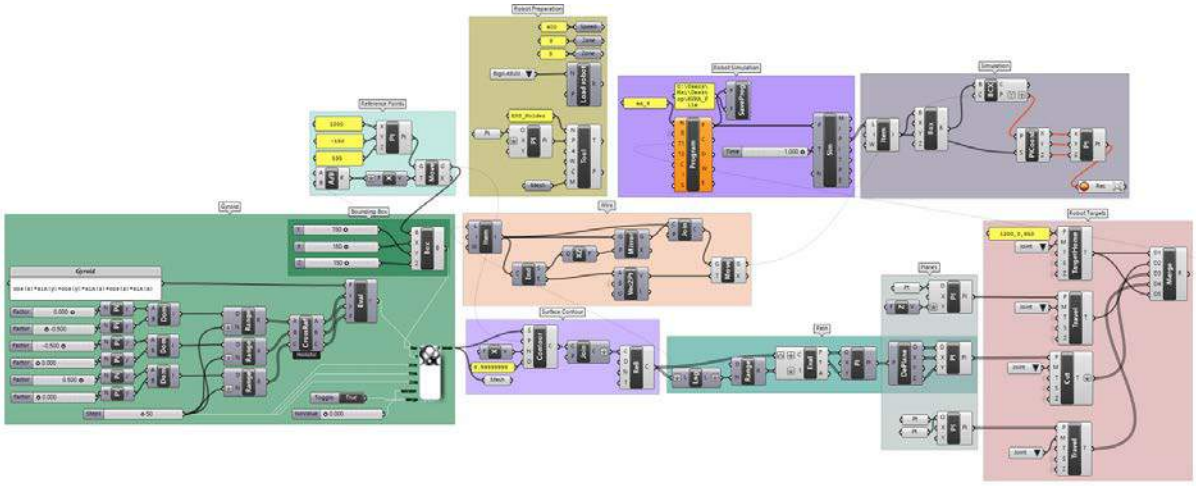

Figure 5.11. Grasshopper definition of experiment #4

Robots add-on does not simulate the product but, some information like the movement, planes, TCP can be obtained with the outputs of the **Program Simulation** component. In experiment #4 simulation, these outputs used to a minimum. In previous experiments, the front and the back edge of the Gyroid fundamental patch cut correctly. However, side edges not. This simulation basically coded to see the geometry of the side surfaces at the end of the cut. To achieve this, the intersection points of the wire with the EPS block attached to the robot along with the cut simulated.

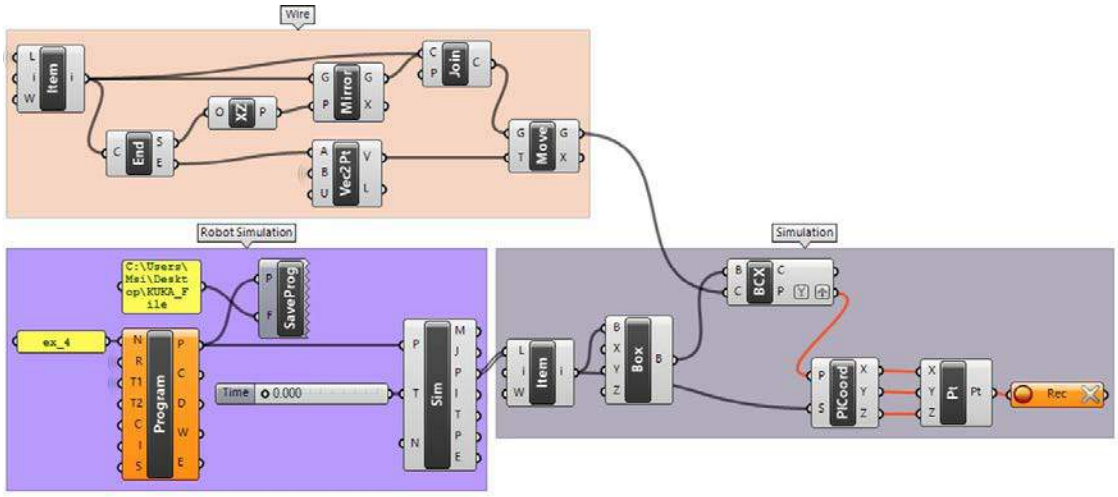

Figure 5.12. Grasshopper definition of the simulation in experiment #4

P output of the **Program Simulation**, which gives the TCP position planes as a list, connected to the **L** (Base List) input of the **List Item** component, which retrieves a specific item from a list. A box with the EPS foam block sizes generated with the **Box** component and **B** (Base) input connected with the **I** (item) output of the **List Item**. Through this connection, the box located in the same number and sequence where the TCP located. **BCX** (Brep | Curve) component used to solve intersection events for a curve and a brep, which are hot-wire curve, **G** output of the **Move** component, and EPS block, **B** output of the **Box** component. The intersection of these two items is two points in every position of the movement. To arrange the intersection points with the same sequence with the movement, the **PlCoord** (Plane Coordinates) component used, which gets the coordinates of a point in a plane axis system. In this file point to be coordinate is the output of the intersection and plane system is the TCP plane. Therefore, **P** input of the **PlCoord**

connected with the **P** output of the **BCX** component and **S** input connected with the **i** output of the **List Item**. **Construct Point** component used for recreating points with the same order on the (0,0,0) coordinate.

The output of the intersection changes through the movement. To make a simulation with all intersection points, they need to be collected. **Data Recorder** component used for collecting intersection points through the movement. The output of the **Construct Point** connected with the input of the **Data Record** component.

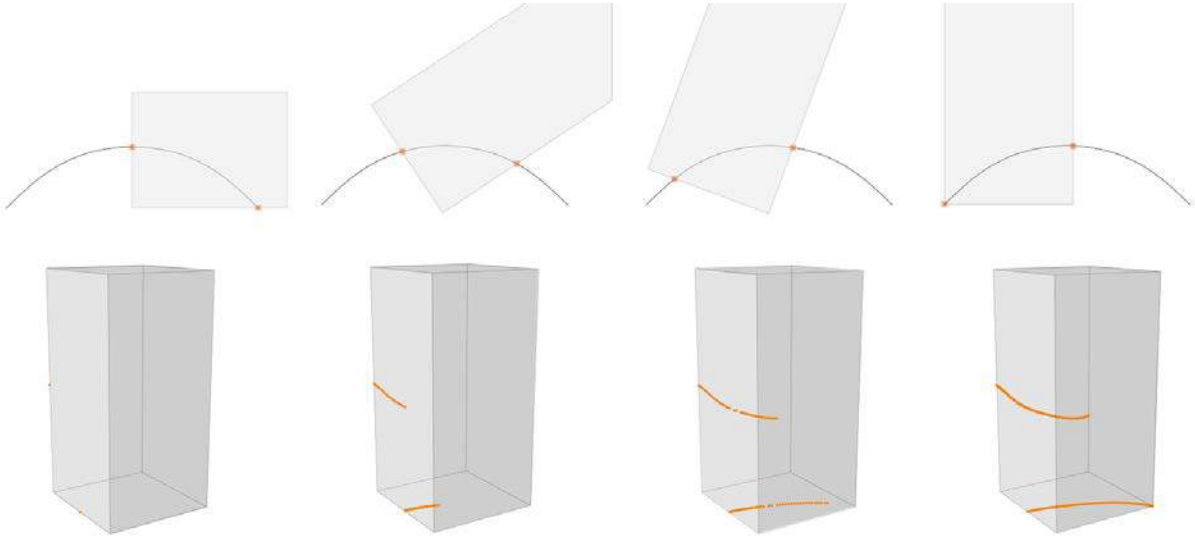

Figure 5.13. Experiment #4 simulation output

Simulation in Experiment #5

In experiment #5, a new simulation cod prepared, which generates sections of the final product with intersections of the EPS foam block and a surface formed from the wire geometry.

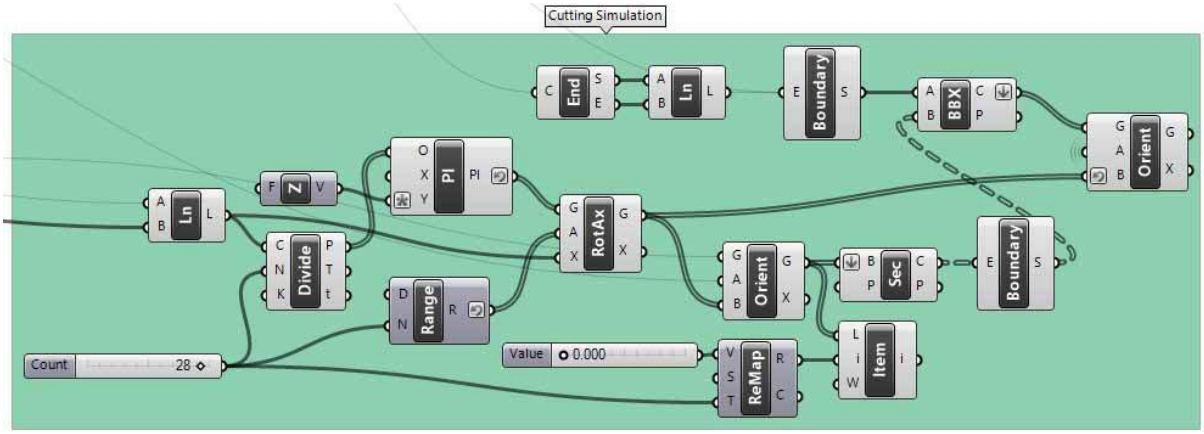

Figure 5.14. Grasshopper definition of the simulation in experiment #5

The block needs to be placed in the same order and rotation with the movement to intersect the EPS block geometry with the wire. Therefore the movement path, which is a straight line, divided into several segments defined by the user and placed planes that rotated to 90-degree on the division points. Block geometries with the same count placed on those planes by their TCP's with the **Orient** component. Sections of the block on a plane, where the wire located, generated with the **Blep | Plane** component. Those sections become surfaces with the **Boundary Surface** component. With another **Boundary Surface** component, a surface generated with the wire geometry and projection of it. The intersection of those two **Boundary Surface** components generated with the **Brep | Brep** component and intersections placed to the planes on the movement path them to be positioned in the correct order.

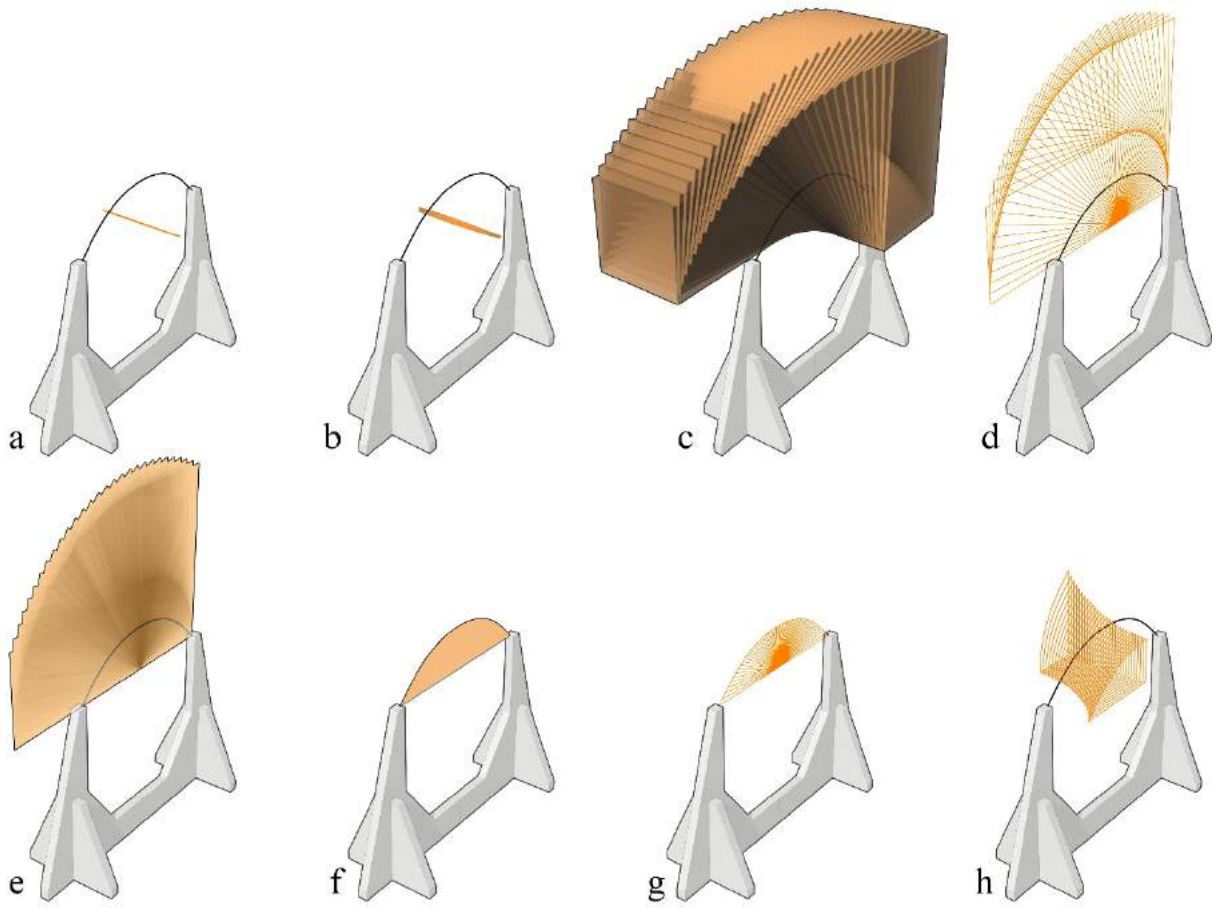

Figure 5.15. Experiment#5 simulation output **(a)** Movement path **(b)** Rotated planes on the movement path **(c)**Block placed to the planes **(d)** Sections of the blocks **(e)**Surfaces of the sections **(f)** Surface of the wire and projection **(g)** Intersections of the **(e)** and **(f) (h)** Final production simulation

The movement of the block in the simulation controlled by a slider called **Value**, which connected to the **ReMap** component. The final product of the cut simulated with the Orient component as subsequent sections. The number of sections controlled by the **Count Slider** connected to the **Divide**, **Range** and **ReMap** components

Simulation for All Experiments

The previous simulation works for only experiment#5 and mirror of it because of the movement paths are a straight line. Therefore, a new simulation code, which can work for any movement path, generated. In this simulation, the final digital product is a surface.

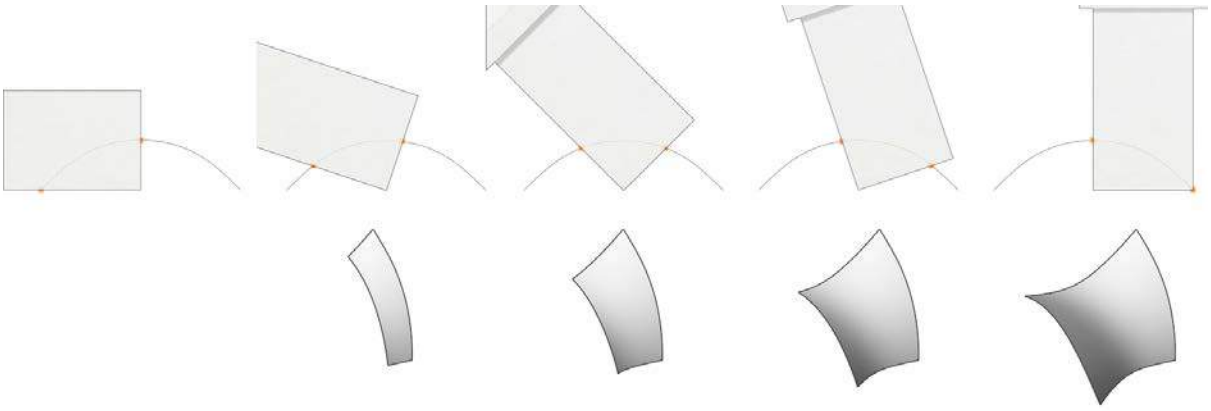

Figure 5.16. Simulation steps of the experiment#5 mirror with the simulation code

Every path has its own parameters, which others do not have. In order to generate a simulation code that fits every movement path, a component that each code has and TCP positions of the robot's movement of any movement is needed. The **Program Simulation** component outputs have both of the features that needed to create the simulation code. Other components and groups that every code collaboratively uses are the **Cutting Wire** group, **Robot Simulation** group, and **Load Robot** component. A new group as **System** generated, which includes all of those components. The simulation generates by intersection through the movement of the wire curve and the block.

M (System Meshes) and **P** (Plane) outputs of the **Program Simulation** component used and both of them separately connected to **L** (Base List) input of a **List Item** component. **P** output of the **Program Simulation** gives the TCP position planes as a list, **M** output gives system meshes as a list, which becomes the EPS block holder tool and block when they connected. **Mesh | Curve** (MCX) component used to make the intersection of the block and the wire. **X** (Points) output of the **Mesh | Curve** component connected to the **Curve Closest Point** components **P** (Point) input. **Curve Closest Point** component used for generating parameters of the point lists. **T** output of the **Curve Closest Point** component connected to the **L** (Base List) input of a **List Item** component. Outputs of the **List Item** component connected with the **Construct Domain** component. With domain and wire, the intersection curve can be generated by the **Sub Curve** component. Intersection curves placed according to TCP planes and origin point by **Orient**

component. **G** (Geometry) output of the **Orient** connected with the input of the **Data Record** component for collecting intersection points through the movement.

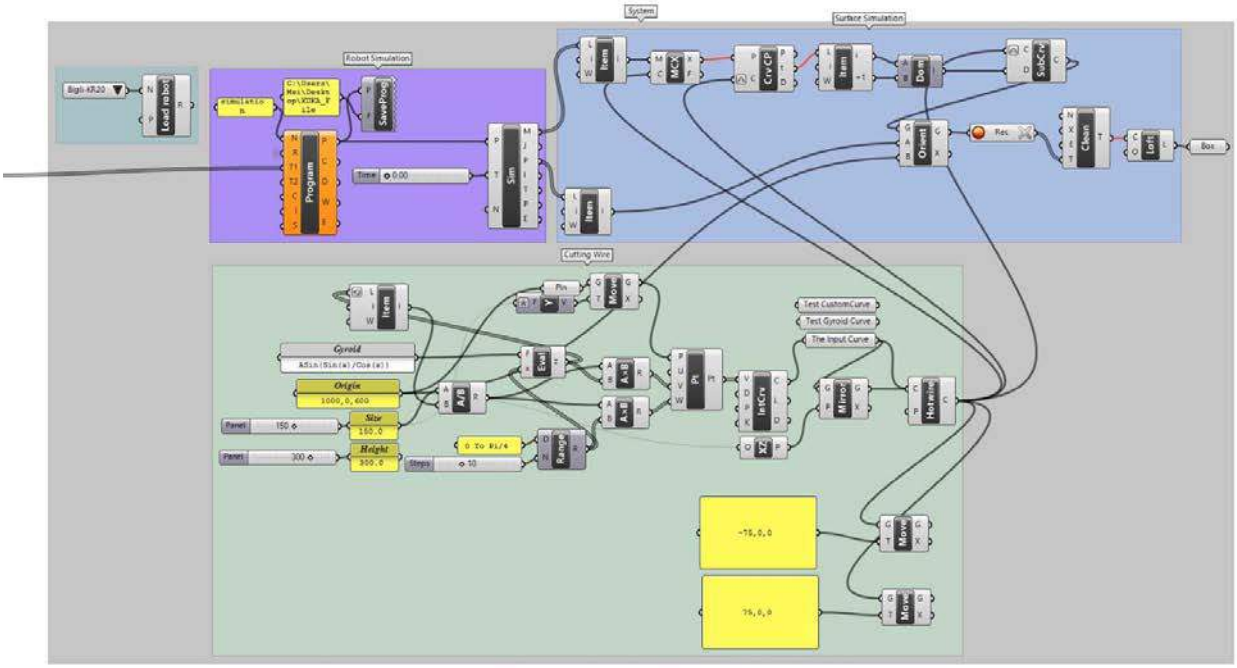

Figure 5.17. The simulation code

All six experiments added to the simulation code for simulating and comparing the digital and physical production. The output of the **Merge** component of the experiment needs to be connected to the **T1** input of the **Program** component to simulate any of them. For generating the final product surface, the **Data Record** component needs to reset, and **Number Slider,** which connected with the **T** input of the **Robot Simulation** component, needs to be slid. The **Number Slider** used for sliding the movement time. Sliding speed adjusts the number of the intersections, therefore, the resolution of the surface. The robot does not have to be moved by the **Number Slider**. A free-hand movement can play and control the speed by **Open Controls** panel, which opens with the right click to the **Robot Simulation.**

Final Generation and Simulation Code

It is possible to generate a Gyroid fundamental patch and variations of it by using the same logic and different wire with pervious simulation code. For simulating the output of the cut, the automatic time control system in the Open Control segment used. However, it observed that different simulations with the same speed generated fundamental patches with different dimensions. The error occurs due to the compulsion by collecting intersections of the wire and block with the **Record** component. In the meantime creating a loft the curves. Creating the patch in two phases as creating the curves first, then creating a loft with them could solve this problem. Therefore simulations created and bounding boxes dimensions of the outputs compared. More than a 3.6 mm difference observed between Gyroid fundamental patches created with 903 curves and a surface (Figure 5.18).

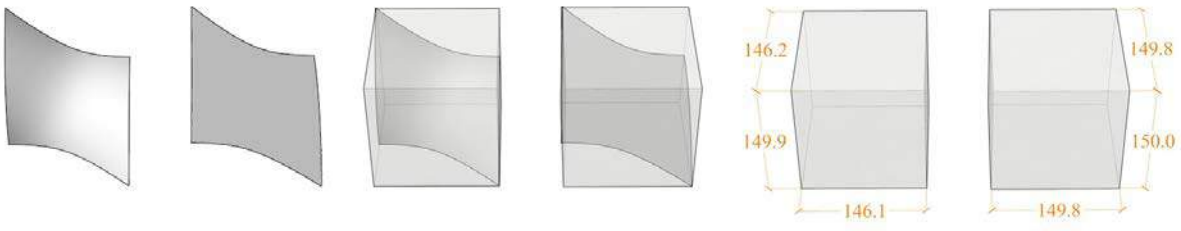

Figure 5.18. Comparing the result of the bounding boxes dimensions of the outputs of the simulations

Because of the error of the simulation, a new code created. Intersection curves placed with an **Orient** component instead of the **Record** component and time control made with the **Range** component. Intersections of the very first and last movement with the wire create the error for **Loft**. Therefore, the **Domain** of the **Range** component defined as 0.0001 to 0.99999.

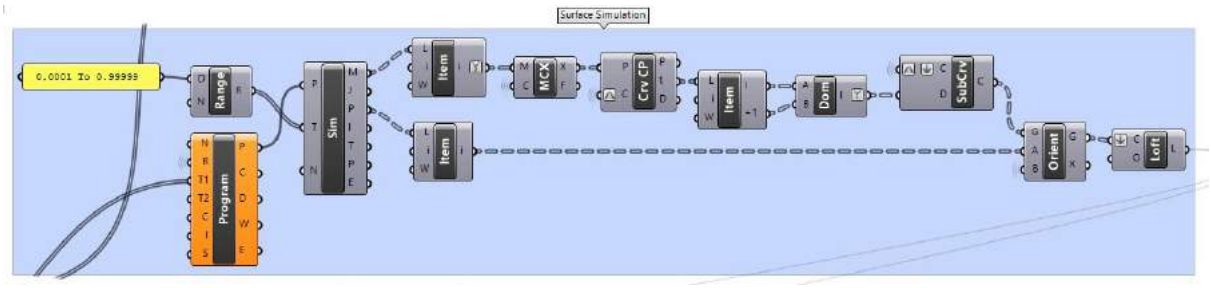

Figure 5.19. Surface simulation group of the final simulation code

Error Rate and Accuracy

The main objective of the thesis is not to create a 1 to 1 Gyroid, but to create a workflow with the Grasshopper and the robot, to turn this workflow into a design tool. Therefore, the produced unit is not a 1 to 1 Gyroid, but a Gyroid approximation. It aimed to test the production of the result of the designed workflow with the fabrication experiments. The research developed by the detected and corrected errors in the experiments throughout the process. After the completion of the workflow, the error rates determined of the fabrications made by using the final code. Thus, the causes and solutions for possible errors in production can be explained.

Primarily the code errors tested with the simulation code. The bounding box of the Gyroid fundamental curve generated with the simulation code should be 150x150x150 mm^3. If the code generates a wrong geometry, as a result, bounding box dimensions would be different from what should be. However, as a result of the test, the dimensions of the bounding box were 149.8x149.8x150 mm^3 (Figure 5.20).

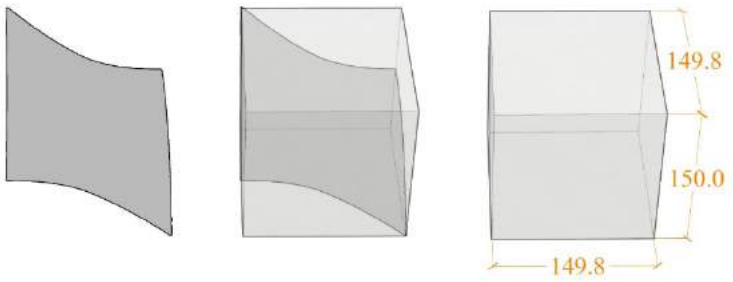

Figure 5.20. The result of the bounding box dimensions of the output of the final simulation

Since the error rate of the code is meager, it focused on the errors that may occur in operation. The interrupting unit modeled with a 3D scan and compared with the result of the equation to detect these errors.

The ideal Gyroid fundamental surface is the output of the equation. Therefore, to calculate the error rate, the distance of the two surfaces should be determined. A 3D scan model of the physical product created to find the error rate between the Gyroid equation model and

experiment#5 cut. To analyze the rate between two models, a code written in which the rate will be calculated by the distances of the point clouds to be generated on both meshes.

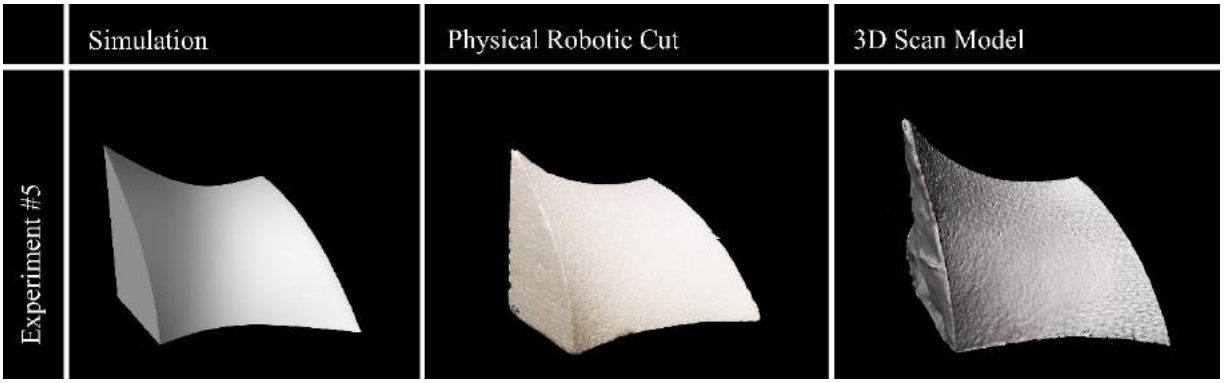

Figure 5.21. Comparison of simulation, physical and 3D scan outputs of the experiment#5

3D scan mesh consists of many small triangular meshes; therefore, the point cloud on the 3D scan model generated by the corners of the triangular meshes with the **Deconstruct Mesh** (DeMesh) component. Closest point projections of the point cloud on the equation mesh generated with the **Mesh Closest Point** (MeshCP) component. With the **Distance** (Dist) component, the distance difference between ideal and fabricated Gyroid fundamental patch surfaces can be calculated.

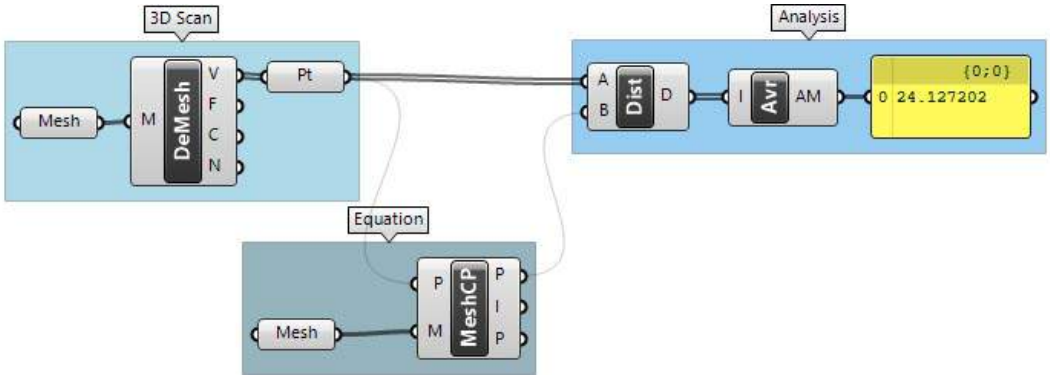

Figure 5.22. Error rate analysis code of the 3D scan and digital equation outputs of the experiment#5

The output of the error rate analysis is 24 mm. This analysis system can be used for every physical output in this research.

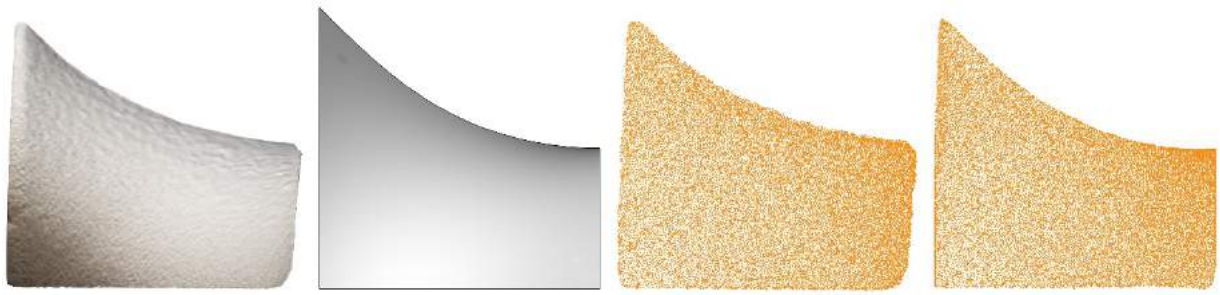

Figure 5.23. From left to right: 3D scan model; Equation output; Mesh endpoints of the 3D scan model; Closest points of the equation mesh and point cloud of the 3D scan model

The main reason for the errors in the unit is the sensitivity problem of the parameters used in operation. It is possible to divide the sensitivity errors that cause the wrong results of production into two groups as process and material. Errors that may arise from incomplete or incorrect operations during the process can be analyzed in two groups as calibration and tool. These errors can be corrected, improved, or completed by increasing sensitivity.

Tools can cause some errors in the process. Incorrect production of the form or dimensions of the frame of the hot wire cutter tool affects the form of the wire and causes the form to deform. In addition, because the dimensions of the frame differ from those of the digital model, the EPS block hitting the frame causes an incorrect cut.

If the EPS holder tool, which is attached to the end effector of the robot and holds the foam block, is not correct in size and holds the foam incorrectly or the foam is not constant throughout the process in the tool, the cut results in an error. Although the tool that holds the EPS block has been developed throughout the process, it is not functional enough. If this research repeated, the EPS holder tool should be reconsidered.

Calibration is another topic that affects the process of errors and causes the information transferred between the computer and the physical environment to be inaccurate. Correct calibration of the robot, base, the tool is important to reduce the error rate.

The unevenness of the ground on which the robot and the base located induce errors in the process. For this reason, the correct calibration of the tools and the transfer of the coordinate information to the digital environment ensure that the ground problems minimized.

Incorrect calibration of the robot causes the coordinates in which the TCP defined to be incorrect in the physical environment. This error causes the robot to follow coordinates other than the movement path. Inaccurate calibration of the base occasions the cutting to be incorrect due to the hot-wire cutting tool being placed on the base.

Tool calibration is important to ensure that the coordinates in which the wire positioned in the physical environment with the position defined in the computer environment are consistent. Otherwise, the cutting will be wrong even if the robot's movement path is correct.

As discussed above, the issue of calibration is a matter that needs to be considered for correct cutting. This problem should be considered in order to avoid communication problems between robot and Grasshopper.

Errors caused by material structure and interaction grouped according to the materials used in the research. Errors grouped as wire and EPS are less controllable than process errors.

Due to the heating of the wire, the expansion and deforming of the form cause faulty cutting. The subject of development, which varies according to the type of wire, can be minimized by choosing the wire considering this possible error.

The wrong form of the wire also causes errors in the resulting product, even if all details of the cut are correct. In this particular study, the wire should be precisely the same form of the Gyroid fundamental curve. The slightest change in the form causes errors in the cut. The thin wire is quite challenging to be inserted into a certain double curvature form. In the research process, different wires tried, and it decided that Nitinol wire was the most efficient.

The cooling of the wire in interaction with the EPS causes cut quality to deteriorate, and the wire to be entrained by the foam. Slightly higher heating of the wire may be the solution to this problem, but it leads to an increased error rate in other matters.

The heat of the wire is directly related to the melting of the foam. As the heat increases, melting increases and causes smaller cuts than required. In case of low temperature, the foam does not cut and creates the form of the wire to deform. The deformation rate of the wire varies by the temperature and the speed of movement of the EPS block.

The wrong size of the EPS block is another factor in the failure of the cut. The movement of the robotic arm, the dimensions of the tool, and the wire adjusted according to EPS block dimensions.

In addition, the newly generated code outcome of each experiment simulated and compared with the physical result of the cuts.

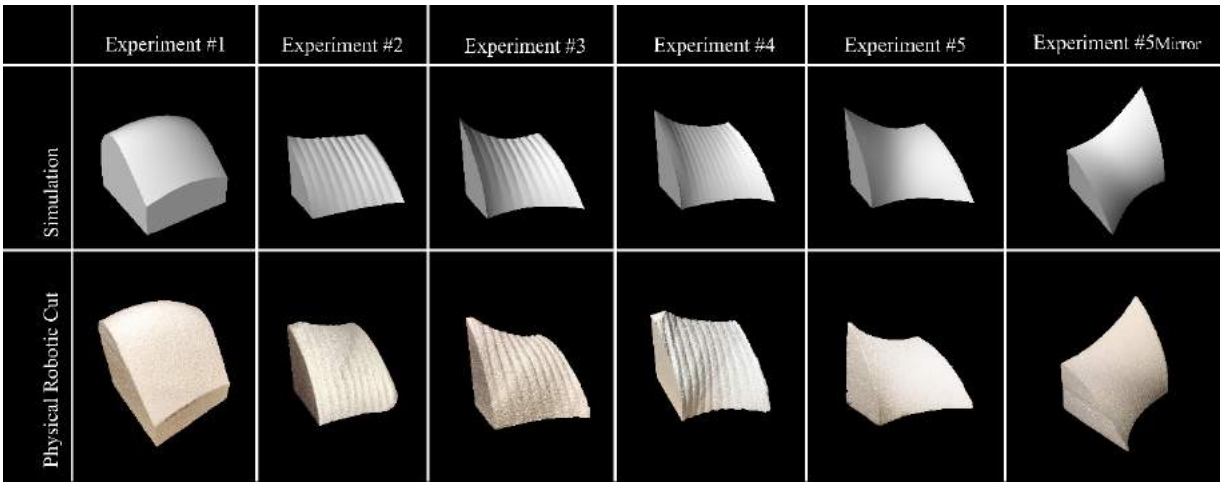

Figure 5.24. Comparison of the physical and digital products

5.3. Generative Design Potentials

The aim of the thesis is to produce a code that will allow the design-production process to operate in a controlled and integrated manner, beyond producing a Gyroid fundamental patch. The final code has been prepared in accordance with this goal. In order for the unit to be produced to grow, triply-periodic multiplication logic of the Gyroid has been added to de final code. With additions to the code, the holistic design can be experienced simultaneously as well as the control of the form of the produced unit.

Therefore, the final code includes five different simulation groups. Robot Simulation group generates robot movement simulation of the travel and cut movements and program creation for translating the code to the KRL. The surface Simulation group has the same simulation and program components with the Robot Simulation group. However, it only connected with the cut movement.

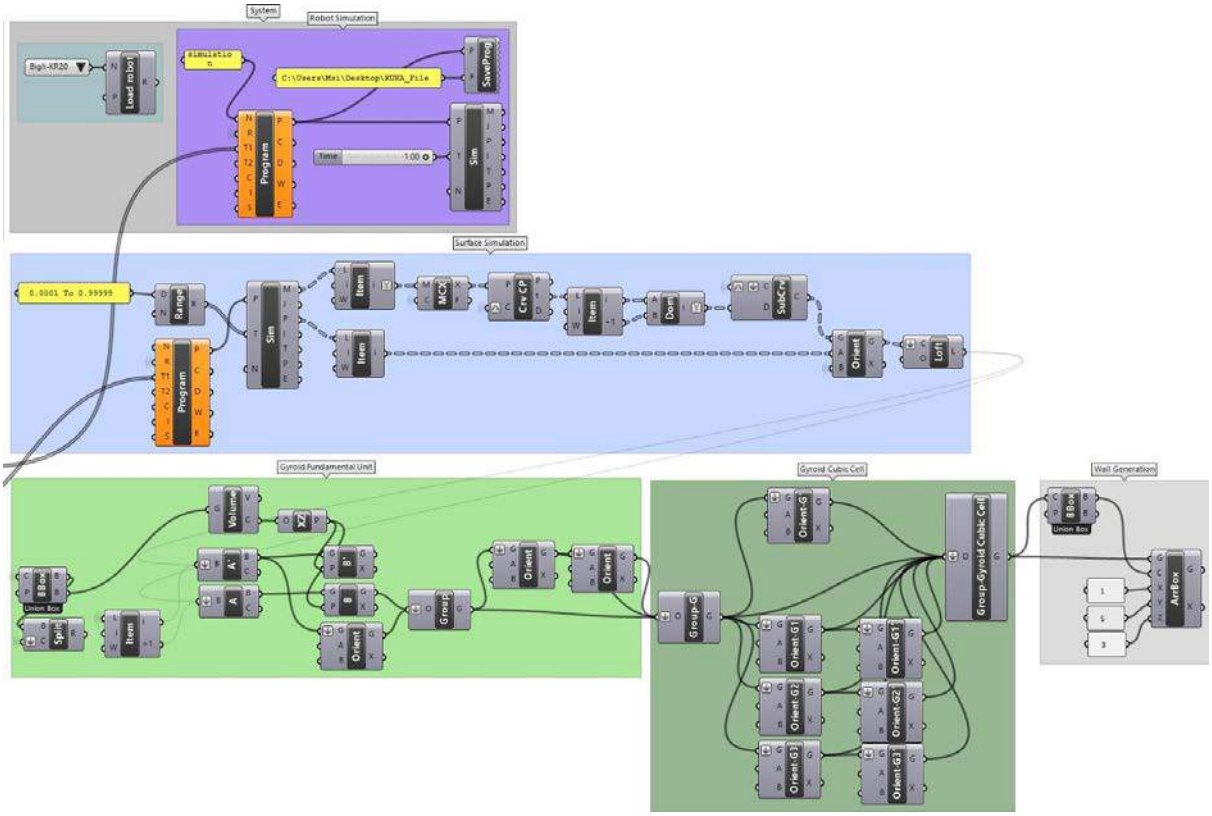

Figure 5.20. Simulation groups in final code

In the Gyroid Fundamental Unit group, bounding boxes of the fundamental patch and mirror of it split by them. As a result, **A, A', B, B'** units created. After creating the split units, a Gyroid fundamental unit generated with three different orientation of the A' and B units. B and A' units set generate a mirror of the created Gyroid fundamental unit. With two copies of a Gyroid fundamental unit and three rotation units of it with the **Orient,** the component generates a Gyroid cubic unit cell. As the final product in the digital environment, a wall generated by duplicating the Gyroid cubic unit cells with the **Array** component.

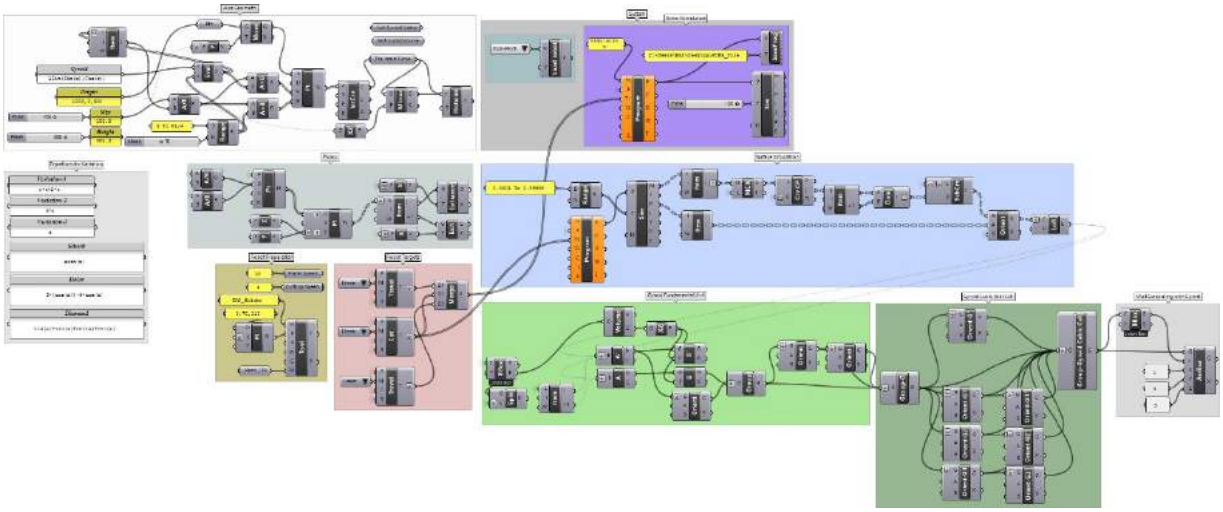

Figure 5.21. The final generation and simulation code

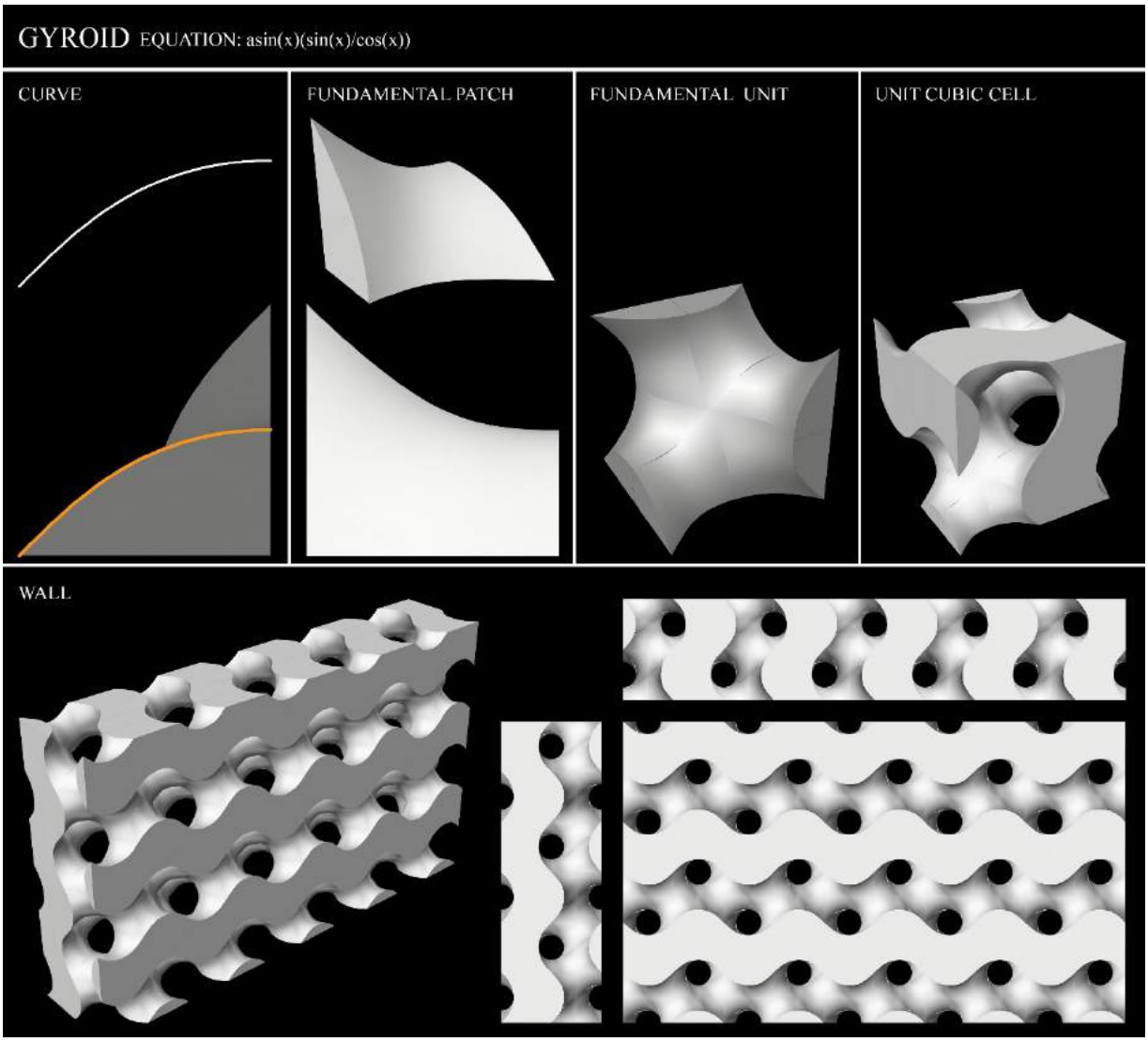

Figure 5.22. Gyroid production wire and final model

Changing the form of the wire and using the same cutting code provides a variation of the resulting form. Variations generate by changing the input component of the **Evaluate** (Eval) component in the Wire Geometry group (Figure 5.21). Wire form could change by defining a manually drawn curve as a wire or changing the equation. Simultaneously generates different wall forms according to the changes in the wire geometry.

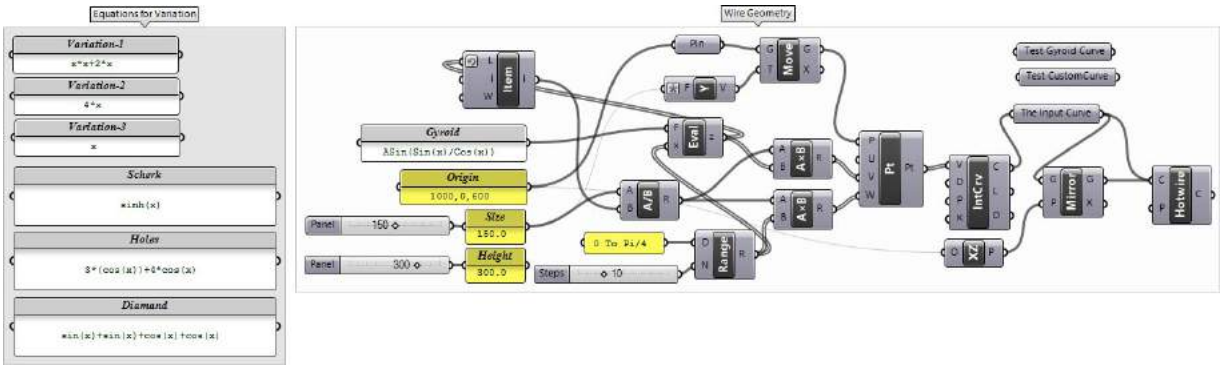

Figure 5.23. Wire geometry code and variation equations

The variation simulations that could occur by redefining the wire form listed with several examples (Figure 5.24.; Appendix B).

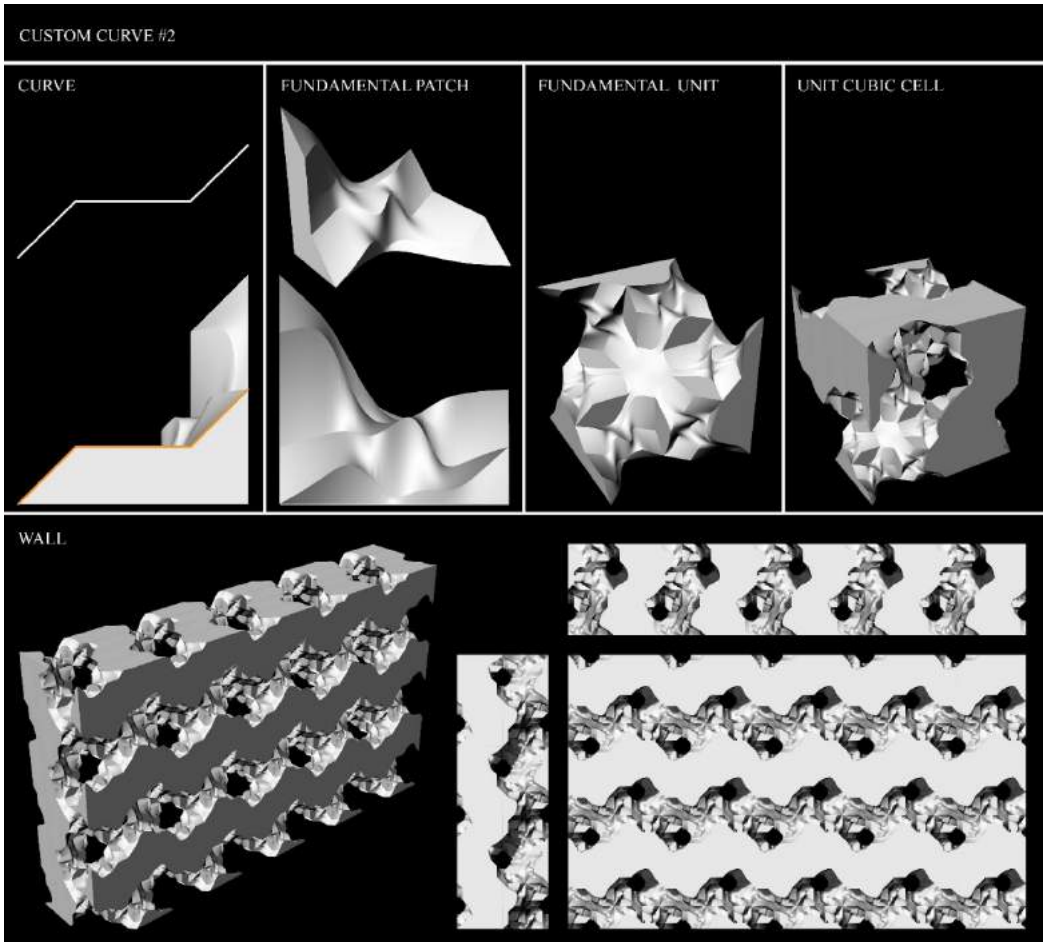

Figure 5.24. Variation #1; Product simulation of manually drawn wire curve

6. CONCLUSIONS

The practical aim of this thesis is to develop a set of workflows to fabricate modular systems that have double-curved surfaces by utilizing a robot-supported wire cutting approach. I call this original workflow as Non-Linear Hot-wire Cutting for future researches

Industrial robotic arms are mass production tools for performing the same job in the same quality and fast. Architectural robotic researches are generally not focusing on the robot's serial fabrication ability but the capability to perform the given job with precision. To provide advanced level researches, researchers work in an interdisciplinary environment and develop knowledge sets for issues like robot programming and manipulating, parametric modeling, and so on.

Within the scope of this thesis, after generating the workflow, the robot arm used as a mass production tool, and connection variation researched with the fabricated units. However, due to the lack of information, the flexibility of the robot fabrication to manufacture differently for each product has not been explored. In this thesis, the industrial robotic arm used as a precise fabrication tool to produce a precise geometry with an inaccurate fabrication method. Therefore, this research focuses not to fabricate exact Gyroid, but generate a workflow as a design tool with the approximation of the Gyroid surface.

New possibilities opened up in design and architecture by position and multi-task potentials of the industrial robots together with parametric design. With future technological developments, digital fabrication tools can be used more actively in the architectural construction field. Robots may need to construct architectural elements, perhaps even how the structures will produce themselves, simultaneously with the designs. In this case, architects may need to design workflows, not just final products. Writing the codes that the customer can determine by playing with the parameters and which can generate the final product, can become the design itself. If workflows are sufficiently parametric, designers may not need to produce a final product.

Practical Conclusions

With the generated workflow, this research proved that it is possible to control the fabrication of double-curved surfaces with robot-supported non-linear hot-wire cutting approach. However, this control required several skills and knowledge sets from the fields of computational design, robot programming, and digital fabrication. Throughout the research, the required skills developed from all three disciplines. The experiments in this research showed that the essential skill set might be right at the intersection of three fields.

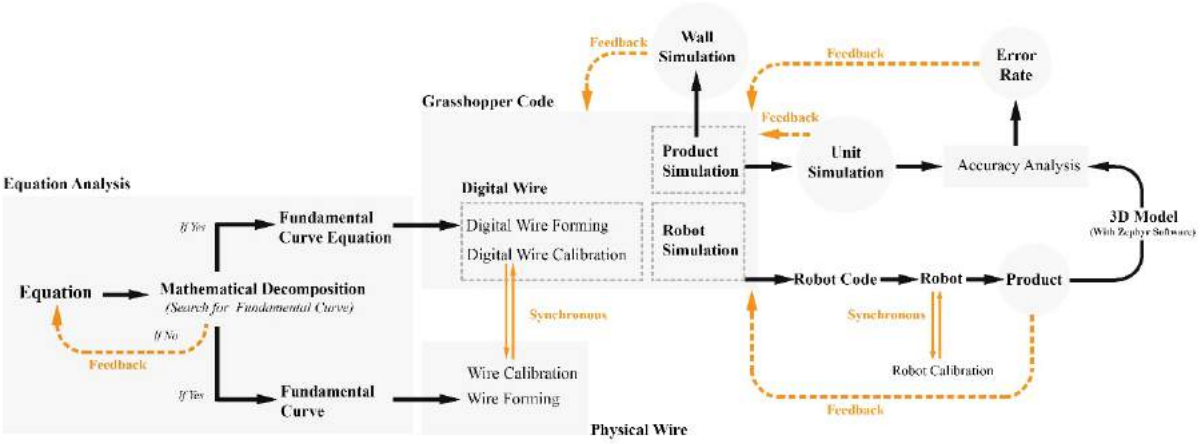

Figure 6.1. Research workflow diagram

During the research, some issues taken into consideration for the correct operation of the workflow. These are;

- The equation should be analyzed, and the fundamental curve equation needed for production should be established.
- The form and calibration of the wire in both digital and physical media should be correct.
- The calibration of the robot should be correct.
- The product should be analyzed and reproduced if necessary.
- Simulation plays an important role in getting feedback without cutting.

In addition, topics like hotwire cutting methods and tools, material research, wire forming, geometric structure of mathematical surfaces researched during workflow generation.

Scope Oriented Conclusions

This research carried out by an architectural researcher who is a non-expert in robot programming and parametric modeling. The outcome of this research could be advanced by developing the potentials of the minimal surface variations, robotic production flexibility, and parametric modeling possibilities.

Architectural-Computational Design Conclusions

The outcomes of the research can be improved, diversified, and error rates reduced in a more controlled environment. Various parameters can be added to the Grasshopper code for different needs. It is possible to produce the research as an architectural element with different scales, diversification, and other materials. The produced EPS modules can be used as molds or base for concrete spraying. Robot supported Non-Linear Hotwire Cutting system can be used for the production of pre-sketch models for the production of double-curved structural elements to be produced by different systems like 3D print or marble carving. Grasshopper code can be used for robot code generation, variation, and simulation in sketch model production.

Computer Programming Outcomes

With the advances in technology and shift in architectural production, architects can also write programs. Most add-ons used by designers have been developed by architects such as Grasshopper, Robots, and Millipede. In this research, which is under the field of architecture, a code was written in which the final product was obtained as intended. However, there have been difficulties with some issues related to code writing. For instance, the module could not be fabricated using any desired geometry and equation and caused the limitation of variation. The reason for the difficulties and deficiencies in code generation is the lack of knowledge. It is possible to optimize, simplify, diversify, and generalize the final code through more interdisciplinary work with the field of computer science.

Digital Robotic Fabrication Conclusions

Robotic arms used in several ways in architecture research. As a non-expert user of the industrial robotic arm and parametric robot control systems, the industrial robotic arm used as a production tool in the basic state in the thesis research. The digital production potentials can incase by manipulating the mechanical structure of the robot system. In the scope of digital robotic fabrication, problems related to sensitivity can be solved through interdisciplinary work with robotic engineering.

In summary, the conclusions of the scope reminded again that, although architects can do many things, architectural-computational design research is an interdisciplinary field.

Outcomes

With the research conducted within the extent of the thesis, the Non-Linear Hotwire Cutting method invented. In thermal cutting, hot blades used when the cutting tool needs to form. With this research, it is revealed that cutting can also be done by giving form to the wire. Nitinol wire used to form the wire by heating through the method of forming the wire. Non-linear hotwire cutting production method has been optimized with the development of topics such as the frame of the wire EPS holder, wire type, wire forming procedure, which were not used for robotic hotwire cutting fabrication with curved wire. Robot code is a unique product that is generated within the scope of the thesis and works in integration with the design-production process. Advanced work with the modules of the Grasshopper code makes it possible to generate the code for the robot to run without the need for a Robots plug-in.

REFERENCES

Akipek, F. Ö. (2018, May). Kent-Doğa Arakesitinde Sıkıştırılmış Toprak Bir Duvar: "Komün-Aksiyon Duvarlar". (D. İncedayı, Ed.) *Mimarist*(62), 28-34.

Aziz, M. S., & El Sherif, A. Y. (2016). Biomimicry as an Approach for Bio-inspired Structure with the Aid of Computation. *Alexandria Engineering Journal*, *55*(1), 707-714. doi:10.1016/j.aej.2015.10.015.

Bognar, B. (2017, May 8-9). Structure and Space Realization of Toyo Ito's National Taichung Theater. In M. Anderson, & P. Anderson (Ed.), *Proceedings of the 5th Annual International Conference on Architecture and Civil Engineering*, (pp. 307-316). Singapore. doi:10.5176/2301-394X_ACE17.86

Braumann, J., & Brell-Cokcan, S. (2012). Digital and Physical Computing for Industrial Robots in Architecture. In T. Fischer, K. De Biswas, J. J. Ham, R. Naka, & W. X. Huang (Ed.), *Beyond Codes and Pixels: 17th International Conference on Computer-Aided Architectural Design Research in Asia (CAADRIA)*, (pp. 317–326). Hong Kong.

Chen, J. (2016). *The Minimal Surface Problem.* Master Thesis, University of California.

Dönmez, B., Özkan, B., & Kadıoğlu, S. (2010). Precise Position Control Using Shape Memory Alloy Wires. *Turkısh Journal Of Electrıcal Engıneerıng & Computer Scıences*, 899-912.

FABLAB. (2017). MATTER & MAKING. (R. Glynn, & B. Sheil, Eds.) *Fabricate 2011: Making Digital Architecture*, pp. 73-84.

Felbrich, B., Früh, N., Prado, M., Saffarian, S., Solly, J., Vasey, L., . . . Menges, A. (2017). Multi-Machine Fabrication: An Integrative Design Process Utilising an Autonomous UAV and Industrial Robots for the Fabrication of Long-Span Composite Structures. In T. Nagakura, S. Tibbits, & C. Mueller (Ed.), *Disciplines & Disruption : Projects Catalog of the 37th Annual Conference of the Association for Computer Aided Design in Architecture (ACADIA)*, (pp. 248-259). Cambridge, MA.

Fritschi, L. E., Reiter, L., Wangler, T., Gramazio, F., Kohler, M., & Flatt, R. J. (2017). Smart Dynamic Casting Slipforming with Flexible Formwork-Inline Measurement and Control. *Second Concrete Innovation Conference (2nd CIC).* Tromsø.

Gandy, P. J., & Klinowski, J. (2000). Exact Computation of the Triply Periodic G (`Gyroid') Minimal Surface. *Chemical Physics Letters, 321*(5-6), 363-371.

Gasparetto, A., & Scalera, L. (2019). A Brief History of Industrial Robotics in the 20th Century. *Advances in Historical Studies, 8*(01), 24-35. doi:10.4236/ahs.2019.81002

Hua, H., & Jia, T. (2018). Wire Cut of Double-Sided Minimal Surfaces. *The Visual Computer, 6-8*(26), 985-995. doi:10.1007/s00371-018-1548-0

Ichbiah, D. (2005). *Robots : From Science Fiction to Technological Revolution.* (K. Kincaid, Trans.) New York: Harry N. Abrams.

Ito, T. (2006). Change the Geometry to Change the Architecture. *Proceedings of the 11th International Conference on Computer Aided Architectural Design Research in Asia*, (pp. 7-18). Kumamoto, Japan.

Ito, T. (2016, December). Grand Opera. (N. R. Pollock, Interviewer) Retrieved November 18, 2019, from https://www.architecturalrecord.com/articles/12040-national-taichung-theater-by-toyo-ito-associates

Ivanovskis, L. (2017). *Four Axis Hot-Wire Foam Cutter Controlled by Mindstorms EV3.* Degree Programme in Mechanical Engineering and Production Technology Thesis, The Saimaa University of Applied Sciences.

Jani, J. M., Leary, M., Subic, A., & Gibson, M. A. (2014). A Review of Shape Memory Alloy Research, Applications and Opportunities. *Materials & Design (1980-2015), 56*, 1078-1113. doi:10.1016/j.matdes.2013.11.084

Jobes, C. C. (1988). *Robot Programming.* Pleasant Hills, PA: Boeing Services International.

Jovanović, M., Vucic, M., Mitov, D., Tepavčević, B., Stojakovic, V., & Bajsanski, I. (2017). Case Specific Robotic Fabrication of Foam Shell Structures. In A. Fioravanti, S. Cursi, S. Elahmar, S. Gargaro, G. Loffreda, G. Novembre, & A. Trento (Ed.), *Proceedings of the 35th International Conference on Education and Research in Computer Aided Architectural Design in Europe (eCAADe), 2*, pp. 135-142. Rome, Italy.

Kaftan, M., & Stravric, M. (2013). Robotic Fabrication of Modular Formwork. In R. Stouffs, P. Janssen, S. Roudavski, & B. Tunçer (Ed.), *Proceedings of the 18th International Conference on Computer-Aided Architectural Design Research in Asia (CAADRIA),* (pp. 75-84). Singapore.

Moran, M. E. (2007, June). Evolution of Robotic Arms. *Journal of Robotic Surgery, 1*(2), 103-111. doi:10.1007/s11701-006-0002-x

Niemeyer, G., Preusche, C., & Hirzinger, G. (2008). Telerobotics. In B. Siciliano, & O. Khatib (Eds.), *Springer Handbook of Robotics* (pp. 1085-1105). Springer.

Niku, S. B. (2001). *An Introduction to Robotics Analysis, Systems, Applications.* Upper Saddle River: Prentice Hall.

Pollock, N. R. (2016, December). *Grand Opera.* Retrieved November 18, 2019, from Architectural Record: https://www.architecturalrecord.com/articles/12040-national-taichung-theater-by-toyo-ito-associates

Rossi, M., & Buratti, G. (2017). Form is Matter. Triply Periodic Minimal Surface Structures by Digital Design Tools. In A. Fioravanti, S. Cursi, S. Elahmar, S. Gargaro, G. Loffreda, G. Novembri, & A. Trento (Ed.), *ShoCK – Sharing of Computable Knowledge - Proceedings of the 35th International Conference on Education and Research in Computer Aided Architectural Design in Europe*, (pp. 259-268). Rome.

Rust, R., Gramazio, F., & Kohler, M. (2016). Force Adaptive Hot-Wire Cutting: Integrated Design, Simulation, and Fabrication of Double-Curved Surface Geometries. In A. Menges, & M. Pauly (Ed.), *Proceedings of the Advances in Architectural Geometry*, (pp. 288-305). Zurich, Switzerland. doi:10.3218/3778-4_20.

Schoen, A. H. (1970). *Infinite Periodic Minimal Surfaces Without Self-intersections.* NASA TN D. National Aeronautics and Space Administration.

Sierra, F., & Rodriguez, C. M. (2014, December 1). Architectural Envelope Systems Based on Triply Periodic Minimal Surfaces. *International Journal of Space Structures*, *29*(4),

Stereotomy of Wave Jointed Blocks. (2016). In D. Reinhardt, R. Saunders, & J. Burry (Eds.), *Robotic Fabrication in Architecture, Art and Design* (pp. 284-293). Switzerland: Springer International Publishing.

Tenu, V. (2009). *Minimal surfaces as self-organizing systems: a particle-spring system simulation for generating triply periodic minimal surface tensegrity structure.* Masters Thesis, UCL (University College London).

Vamvakidis, S. (2007). The Sponge Epidermis: A Study on Minimal Surfaces & Porosity. *Proceedings of the 25th eCAADe Conference*, (pp. 927-934). Frankfurt, Germany.

Wallén, J. (2008). *The History of the Industrial Robot.* Linköpings Universitet, Electrical Engineering, Linköping.

Weber, M., & Wolf, M. C. (2011). About the Cover: Early Images of Minimal Surfaces. *Bulletin of the American Mathematical Society*, *48*, 457-460.

URL REFERENCES

URL-1 <https://www.archdaily.com/157658/ad-classics-expo-58-philips-pavilion-le-corbusier-and-iannis-xenaki> Retrieved 15.11.2019

URL-2 <https://www.youtube.com/watch?time_continue=3&v=-IW7o25NmeA&feature=emb_logo> Retrieved 15.11.2019

URL-3 <https://www.archdaily.com/623689/ad-classics-german-pavilion-expo-67-frei-otto-and-rolf-gutbrod> Retrieved 15.11.2019

URL-4 <https://www.sciencedirect.com/science/article/pii/S0141029618339786#f0005> Retrieved 15.11.2019

URL-5 <https://medium.com/designscience/1976-57636ff1f122> Retrieved 15.11.2019

URL-6 <http://apps.baltimorecity.gov/Art_Culture_Map/public/130.html> Retrieved 15.11.2019

URL-7 <http://www.bridgesmathart.org/art-exhibits/jmm08/sequin.html> Retrieved 15.11.2019

URL-8 <http://www.vladtenu.com/2011/minimal-surfaces-as-architectural-prototypes/> Retrieved 15.11.2019

URL-9 <https://74fdc.wordpress.com/2012/02/23/erwin-hauer-modular-constructivist/> Retrieved 16.11.2019

URL-10 <https://www.architecture.yale.edu/exhibitions/62-still-facing-infinity-the-tectonic-sculptures-of-erwin-hauer> Retrieved 16.11.2019

URL-11 <https://www.archdaily.com/796428/toyo-itos-taichung-metropolitan-opera-house-photographed-by-lucas-k-doolan> Retrieved 16.11.2019

URL-12 <https://external-preview.redd.it/c8IeiqcSseJhiCVUkas0L7NWXIbhfB6MkRUuELjCSwc.jpg?auto=webp&s=4dab8bdafd713e7aa5ec5a77a65e5b16f10e5a76> Retrieved 16.11.2019

URL-13 <https://www.archdaily.com/796428/toyo-itos-taichung-metropolitan-opera-house-photographed-by-lucas-k-doolan> Retrieved 16.11.2019

URL-14 <http://www.khoavu.com/projects#/new-page-2/> Retrieved 18.11.2019

URL-15 <http://www.khoavu.com/meditationclub/> Retrieved 18.11.2019

URL-16 <https://parametricmonkey.com/teaching/hku-groovy-tectonics/>
Retrieved 18.11.2019

URL-17 < http://www.matterdesignstudio.com/#/periscope/ > Retrieved 20.11.2019

URL-18 < https://www.semanticscholar.org/paper/Case-Specific-Robotic-Fabrication-of-Foam-Shell-Jovanovi%C4%87-Vucic/e8e81595df7ebcf1453623ac6fe4211868e9e240 >
Retrieved 22.11.2019

URL-19 < https://gizmodo.com/how-the-atomic-age-gave-us-robot-surgeons-1704168204 >
Retrieved 02.12.2019

URL-20 < http://cyberneticzoo.com/teleoperators/1954-electromechanical-manipulator-ray-goertz-american/ > Retrieved 02.12.2019

URL-21 < https://ifr.org/robot-history > Retrieved 05.12.2019

URL-22 < http://gramaziokohler.arch.ethz.ch/web/e/forschung/223.html >
Retrieved 06.12.2019

URL-23 <https://www.archdaily.com/869450/icd-itke-research-pavilion-2016-17-icd-itke-university-of-stuttgart?ad_medium=gallery> Retrieved 06.12.2019

URL-24 < http://facstaff.susqu.edu/b/brakke/evolver/examples/periodic/periodic.html >
Retrieved 08.11.2019

URL-25 < http://erwinhauer.com/eh/about/#2 > Retrieved 16.11.2019

URL-26 < https://www.robots.com/robots/kuka-kr-20-3 > Retrieved 27.09.2019

URL-27 < https://www.spinneybeck.com/index.php?/collaborators/view/erwin-hauer >
Retrieved 16.11.2019

URL-28 < https://roboticsbook.com/milling-cnc-machine-vs-industrial-robot/>
Retrieved 04.10.2019

URL-29 < https://wewanttolearn.wordpress.com/2019/02/03/triply-periodic-minimal-surfaces/ > Retrieved 12.06.2019

URL-30 < http://potplus.org/tr/komun-aksiyon-duvarlar-1/ > Retrieved 16.02.2020

URL-31< https://www.semanticscholar.org/paper/Wire-cut-of-double-sided-minimal-surfaces-Hua-Jia/8d63f3d479d373e1382fdc6c1e94480d929160d6 >
Retrieved 17.02.2020

APPENDIX-A: Deformation Research of Minimal Surfaces

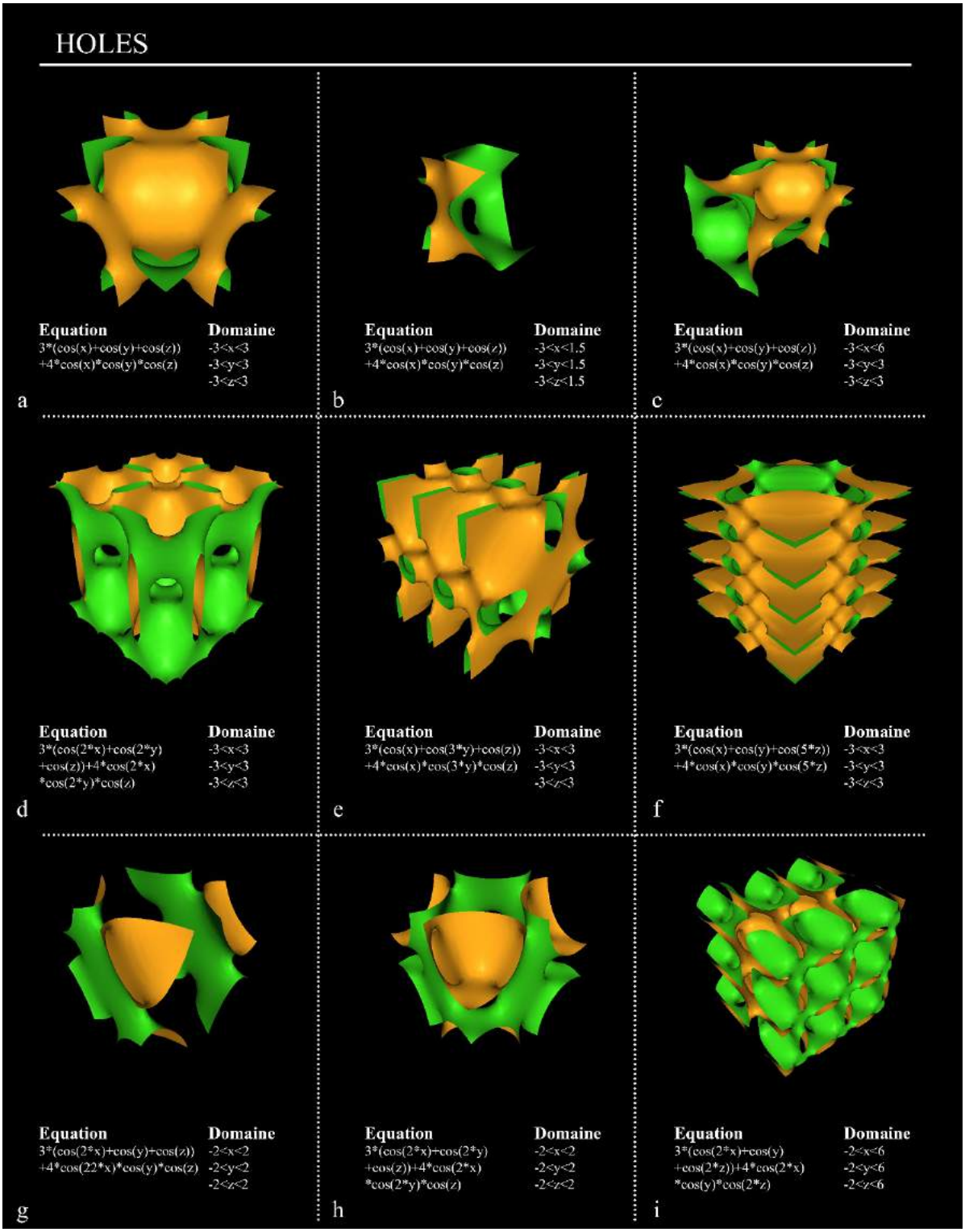

Figure A.1 Variation of Holes minimal surface by changing the equation

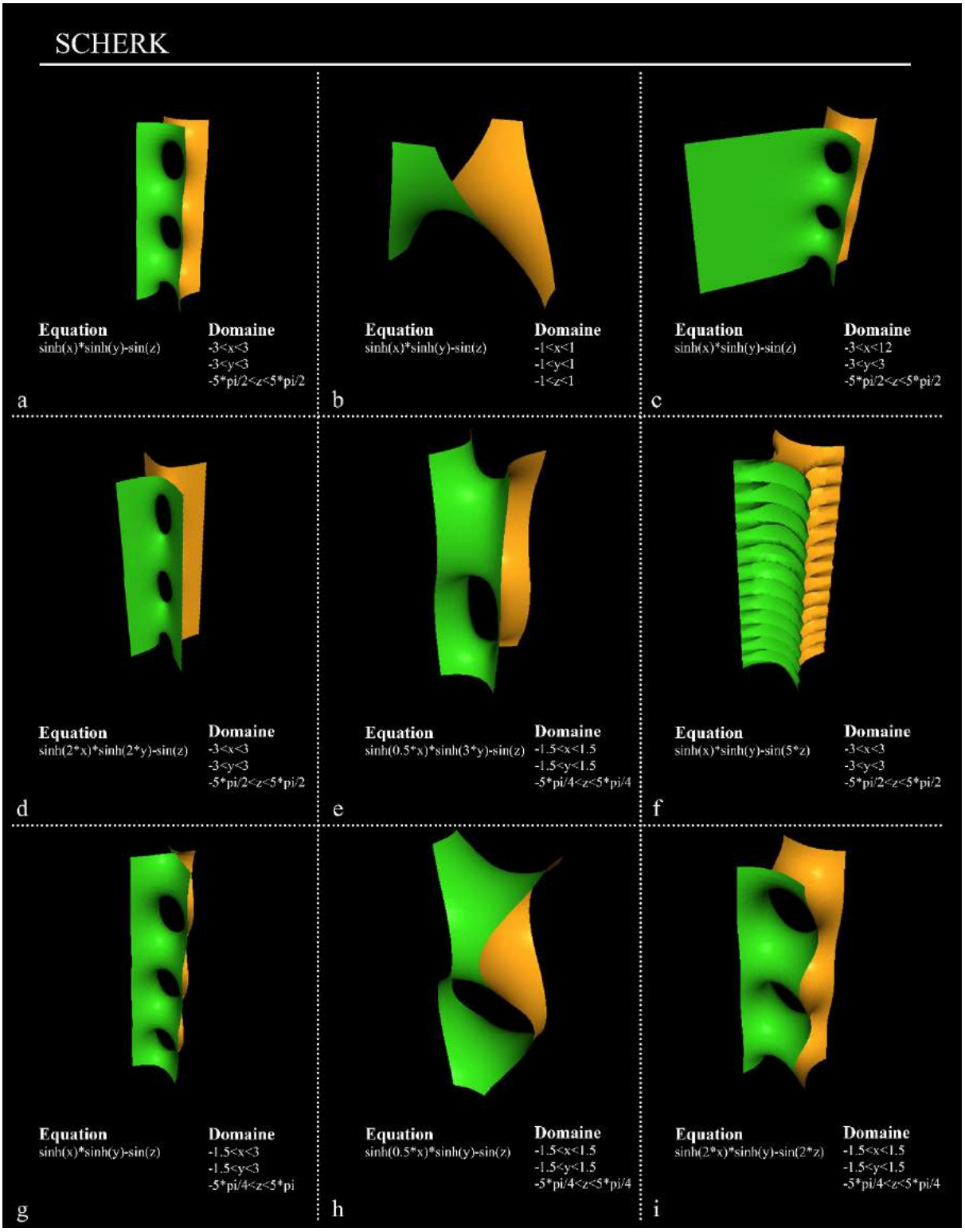

Figure A.2. Variation of Scherk minimal surface by changing the equation

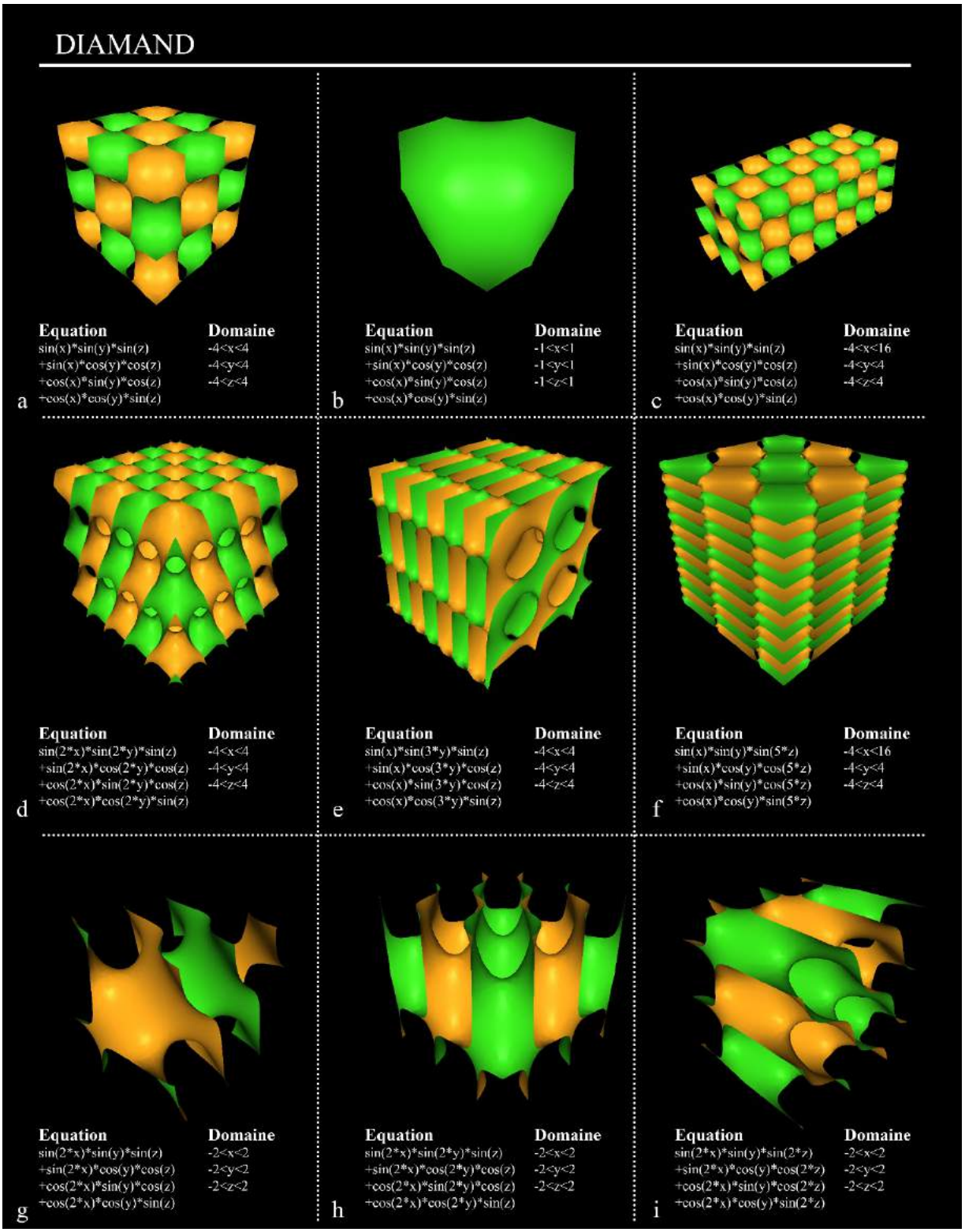

Figure A.3. Variation of Daimand minimal surface by changing the equation

APPENDIX-B: Fundamental Patch Connection Lists

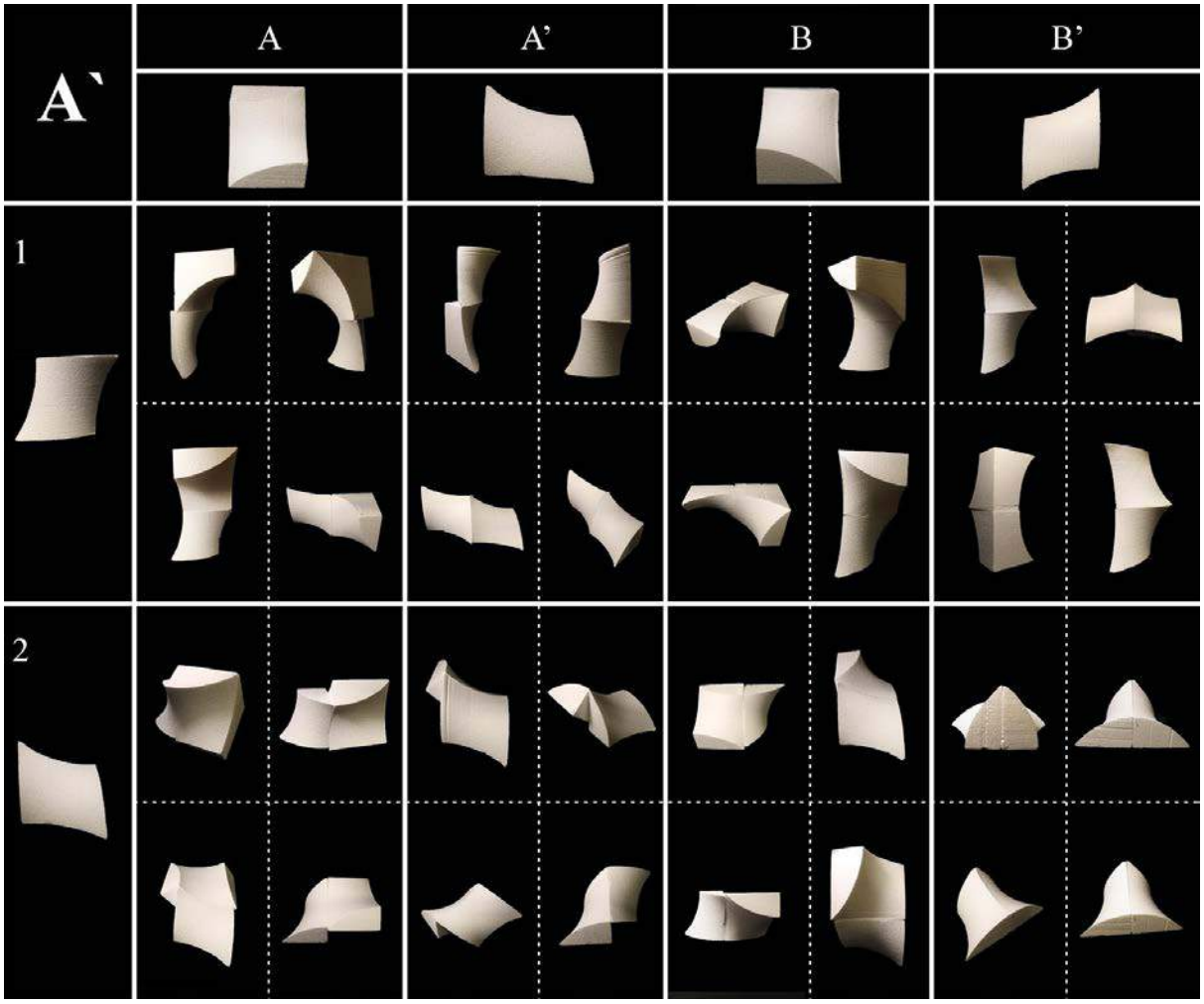

Figure B.1. Connection combination list of A' fundamental patch

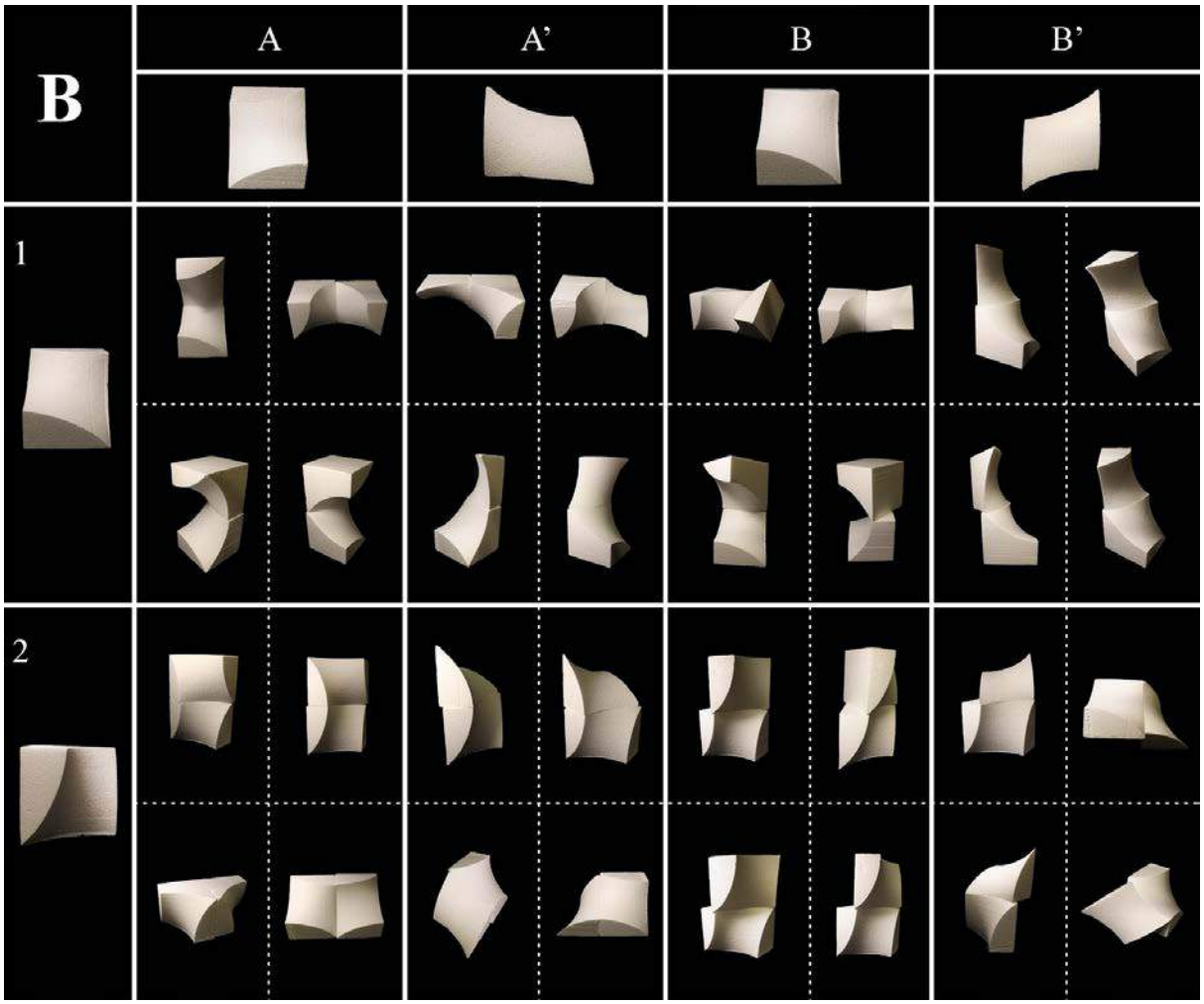

Figure B.2. Connection combination list of B fundamental patch

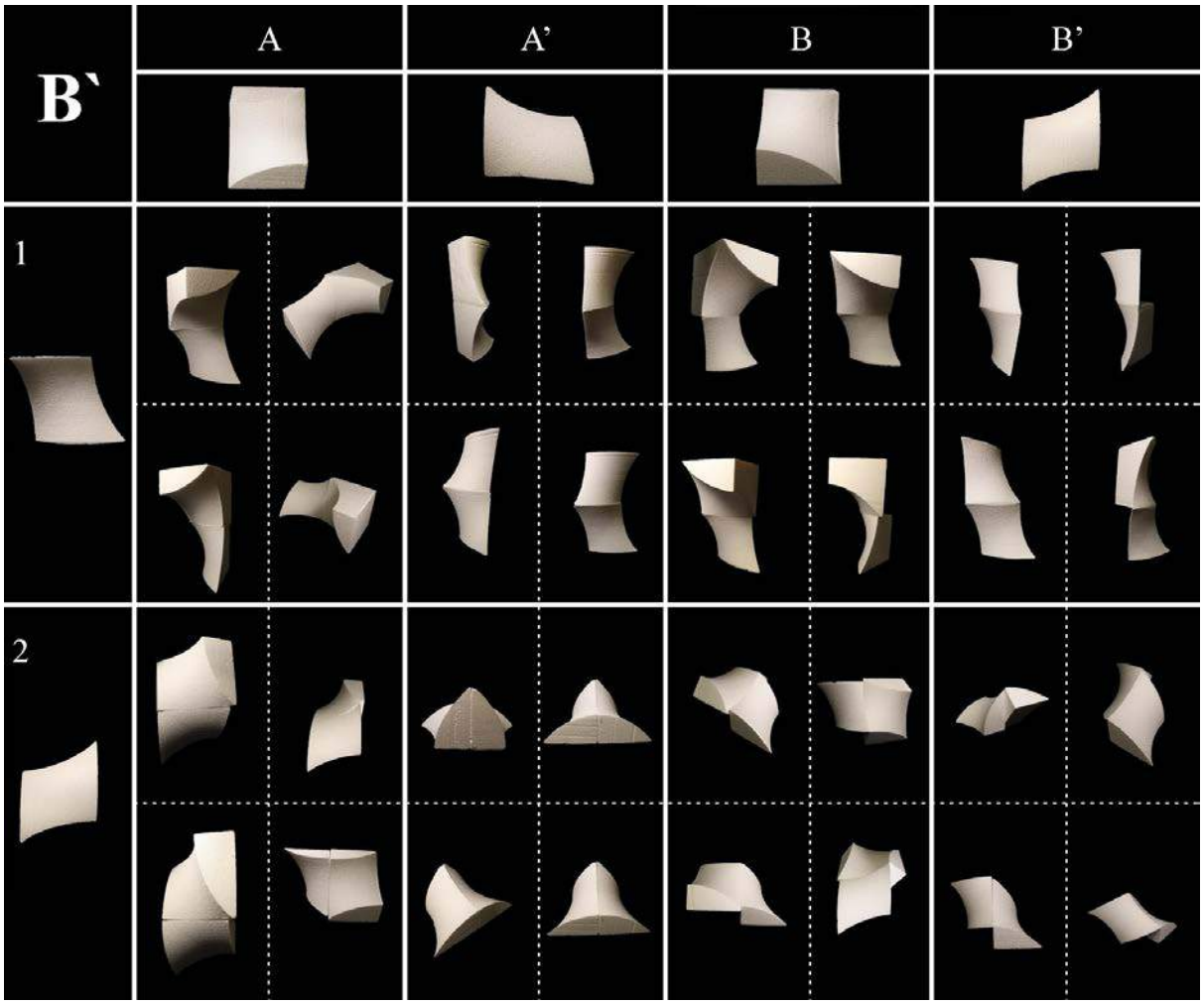

Figure B.3. Connection combination list of B’ fundamental patch

APPENDIX-C: Unit Combinations

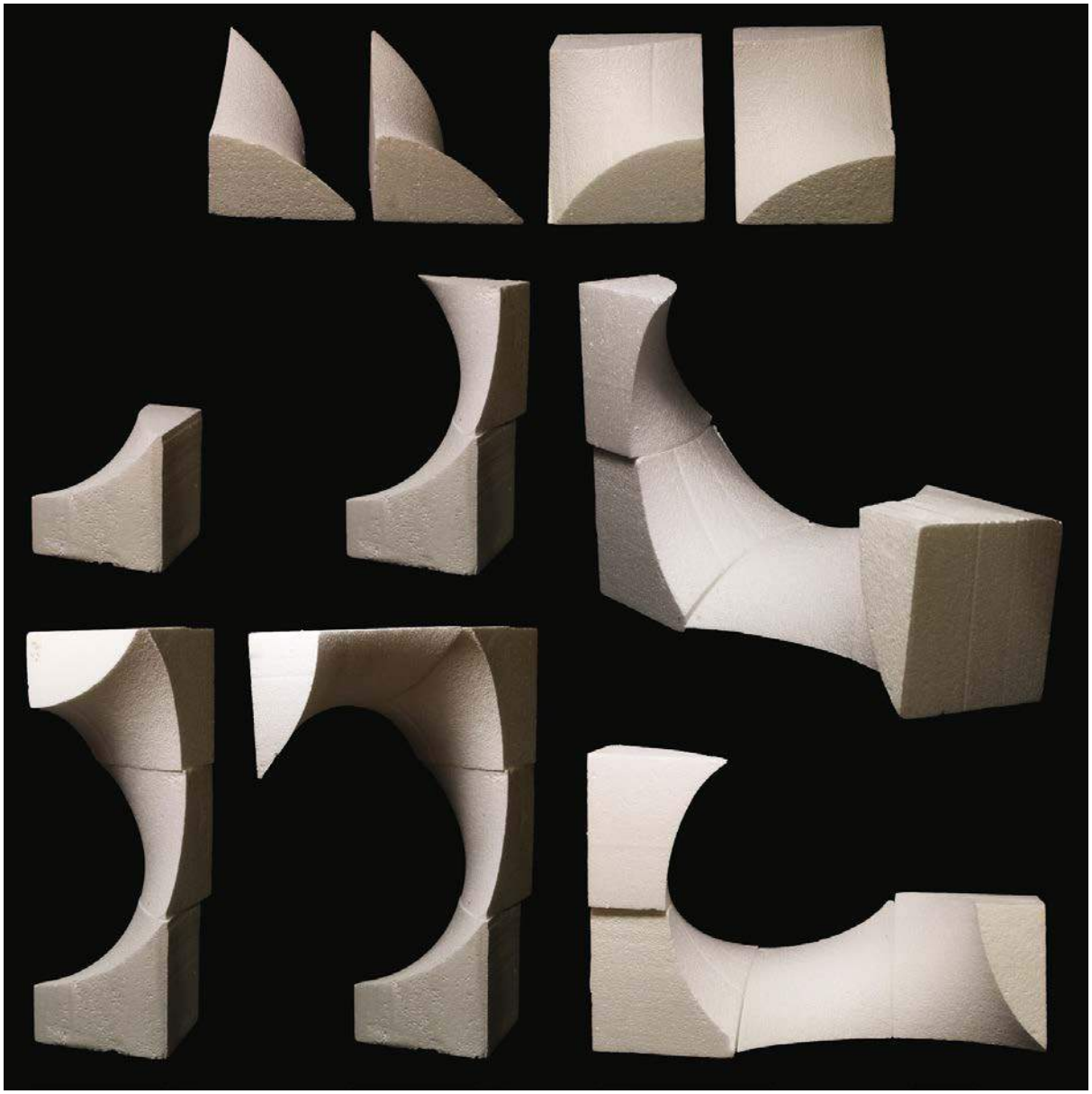

Figure C.1. A17, A16, B’11, B’12

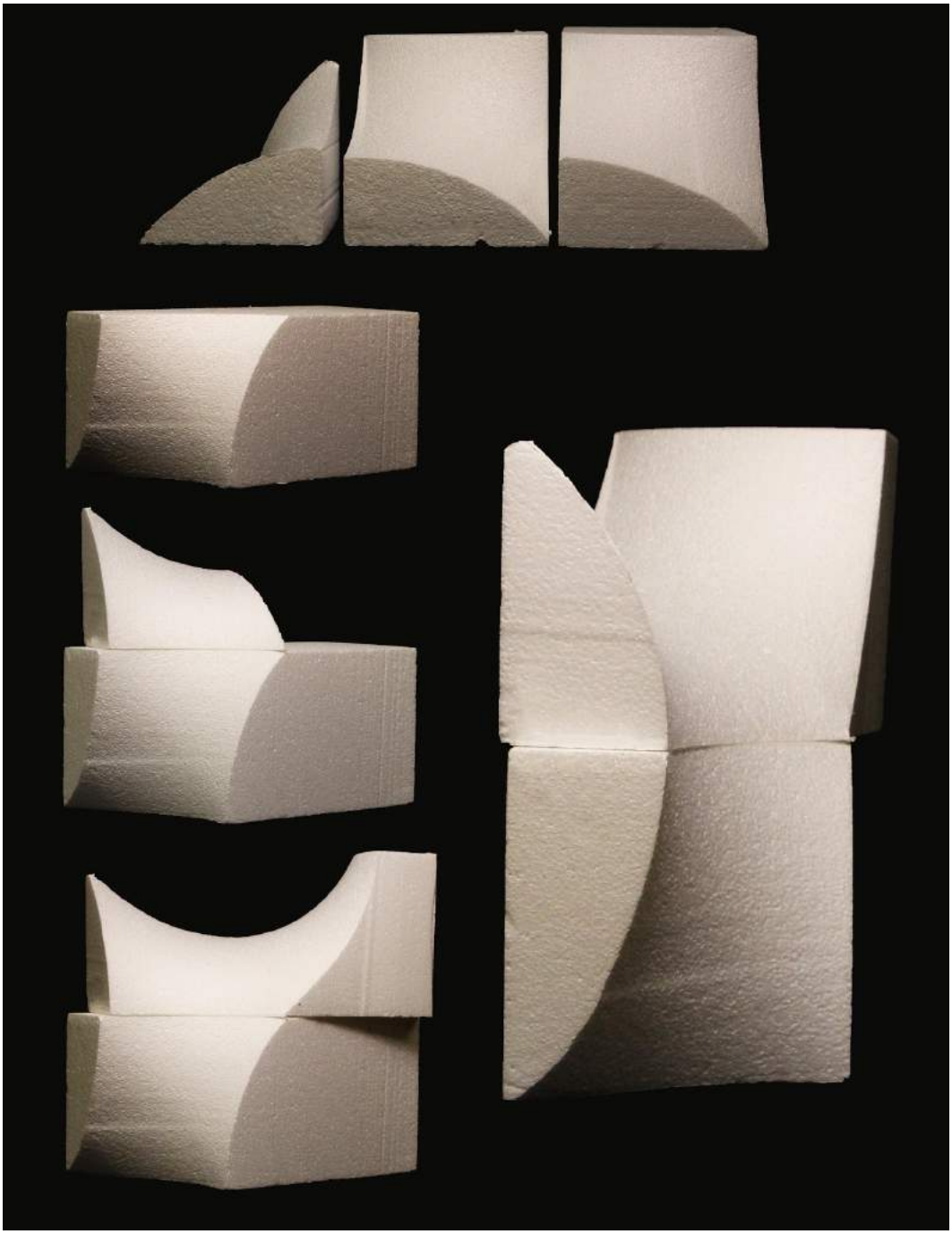

Figure C.2. A’3, B4, B17

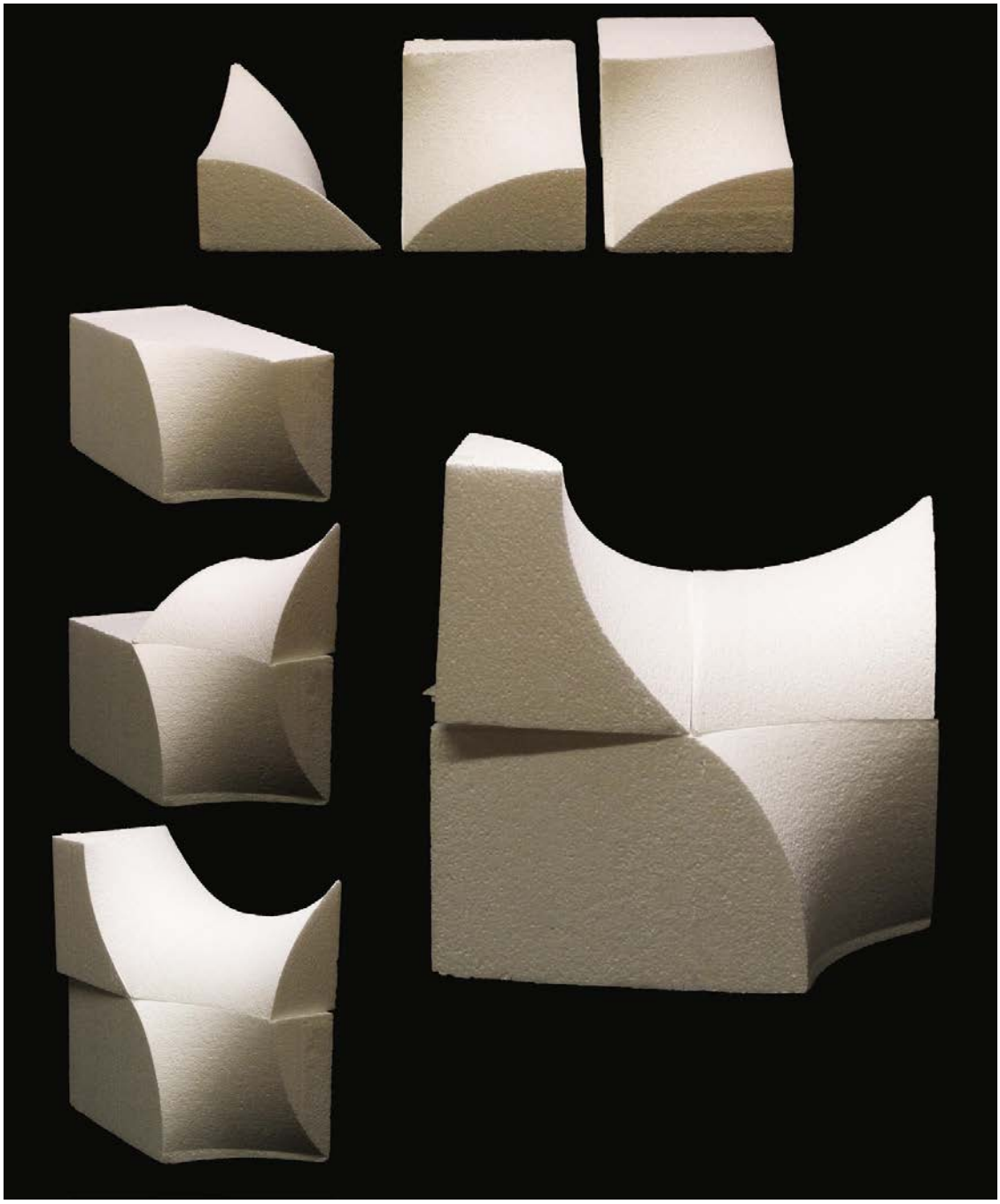

Figure C.3. A3, A10, B’10

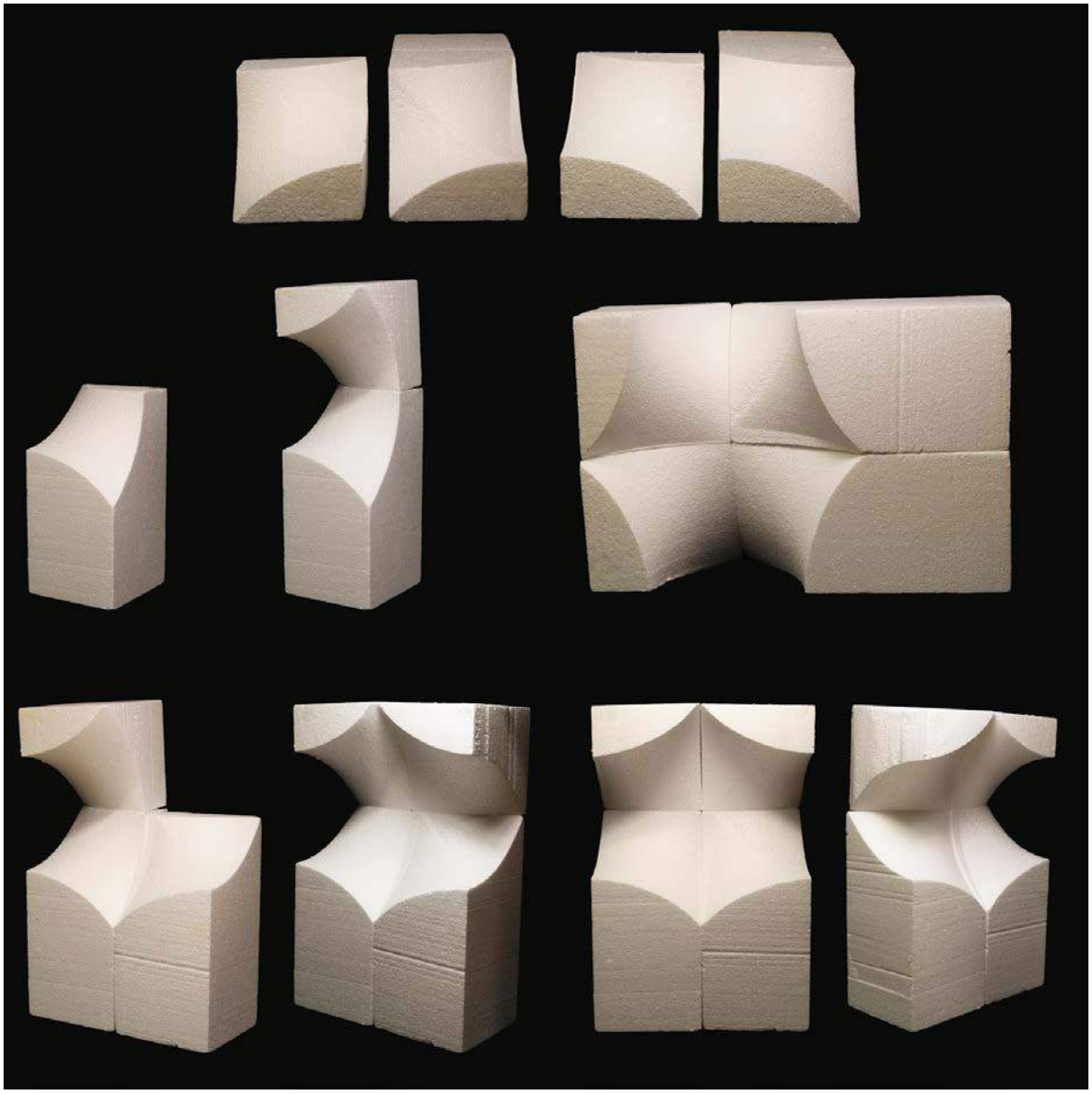

Figure C.4. A9, A16, B1, B8

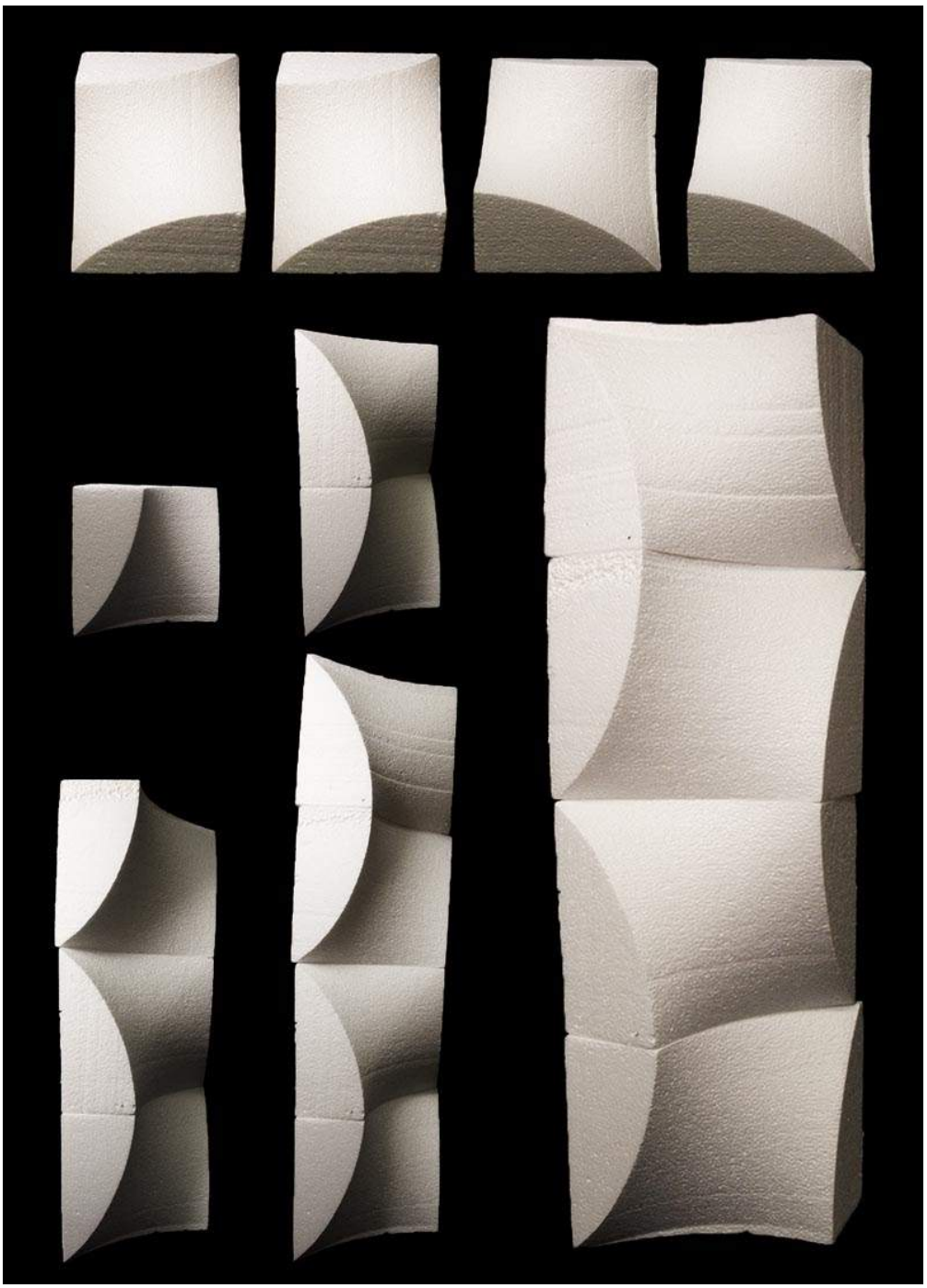

Figure C.5. A7, A2, B5, B13

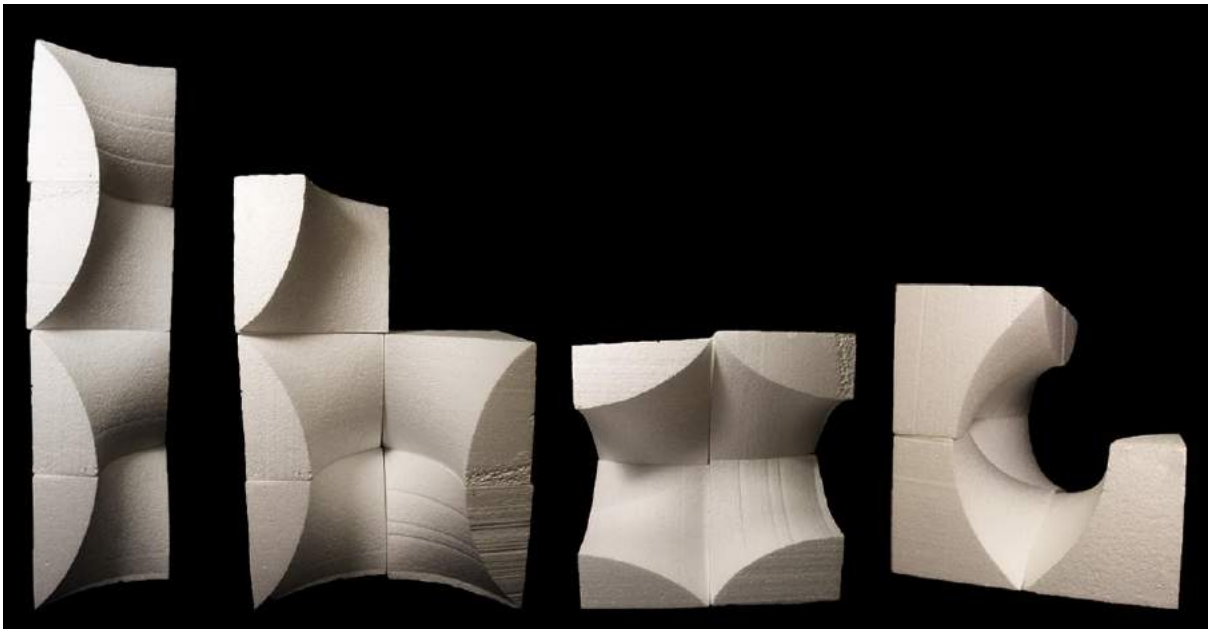

Figure C.6. Variation of A7, A2, B5, B13 patches

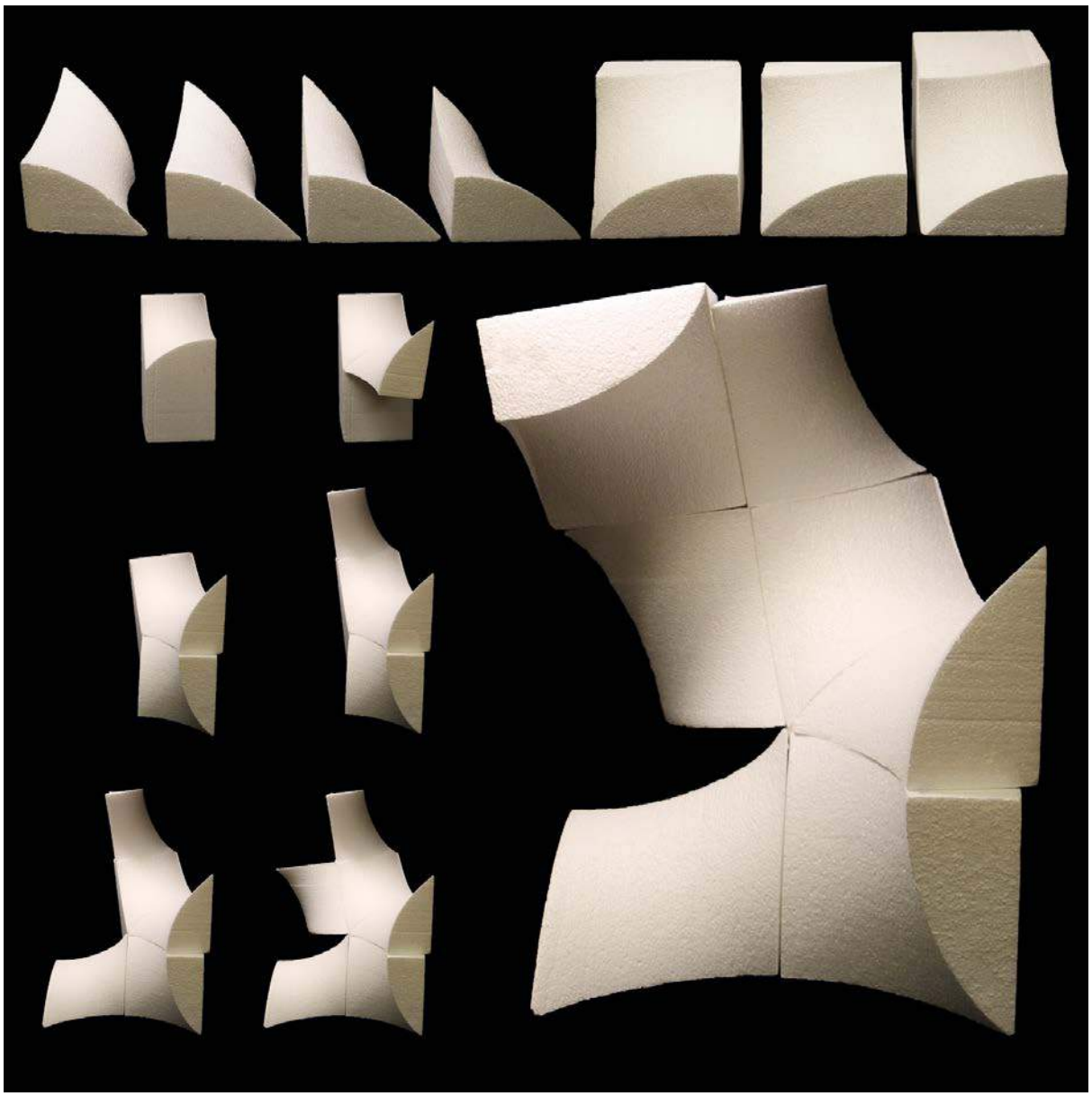

Figure C.7. A4, A8, A15, B’2, B’3, B’4, B’8

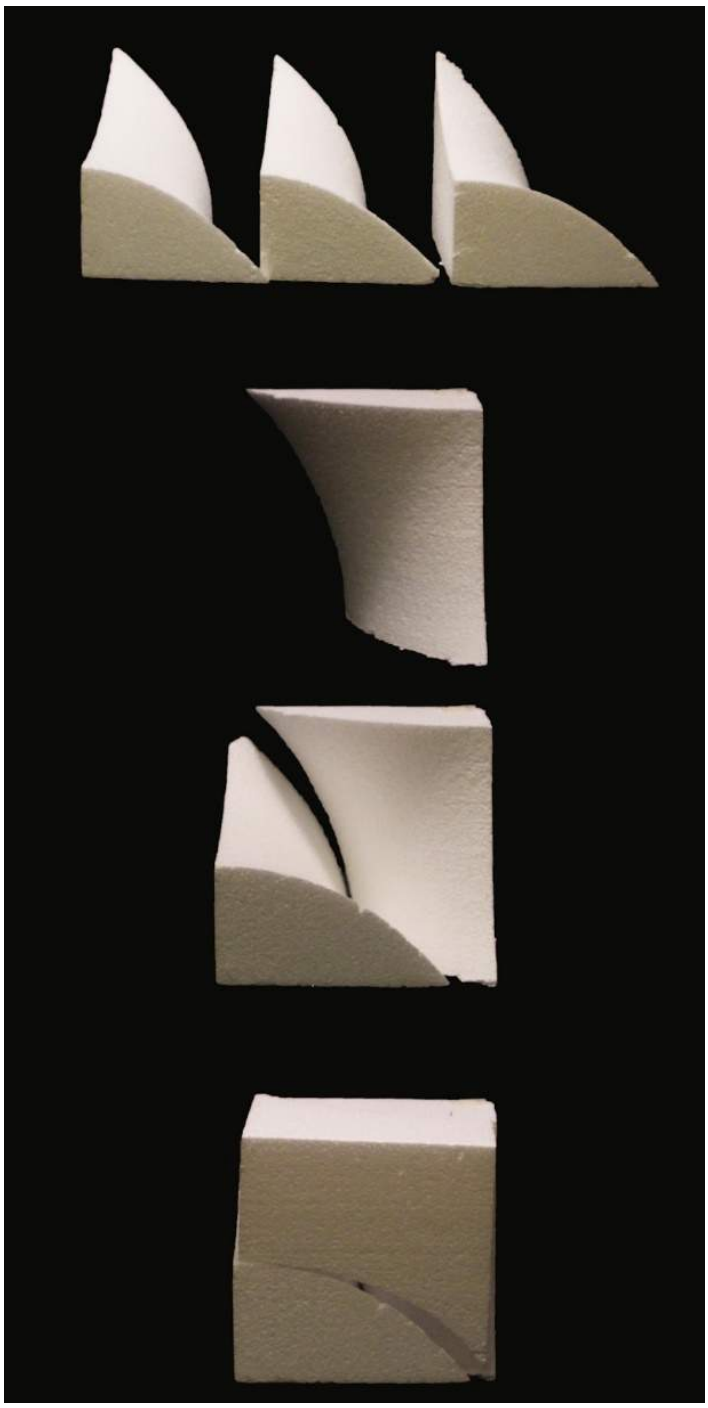

Figure C.8. B’6, B’4, B’12

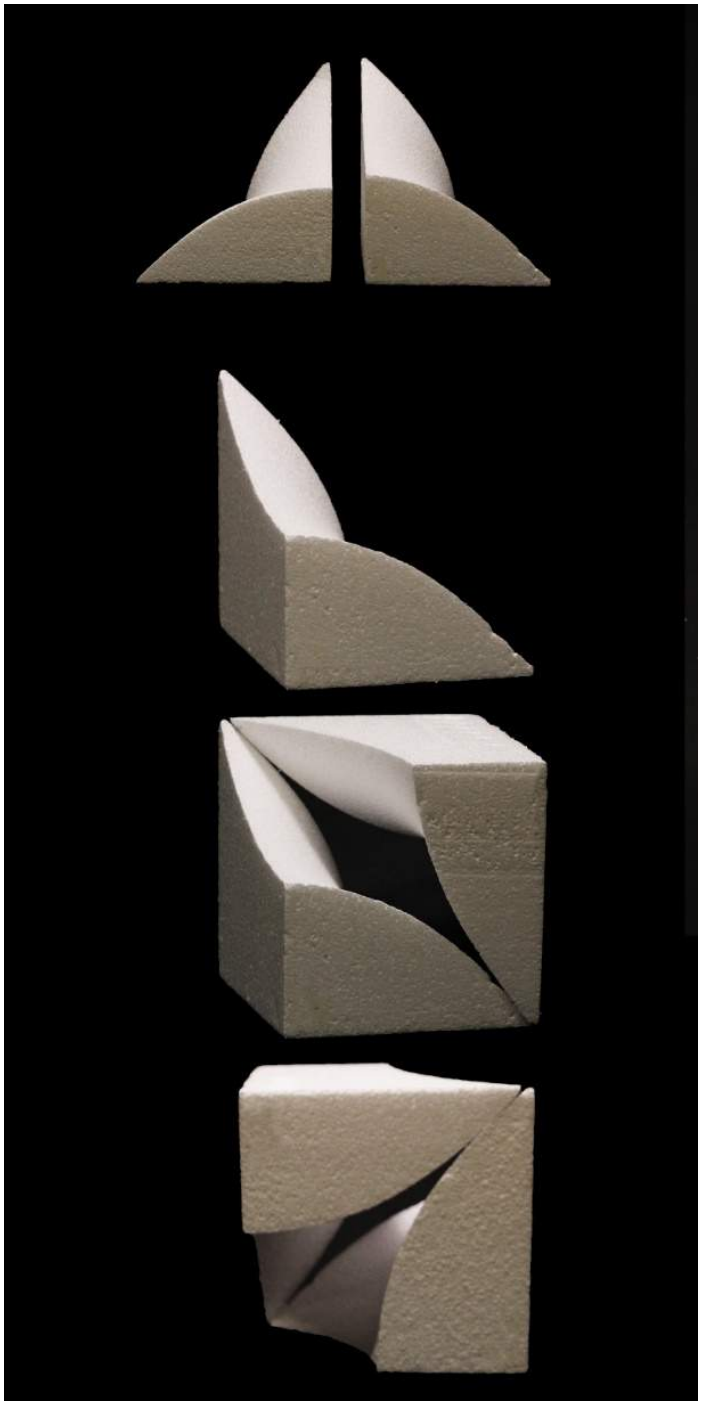

Figure C.9. A’2, B’5

Figure C.10. A9, A15, B’1, B’11

APPENDIX-D: Variations by Changing Wire Geometry

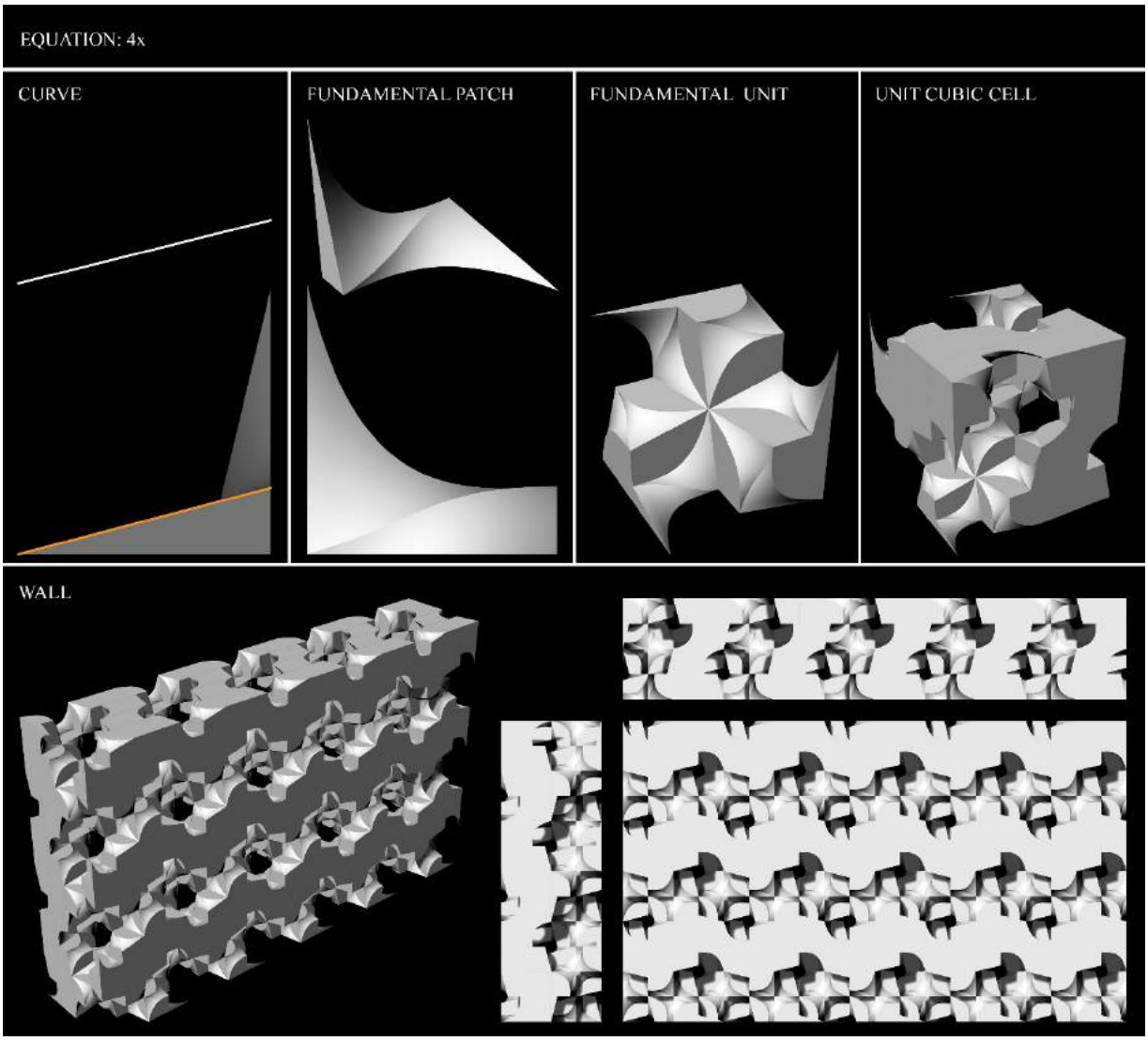

Figure D.1. Variation #3

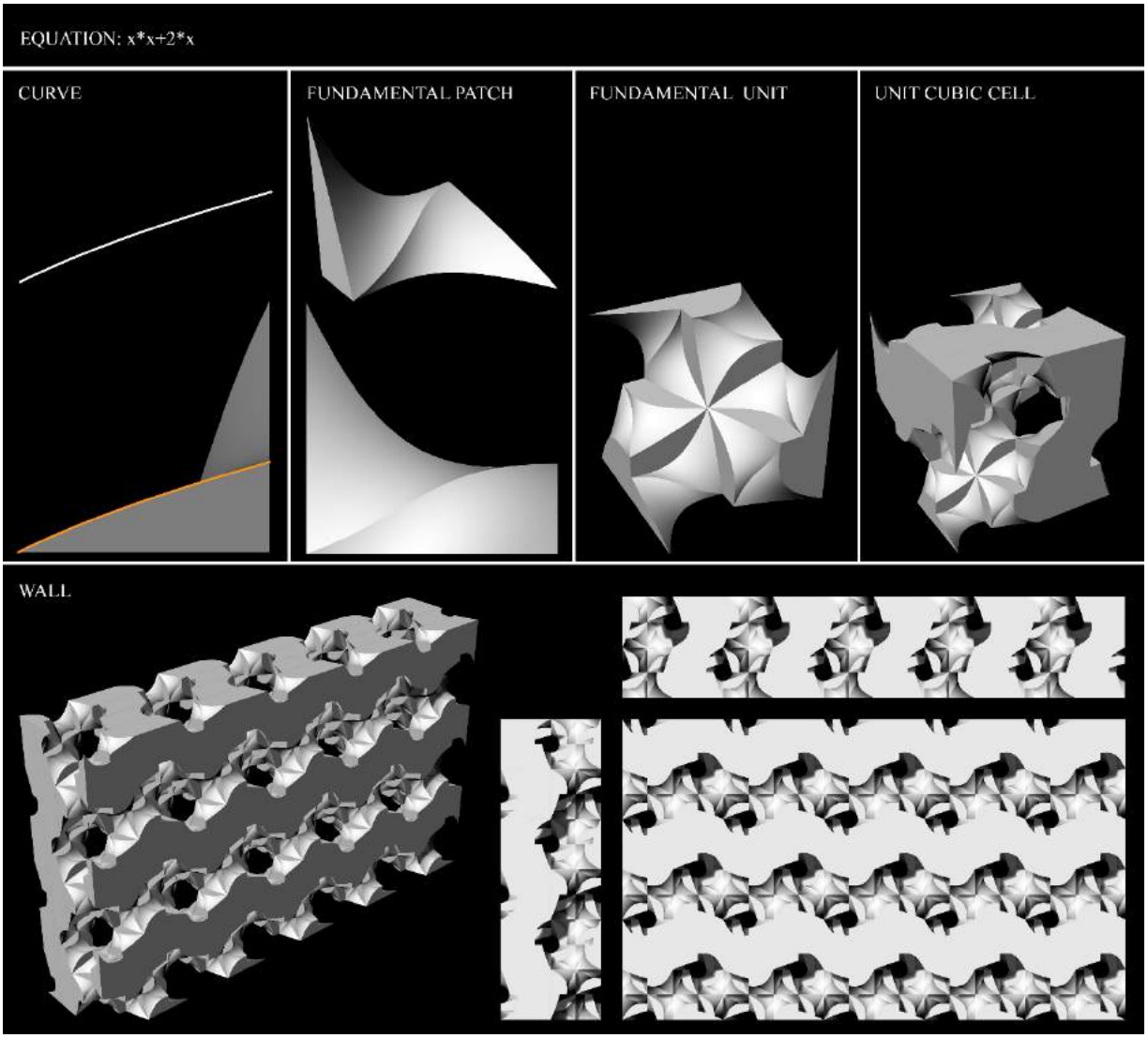

Figure D.2. Variation #4

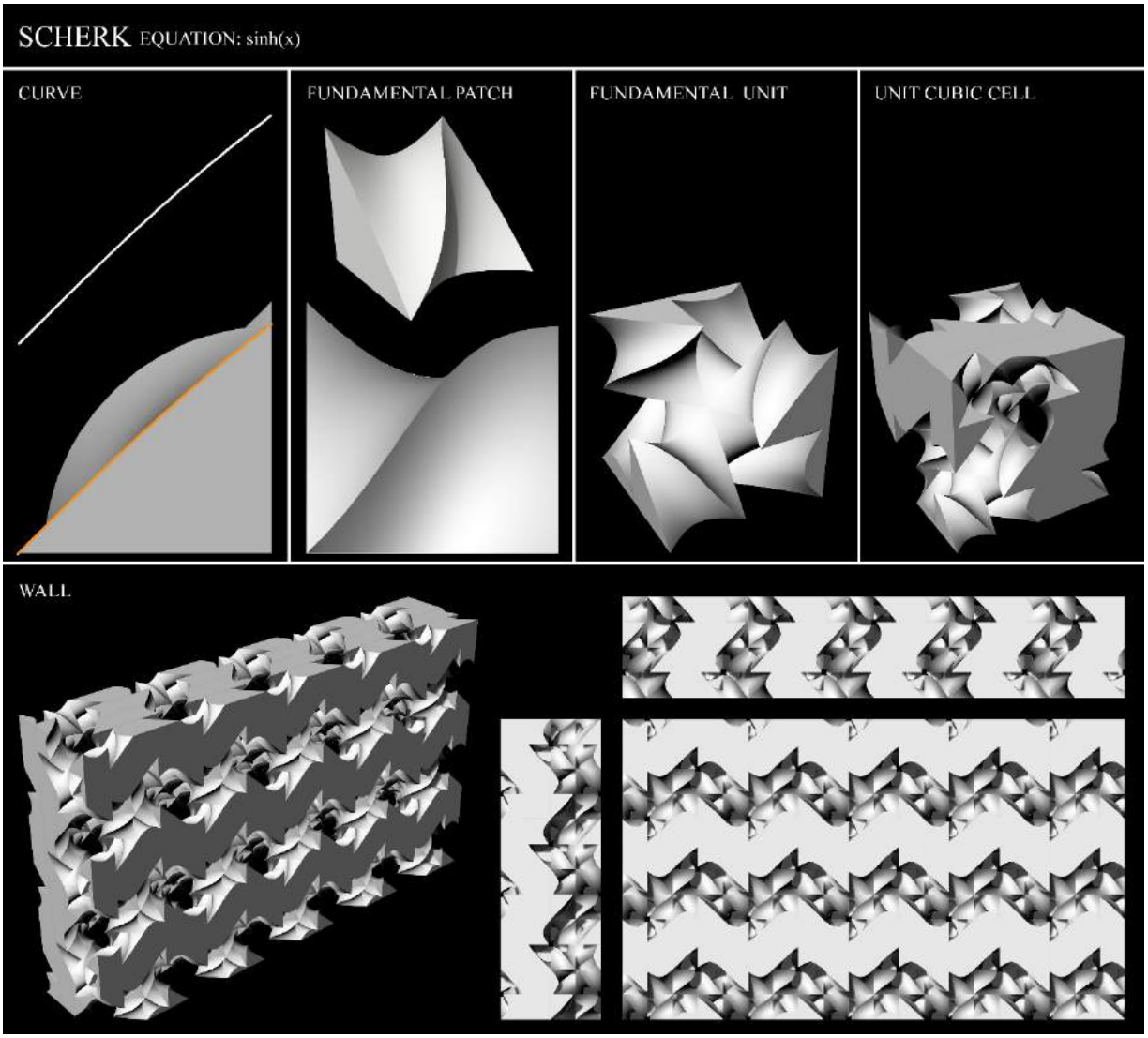

Figure D.3. Variation #5

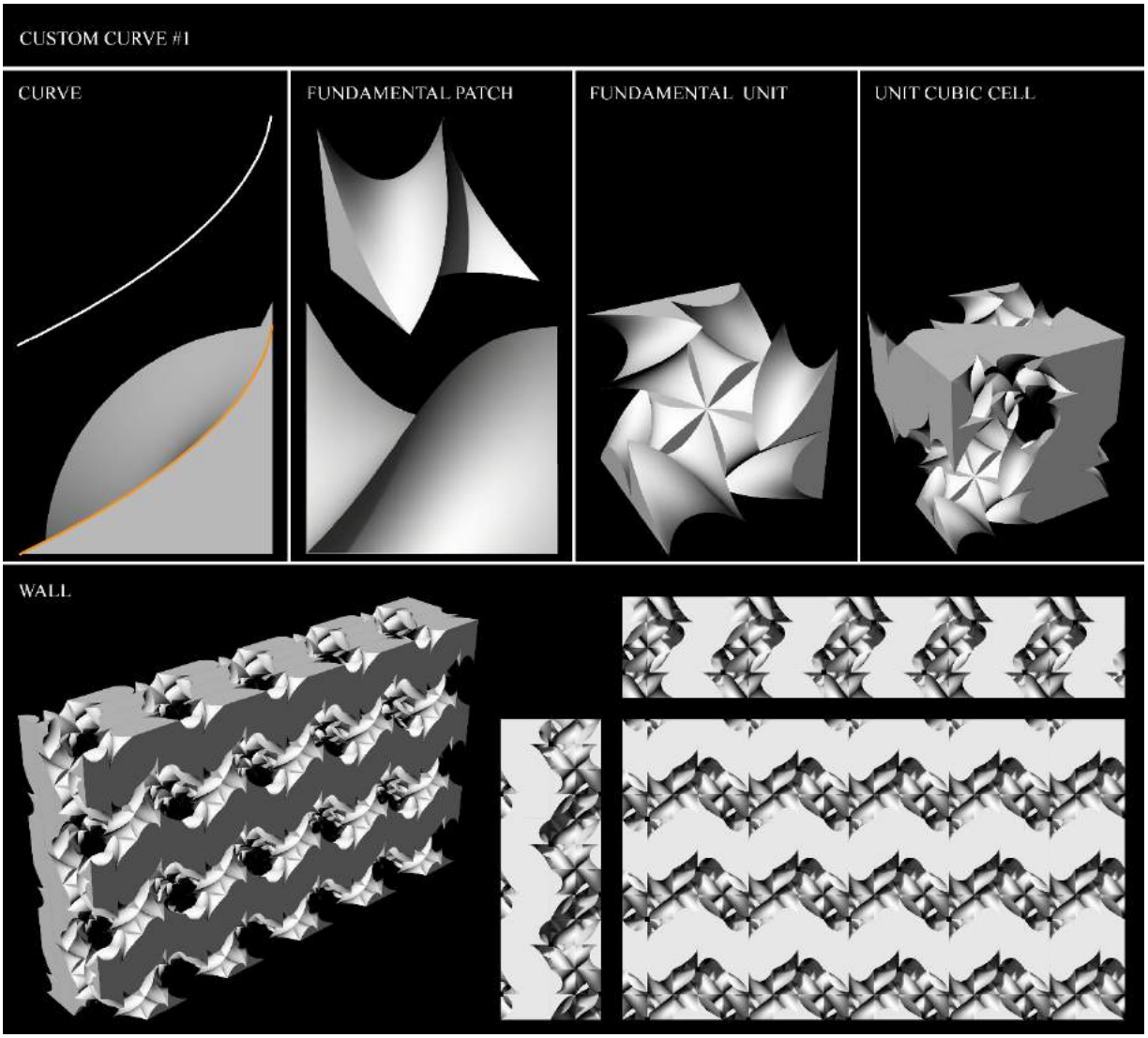

Figure D.4. Variation #6

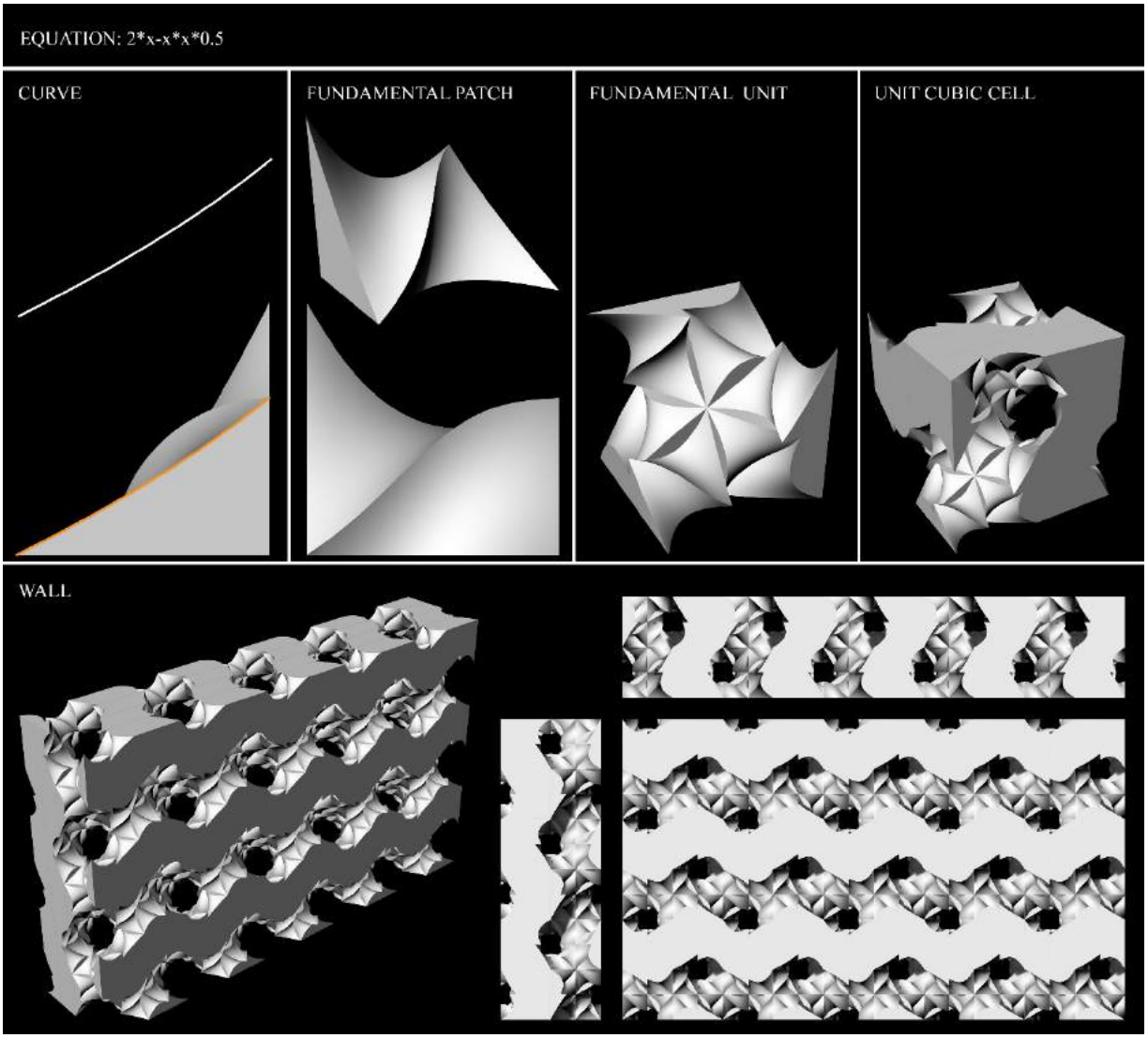

Figure D.5. Variation #7

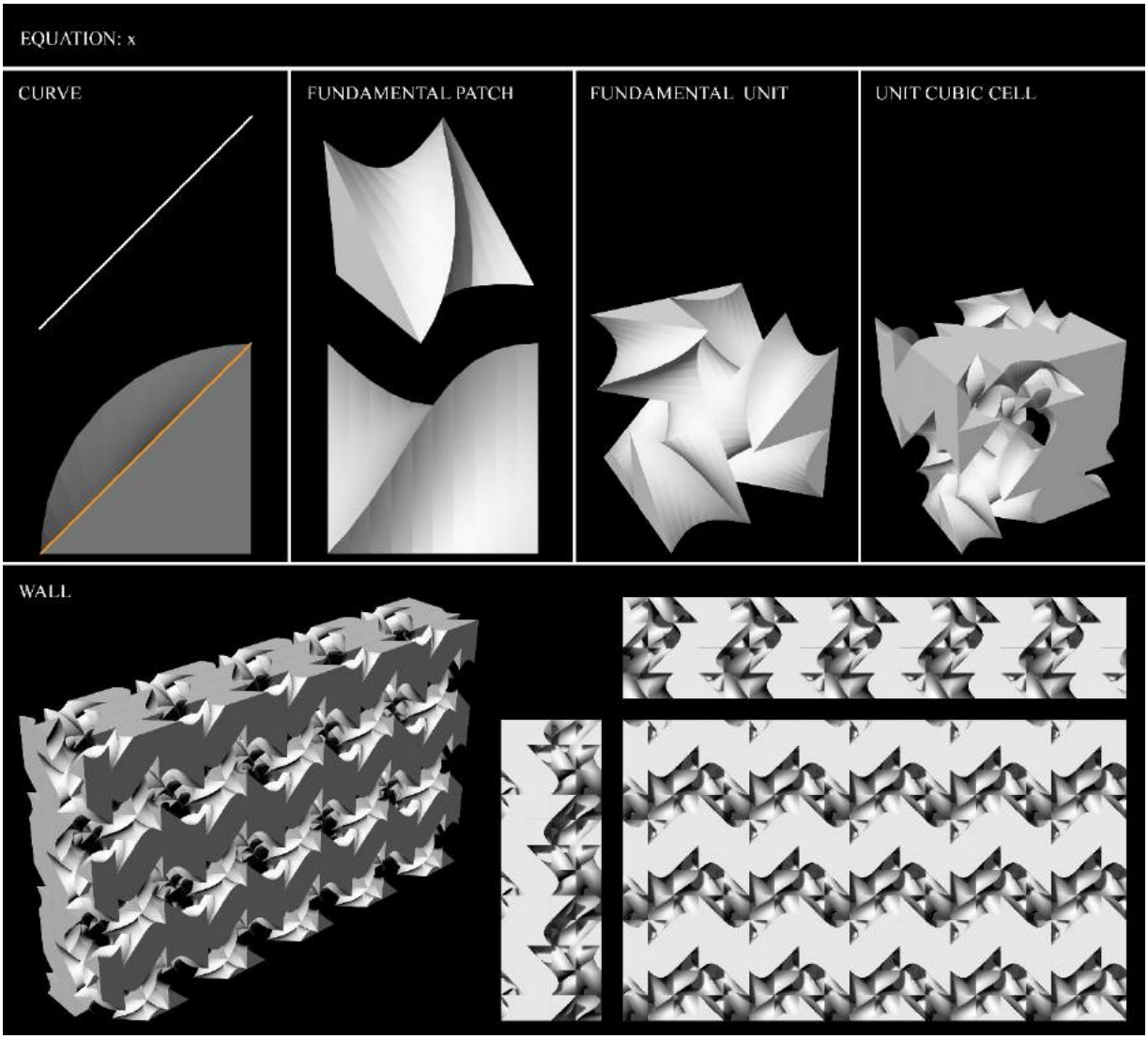

Figure D.6. Variation #8

APPENDIX-E : The Final Generation and Simulation Code

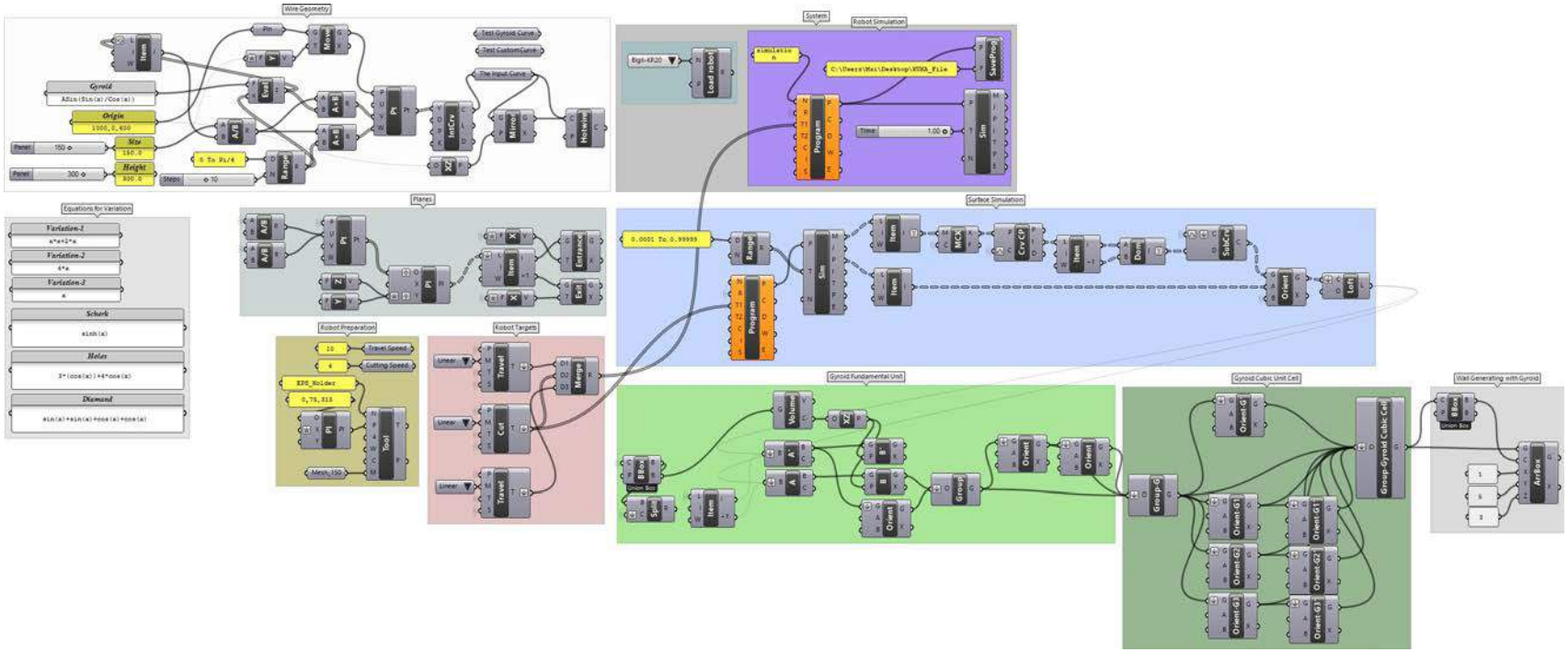

Figure E.1. Final code

APPENDIX-F: The Final Workflow Diagram

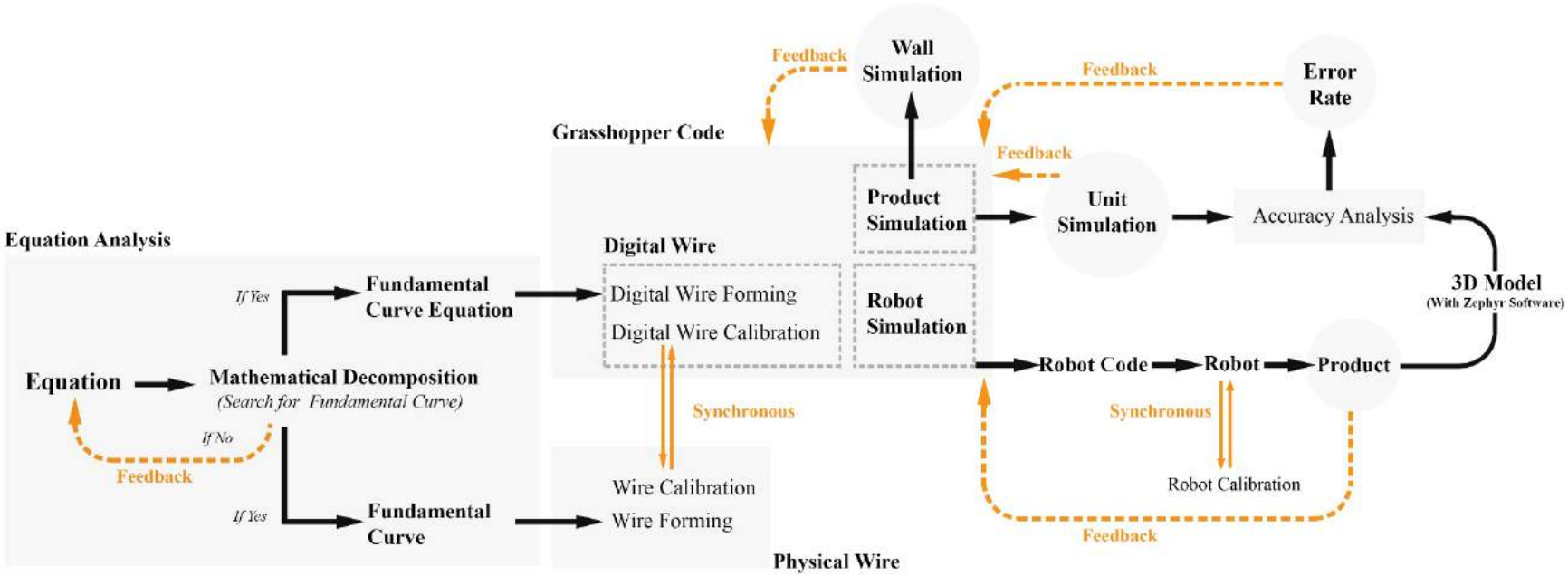

Figure F.1. The final workflow diagram of the research